Development of core-shell nanostructure encapsulating gentamicin as efficient drug delivery system for intracellular Salmonella

Ashish Ranjan

Dissertation outline submitted to the faculty of the Virginia Polytechnic Institute and State University in partial fulfillment of the requirement of the degree of

Doctor of Philosophy
In
Biomedical and Veterinary Sciences

Dr. Ramanathan Kasimanickam (Chair)

Dr. N. Sriranganathan

Dr. William S. Swecker

Dr. Kevin Pelzer

Dr. Judy Riffle

Dr. Gary Pickrell

September 10th 2009
Blacksburg, VA

Keywords: *Salmonella,* Nanostructures, Gentamicin, Drug delivery

Development of efficient drug delivery system against intracellular *Salmonella*

Ashish Ranjan

ABSTRACT

Intracellular pathogens like *Salmonella* have developed various mechanisms to evade host defenses, and they can establish infections. Treatment and eradication are difficult due to our inability in achieving the optimum concentrations of cell-impermeable aminoglycosides like gentamicin within these cells. In this dissertation, we hypothesize that developing a novel core-shell methodology for incorporating high amounts of gentamicin into the cores with either hydrophilic or amphiphilic shell will be more effective than the free gentamicin in clearing intracellular *Salmonella* infection.

Hydrophilic core-shell nanostructures (N1) were made with block co-polymers of poly (ethylene oxide-*b*-sodium acrylate) blended with sodium polyacrylate ($PAA^{-+}Na$) and complexed with the polycationic antibiotic gentamicin. N1 showed 20-25 fold higher gentamicin loading than the currently existing materials and reduced numbers of viable *Salmonella* in the liver and spleen compared to free gentamicin. To further improve the rate and route of uptake, the shell of the nanostructures were made amphiphilic by incorporating pluronics F68 $(PPO)_{68}$ in the block copolymer. We showed that core-shell nanostructures encapsulating gentamicin having $(PPO)_{68}$ in the shell (N2) enhances the rate and modulates the route of uptake into macrophages, thus promoting significant reduction in the intracellular *Salmonella in-vitro* and *in-vivo*.

The main drawback of N2 was its poor stability at physiological pH of 7.4, 0.1 M NaCl. Therefore, core-shell nanostructures encapsulating gentamicin containing pluronic P85 $(PPO)_{85}$ in the shell (N3) with improved colloidal and ionic stability were designed. N3 achieved significant intracellular reduction of vacuolar *Salmonella* (0.53 $\log_{10}$) and cytoplasm resident *Listeria* (3.11 $\log_{10}$) compared to free gentamicin *in-vitro*. However, greater reduction of *Listeria* suggested that sub-cellular localization of bacterium influences targeting by N3. Even though oral administration of N3 was not effective compared to free gentamicin, parenteral (I.P.) administration significantly reduced the intracellular *Salmonella* from liver and spleen compared to free gentamicin and appeared to have no abnormal *in-vivo* toxicity.

In summary, core-shell nanostructures encapsulating gentamicin (N) with improved encapsulation efficiency and different shell chemistry (N1, N2 and N3) were developed with enhanced efficacy against intracellular Salmonella. The novel gentamicin delivery approach developed in this study may be applicable for therapy of many intracellular infections.

Acknowledgement

I am heartily thankful to my supervisor, Dr. Ramanathan Kasimanickam, whose encouragement, guidance and support from the initial to the final level enabled me to develop an understanding of the subject. He showed me different ways to approach a research problem and the need to be persistent to accomplish any goal. Dr. Ram had confidence in me when I doubted myself. He was always there to meet and talk about my ideas and ask me good questions to help me think through my problems. I would also like to thank him for being as much as a friend as a mentor.

I would like to especially thank to Dr. Nammalwar Sriranganathan for his support in my development as a scientist. I am grateful to him for his generosity, guidance and enthusiasm in my research progress. Without his support, knowledge, inputs and pushing me hard to perfection I would never have achieved all this. He was inspiration in motivating me to excel and understand the importance of truthful scientific exploration. I will always remember his quote "You don't convince anyone else in science except yourself". I am grateful to Dr. Nathan for instilling a sense of responsibility, patience and team building skills which immensely developed my self-confidence.

This research would not have been possible without the valuable contribution of our collaborators, Dr. Judy Riffle and her team. Dr. Riffle's suggestion, feedback, and guidance really shaped my course of research. I also believe that her efficient reading of manuscripts, ability to impart manuscript writing skills and her constructive criticisms will determine my future course of development as a scientist. I would like to extend my warm appreciations to Dr. Gary Pickrell who was instrumental in bringing me to the field of nanomedicine research. I liked Dr. Pickrell's philosophy of understanding the objectives of an experiment well and designing the experiment accordingly. This helped me focused my goals more accurately and in a time efficient manner. I would like to thank my other committee members Dr. Kevin Pelzer and Dr. William Swecker for their insightful comments and inputs that always helped me to keep the big clinical picture in my perspective as my research evolved during the course of my study.

My special thanks to Nikorn Pothayee for his efforts in ensuring the successful completion of this project. Nikorn was responsible for the synthesis of drug carriers which were crucial for all of my experiments. The technical and non-technical discussion with Nikorn helped immensely in

executing the experimental plans well. I would like to thank Dr. Mohammed N. Seleem for his guidance, timely help with my experimental works and reviewing my works at a short notice. My thanks are due to Dr. Ron Tyler, Dr. Dave Caudell and Dr. Bonnie Brenseke for carrying out histo-pathological analysis of tissues during the study. I am thankful to my lab-mates Neeta, Gade and Eva for their friendship, encouragement and hard questions. I especially thank Kay Carlson for ensuring the timely availability of lab supplies, for being a friend, teaching me good laboratory practices and supporting my endeavor.

I gratefully acknowledge and thank the Virginia-Maryland Regional College of Veterinary Medicine, Department of Large Animal Clinical Sciences and Research & Graduate Studies for financial support and assistantship during my study.

I would like to thank my friends Umesh, Sai, Parthiban, Neeraj, Gautham, Naveen and Clifton for making my stay in Blacksburg wonderful, timely assistance and support during my study. Finally, I thank my parents, brothers and my wife for always being in my side in thick and thin, unwavering commitment and supporting my ambition. They have been and will remain the source of my aspirations.

Tables of Contents

LIST OF FIGURES

LIST OF TABLES

List of Abbreviations

TTSS: Type three (III) secretion systems

SCV: *Salmonella* containing vacuoles

SPI-1: *Salmonella* pathogenicity island 1

SPI-2: *Salmonella* pathogenicity island 2

AMP: Antimicrobial peptides

RND: Resistance-nodulation-division

MIC: Minimum inhibitory concentration

MRI: Magnetic resonance imaging

DDS: Drug delivery system

DOPE: Dioleoylphosphatidylethanolamine

LLO: Listeriolysin-O

PLA/PEG: Polylactic acid/ Polyethylene glycol

$PAA^{-}{}^{+}Na$: Poly(sodium acrylate)

PEO-*b*-$PAA^{-}{}^{+}Na$: Poly(ethylene oxide-*b*-sodium acrylate)

(PEO-*b*-$PMA^{-}{}^{+}Na$): Poly(ethylene oxide-*b*-sodium methacrylate)

$(PPO)_{68}$: Pluronic-F68

$(PPO)_{85}$: Pluronic-P85

PMPG: Gentamicin nanoplexes encapsulated in PEO-*b*-$PMA^{-}{}^{+}Na$/$PAA^{-}{}^{+}Na$

PAPG: Gentamicin nanoplexes encapsulated in PEO-*b*-$PAA^{-}{}^{+}Na$/$PAA^{-}{}^{+}Na$

^{1}H NMR: Nuclear Magnetic Resonance spectroscopy

CFU: Colony forming units

IP: Intraperitoneal

PO: Par oral

PBS: Phosphate buffer saline

N1: Block copolymer nanostructures encapsulating gentamicin with amphiphilic surface

N2: Block copolymer nanostructures encapsulating gentamicin with hydrophilic surface

PPO: Poly(propylene oxide)

GFP: Green Fluorescent Protein

MCS: Multiple cloning site

D1: Mice treated with 5µg g^{-1} body weight

D2: Mice treated with 15µg g^{-1} body weight

MTS: (3-(4,5-dimethylthiazol-2-yl)-5-(3-carboxymethoxyphenyl)-2-(4-sulfophenyl)-2H-tetrazolium)

FBS: Fetal bovine serum

DMEM: Dulbecco Modified Eagle Medium

HBBS: Hanks Balanced Salt solution

HN: Hydrophilic Nanostructures

PN: Amphiphilic Nanostructure

FITC: Fluorescin Isothiocynanate

ATP: Adenosine triphosphate

THF: TetroHydroFuran

MWCO: Molecular weight cut off

DLS: Dynamic Light Scattering

NG: Nanostructure

FG: Free gentamicin

Chapter 1

Literature review

Nanomedicine in the Chemotherapy of Salmonellosis

(To be submitted)

Abstract

Intracellular pathogens like *Salmonella* evade host phagocytic killing by various mechanisms, and multiply in specialized niche inside the cells. Classical antimicrobial therapy requires multiple dosages and frequent administration of drugs to the patient for long duration. Indiscriminate drug use and patient non-compliance has the potential to create chronic carriers. Specific intracellular delivery of cell impermeable antimicrobials using nanoparticulate carriers may effectively reduce the dosage, frequency of administration, toxicity of antimicrobial resulting in significant bacterial clearance from the infected patients. In the last decade, nanomedicine has been increasingly applied to devise alternative therapy for many intracellular infections. However, the nanoparticulate carriers have poor stability, minimal drug loading capacity and inefficient drug releasing. This review will address the mechanisms used by *Salmonella* to avoid host pathogenic killing, reasons for therapeutic failure, advances in drug delivery methodology and development of alternative drug delivery strategy to achieve efficient intracellular bacterial clearance.

1. Introduction

In the last few decades, intracellular infections and development of chronic carriers of bacterial organisms like *Salmonella* has increasingly become a global health concern and created new challenges for humans (53). *Salmonellae are* rod-shaped, gram-negative, facultative anaerobes in the family *Enterobacteriaceae* (51). Clinically, *Salmonella spp*. are classified as enteric (typhoid form) and gastroenteritis types (non-typhoidal form) (60). Enteric forms are seen exclusively in humans beings caused by *S. paratyphi* and *S. typhi* (13). In contrast, gastroenteritis is a self limiting disease condition seen both in humans and various animal species including birds, cattle and pigs and is caused mainly by *S. typhimurium (33, 38)*. Based on serotyping studies in humans by the Center of Disease Control and Prevention (CDC, USA), *S.* Typhimurium was the most frequently found *Salmonella* strain with a prevalence rate of 22.1% of total serotypes (10). In addition, risk assessment studies in the USA and the world for salmonellosis indicate high mortality and morbidity in human and animal populations with economic losses in billions of dollars (16, 34).

Patients suffering from salmonellosis may be infected resulting in either an acute or chronic state. Acute salmonellosis can be treated with aminoglycoside and quinolone classes of antimicrobials (11). Treatment of chronic salmonellosis is difficult due to drug resistance, poor management practices and presence of a significant percentage of carriers without clinical signs (24, 75). Development of a chronic state is mainly by evasion of host phagocytic killing mechanisms and establishment of specialized intracellular niches sequestered from the host immune system (45). The intracellular localization of *Salmonella spp*. presents unique therapeutic challenges (59). At a cellular level, therapeutically active polar drugs are not able to traverse the mammalian cell membrane efficiently. Consequently, desired intracellular drug levels for bacterial clearance are not met with such drugs. This may result in antimicrobial treatment failure and high relapse rates in salmonellosis.

To prevent treatment failure and relapse, nanotechnology based approaches may be helpful. Nanotechnology can be used to fabricate the particles and cross-link them to a variety of antimicrobials including quinolones and aminoglycosides. Thus, nanotechnology should help in designing and developing new biomedical therapeutics for therapeutic application, particularly in the targeted delivery of antimicrobials to cells with a high intracellular bacterial load (27). This

literature review will give a brief insight into the mechanism of host evasion by *Salmonella spp.*, reasons of therapeutic failure and the potential of nanomedicine in salmonellosis therapy.

1.1 Salmonella and intracellular parasitism

The interaction of *Salmonella spp*. with mammalian phagocytic and non-phagocytic cells is a complex interplay of numerous genes and protein products that is triggered by the bacterium in response to killing by the host (33). *Salmonellae* possess two types of genes encoding type III secretion systems (TTSS); their encoded proteins play an important role in extracellular and intracellular survival as shown schematically in Fig. 1 (65). Upon phagocytosis, the *Salmonellae* are found in the membrane bound vacuoles, also referred to as *Salmonella* containing vacuoles (SCV) (4, 9, 28). The biogenesis of SCV is normally by the activation of invasion associated TTSS encoded by a *Salmonella* pathogenicity island 2 (SPI-2) (12). The SPI-2 upon induction inside the SCV secretes more than 19 effector proteins across the vacuolar membrane. These effector proteins play an important role in SCV membrane integrity, promote subcellular localization, avoid lysosomal killing, prevent the action of intracellular antimicrobial factors and reorganize the host cytoskeleton (66). Thus, formation of SCV results in prevention of direct fusion with late endosomes or lysosomes and evasion of bacterial killing by the host phagocytic cell (2). In contrast, SPI-1 assists in extracellular survival and infection mainly in the intestinal lumen (44). Alternative mechanisms of intracellular survival may be mediated by the *Salmonellae phoP – phoQ* genetic components activating the transcription of other *Salmonella* genes within SCV providing resistance against antimicrobial peptides (AMP) (22). The *phoP – phoQ* proteins in *Salmonellae* produces a remodeling of the lipid A domain of the lipopolysaccharide resulting in an outer membrane that serves as an effective permeability barrier to divalent cations or cationic peptides like AMP's (48). AMP's are an important component of host innate immune system and resistance to AMP aids in intracellular bacterial proliferation (69).

2. Challenges in Salmonellosis therapy

Treatment of intracellular *Salmonella* like any other intracellular infections is associated with unique therapeutic challenges as described below.

2.1: Treatment Failures

The intracellular adaptation and survival of the *Salmonellae* is frequently associated with treatment failure. Treatment failure in patients infected with the pathogen is mainly due to gene mutation, relapse, or persistence of the active infection (81). Moreover, clinical outcomes in diseases like salmonellosis is influenced by wrongful practices, indiscriminate drug use, sub-optimal pharmacokinetics and pharmacodynamics, inaccurate diagnosis and inadequate knowledge of local epidemiology (78). For example, persistent salmonellosis is often associated with reduced susceptibility to antimicrobials like nalidixic acid and ciprofloxacin leading to higher incidences of treatment failure (15). Thus in such cases, a rational therapy should involve an epidemiological assessment for antibiotic resistance and prolonged therapy to define the correct combination of antibiotics (55). However, a long therapeutic regimen is often associated with patient non-compliance contributing to reduced drug accumulation and poor bacterial clearance (77). In addition, *Salmonellae* has also evolved mechanisms to thwart the antibiotic killing effects. The development of highly sophisticated multidrug efflux system in *Salmonellae* is a noteworthy example of a mechanism to reduce the cellular accumulation of drugs. The putative drug efflux system in *Salmonellae* is facilitated by use of pumps belonging to the resistance-nodulation-division (RND) family (61). Such drug efflux system helps the *Salmonellae* to escape both the bactericidal action of bile salts in the intestinal lumen and of AMP's intracellularly. Therefore, a multitude of factors need to be considered to prevent treatment failures.

2.2 Barriers to optimize antimicrobials therapy

Therapeutic success is dependent on an optimal strategy. Any strategy for the efficient treatment of the infected host should assess the initial size of the bacterial population, drug potency, bacteriostatic/ bactericidal characteristics of antimicrobials, pharmacokinetic/pharmacodynamic properties of the drugs, presence of a post antibacterial effect and *in-vivo* toxicity. Also, for chronic salmonellosis, the ability of drug molecules to traverse the eukaryotic cell membrane needs to be evaluated (78). Intracellular penetration of a drug molecule is dependent on its polarity. Polar drugs are poorly permeable across non-polar, lipophilic cell membrane. For example, aminoglycosides like gentamicin are polar and cationic with net charge of +3.5 at pH 7.4. Hence, their permeability across cell membrane is relatively very low (1, 39). Due to

reduced transcellular penetration by the cationic and polar antimicrobials, the bactericidal clearance of *Salmonellae* does not occur as shown schematically in Fig. 2. Along with the cell membrane barriers, active drug molecules should also be protected from endosomal pH since the activity of antimicrobials like gentamicin is dependent on pH. Late endosomal pH 5 can inactivate or increase the minimum inhibitory concentration (MIC) of the drug molecule. For example, gentamicin, a member of aminoglycoside family, shows a 64-fold increase in MIC at pH 5 (26).

3. Nanomedicine and Salmonellosis Chemotherapy

3.1: Antibacterial nanomedicine:

Nanotechnology is a multidisciplinary scientific field dealing with materials whose physical and chemical properties can be controlled at the molecular level by incorporating chemistry, engineering and manufacturing principles (23). Such materials called nanoparticles are microscopic in nature with sizes ranging typically from 1-100 nanometers (70). Nanotechonology is finding important applications in medicine especially in drug targeting and in imaging tools such as magnetic resonance imaging (MRI). The convergence of nanotechnology and medicine suitably called nanomedicine has the potential to bring momentous advances in the fight against a range of diseases (73). Nanomedicine specifically is defined as the use of materials in which at least one of the dimensions that affects their function is in the size range of 1-100 nm, for a specific diagnostic or therapeutic purpose (36). The application of nanomedicine in antibacterial therapy may prolong release, increase solubility, bioavailability, decrease aggregation and improve efficacy (20, 30). Additionally, nanomedicine based site directed drug therapy can reduce dosage and frequency of drug administration especially in chronic intracellular infection (3). For example, encapsulation of aminoglycosides in the liposomes allows a significant reduction (50%) of the total treatment duration in disseminated *Mycobacterium avium* infection in mice relative to the classical antimicrobial therapy (19). Furthermore, conventional prolonged antimicrobial therapy of any intracellular infection including salmonellosis can cause side effects and toxicity. For example, the manifestation of nephrotoxicity and ototoxicity on repeated administration of aminoglycosides or the incidences of liver damage by tetracyclines are known side effects of antimicrobial therapy (68, 84). Development of alternative therapeutic strategies by encapsulating antimicrobials in

nanocarriers can protect against organ toxicity. For instance, reduced accumulation of the gentamicin encapsulated in liposomes was reported in the kidney upon parenteral administration in rats (1). As evidenced by similar studies, reduced accumulation in the kidney may prevent toxicity due to increased mean half life and retention of encapsulated gentamicin in the liver and spleen in mice relative to free drug (76). In addition to preventing toxicity, encapsulating/cross-linking the drug molecules to the nanoparticles may improve site specific intracellular delivery. This is because drugs encapsulated in nanoparticles are recognized as foreign particulate material to the body and are phagocytosed by the cells of the reticulo-endothelial system (RES). The uptake is mainly by the blood monocytes and macrophages of the liver, spleen, and bone marrow (63). The mechanism of uptake of a foreign carrier has similarly been modulated to deliver drugs to the Salmonellae infected macrophage cells of RES as shown schematically in Fig.3. For example, as a proof of concept, increased accumulation of gentamicin encapsulated in liposomes in liver and spleen cells resulted in extremely effective therapy for disseminated Salmonella infections compared to free drug alone in-vivo (25). Therefore, delivery of antimicrobials by encapsulation in a carrier system enhances/limits their distribution to target organ of intracellular infections like liver and spleen, and prevent side effects associated with repeated administration (39).

Site specific delivery of drug molecules to the target organ of infection like the liver/spleen can be further improved by devising ways to prevent pH dependent loss in bioactivity in the endosome particularly in case of aminoglycosides (26). An important component of such strategy can be destabilization of the endosomal membrane. Destabilization will promote rapid escape of drugs from endosomal compartment and reduce the required MIC at the cytoplasmic pH. In this regard, development of membrane destabilizing compounds like cell penetrating peptides, fusogenic lipids, listeriolysin-O and their incorporation onto the nanoparticulate Drug delivery System (DDS) is a significant development (40, 46, 67). The mechanism of endosomal destabilization by these biomolecules could be an interplay of both endosomal pH and its membrane composition (82). For example, fusogenic lipids like dioleoylphosphatidylethanolamine (DOPE) does not form a bilayer in aqueous media, but addition of different lipids may favor a bilayer structure. A negatively charged head group with an appropriate acid dissociation constant (pK_a) in the stabilizing lipid in an acidified endosomal environment neutralizes the lipid charge and reduces the bilayer stabilization. Bilayer

destabilization in presence of DOPE and subsequent fusion with endosomal membranes have reported to increase intracytoplasmic drug concentration (41, 86). A potential benefit of this technique can be an enhancement in the efficacy of membrane-impermeable antibiotics like gentamicin. Research studies have shown that improved delivery of gentamicin, an aminoglycoside encapsulated in pH dependent liposomal formulation resulted in better efficacy in killing intracellular *Salmonellae* or *Listeria monocytogenes in-vitro* compared to nonfusogenic pH insensitive liposomes (41). However, the stability of the carrier in the physiological environment needs further investigation. Alternatively, endosomal membrane destabilization by purified listeriolysin-O (LLO) secreted by the bacterial pathogen *Listeria* can be highly promising. Secretion of LLO by *Listeria* creates pores on the endosomal membrane resulting escape of organism into the cytoplasm (79). LLO is pH dependent with increased activity at low pH. For example, as the pH of the endosomal environment decreases from 7.0 to 5.5, there is a proportional increase in the activity of the LLO protein molecule and greater escape of the pathogen from the endosomal vacuoles (31, 79). Although using purified protein from bacterium in drug carrier is attractive, the chances of the encapsulated LLO protein inducing host immune reactions cannot be ruled out. Most notably, this phenomenon can adversely affect the dosage especially in therapy requiring multiple administrations of drug. Regardless, this suggests that optimizing therapy for intracellular infection should aim to design a DDS which is non-immunogenic and non-toxic with improved characteristics particularly in their capacity to deliver drugs to the intracellular niches where the pathogen is hiding from the host immune system. This will assist in achieving improved intracellular killing of pathogens that adapt to intracellular parasitism as a strategy to avoid host defense (49).

Finally, to realize cell specific delivery, the nanosized carriers should have controlled physico-chemical properties in terms of size, zeta potential, pH sensitivity, surface chemistry in addition to membrane destabilizing properties. For example, nanoparticulated DDS with positive zeta potential and size greater than 80 nm is rapidly taken up by RES cells like macrophages (68, 72). Also, the surface chemistry of the nanoparticulate drug carriers can significantly influence uptake by macrophages. For instance, quantum dots (QD) containing either carboxylate (COOH) or amino (polyethylene glycol) [NH2-(PEG) amino groups shows variable rate of uptake by J774A.1 macrophage cells. Uptake of carboxylate group containing QDs has been found to be relatively higher by the macrophage cells irrespective of size in comparison to QD

containing NH2-(PEG) group (12). Plausible explanation for NH_2 (PEG) QDs not being readily taken up by the macrophages could be due to the PEG coating providing a 'steric-repulsive barrier' against interaction with macrophages. Similarly, the phagocytosis of polylactide (PLA) nanoparticles by the polymorphonuclear cells is more efficient than a blend of polylactic acid/ polyethylene glycol (PLA/PEG) (1:0.25). This is because PLA nanoparticles are more hydrophobic due to the presence of uncapped carboxyl end-groups of the polymer. The presence of hydrophobic uncapped polymer has a stimulatory effect both in adhesion and internalization by the cells (43). Thus, it is safe to hypothesize that greater particle recognition and uptake by the *Salmonella* infected macrophage cells may be correlated with the parameters influencing the particle surface chemistry. Hence, careful control of the characteristics of DDS is important for therapeutic application and is a subject of intense investigation by various research groups.

3.2 Application of nanomedicine in the treatment of Salmonellosis:

Nanoparticle based DDS containing various classes of antimicrobials have been tested *in-vivo* and *in-vitro* against Salmonellosis. Ampicillin belonging to the penicillin group of beta-lactam antibiotics is active against both gram positive and gram negative bacteria. Though the beta-lactam antibiotics are effective against intracellular pathogens, they have low intracellular uptake and diffusion through the lysosomal membrane. The loading of ampicillin into colloidal carriers like polycyanoacrylate nanoparticles *in-vitro* and *in-vivo* may potentially overcome the drawback of classical antimicrobial therapy and reduce intracellular *Salmonella* (6). For example, marked destruction of the intracellular *Salmonella* have been observed in infected peritoneal cells and J774A.1 murine macrophage cells upon treatment with radioactive tritium labeled ampicillin loaded polycyanoacrylate nanoparticle. The killing action of the ampicillin loaded nanoparticles is attributed to the cell wall destruction of the *Salmonella* as evidenced by the presence of numerous spherical bodies with radioactivity in the infected cytoplasm of the macrophages (62).

One important determinant in the antimicrobial activity of the DDS is their ability to release drug intracellularly in a sustained manner for an extended period. It is noteworthy that the bactericidal effects of the ampicillin loaded polycyanoacrylate nanoparticle in the *Salmonella* infected cells is indeed influenced by the duration of treatment. Bacterial destruction was significant in the case of a 12 hour treatment with ampicillin loaded polycyanoacrylate compared to free ampicillin. In contrast, shorter incubation with the radioactive tritium labeled ampicillin loaded

polycyanoacrylate nanoparticles resulted in higher particle uptake compared to free ampicillin, but did not translate into significant reduction in the intracellular *Salmonella* (5). The mechanism of uptake for ampicillin loaded polycyanoacrylate was endosomal, and were mostly concentrated in the phagosome or phagolysosome as observed by transmission electron and confocal microscopy, respectively (62). However, the endosomal pathway has the potential to increase the MIC and reduce the efficacy of aminoglycosides which is a drug of interest against many intracellular pathogens including *Salmonella*. Regardless, these studies suggest that uptake of antibiotic bound to the nanoparticles is indeed possible in the *Salmonella* infected cells.

In addition to greater intracellular uptake, the efficacy of antimicrobial loaded nanoparticles to clear *Salmonella* is dependent on the physiological state, the class of antimicrobial and duration of infection (57). For example, administration of polycyanoacrylate nanoparticles containing ciprofloxacin in persistently *Salmonellae* infected BALB/c mice reportedly results in significant bacterial decrease in liver but an incomplete clearance of the pathogen (56). In contrast, ampicillin loaded polycyanoacrylate nanoparticles are ineffective in treating chronic murine salmonellosis. Thus, the stage of infection viz. chronic or acute state can have a significant impact on rate of bacterial clearance and could be a limiting factor in nanoparticle based therapy. It is interesting to note that mice chronically infected with *Salmonellae* show reduced susceptibility to the antimicrobial loaded nanoparticles, possibly due to changes in the intracellular microenvironment of the infecting pathogen. In contrast, acute *Salmonella* infection is more efficiently cleared by either ampicillin loaded polyisohexylcyanoacrylate nanoparticles, or gentamicin and ciprofloxacin containing liposomes (25, 42, 83) . Furthermore, differences in the efficacy of bacterial clearance may also be due to the different growth states of *Salmonella* in acute vs. chronic states. Ampicillin is more effective against replicating pathogens, which is the case in an acute infection. In contrast, chronic salmonellosis is characterized by a carrier state wherein the patient harbors the dormant bacterium in lymph nodes, spleen and liver and sheds them under stress, thereby making ampicillin ineffective. In addition, *Salmonella* resides in the SCV in chronic carriers; drug molecules may not readily traverse the SCV membrane to aid in clearance.

As described before in the previous sections, in the case of aminoglycosides, bactericidal activity is pH dependent. Though the nanoparticle carrier may improve the bioavailability of drugs, an endocytic uptake can potentially reduce the efficacy. The incorporation of endosomal destabilizing agent in the DDS to improve intracytoplasmic delivery of gentamicin is a significant advancement. For example, pH sensitive liposomal DDSs containing fusogenic lipids designed to undergo controlled fusion with cellular or endosomal membranes drug delivery results in better *Salmonella* clearance (14, 41). Plausible mechanism of the improved efficacy could be concentration dependent bactericidal effect of aminoglycoside. However, the stability of liposomes in the blood stream are a concern since break-up tends to release any encapsulated drugs prematurely. One strategy for improving the stability is to incorporate cholesterol into the bilayers to increase stiffness of the liposome walls (47, 80). But, improving the stability can compromise the liposomal uptake by the macrophages (80).

Finally, physiologically, outcomes of therapy in chronic infections are complicated by an inability of the mammalian cells to take up certain classes of drugs, over-expression of the drug targets, inactivation of the drugs by the cells and an initiation of the drug efflux system from the cells, reducing further the drug intracellular concentrations in chronic salmonellosis (52). In such cases, nanoparticle DDS by virtue of enhanced drug delivery has the potential to improve bioavailability and achieve comparatively better reduction of pathogen load compared to conventional therapy.

General rationale for the present research

Evasion of intracellular phagocytic killing mechanisms by many bacterial pathogens can result in failure of classic antimicrobial therapy. The main drawback of classical antimicrobial therapy is its inability to achieve the recommended amount of cell-impermeable antimicrobials like gentamicin within the cells. Thus, treatment and eradication of intracellular pathogens becomes highly difficult. Several groups have investigated to improve intracellular drug delivery but the DDS have poor encapsulation, stability and release efficiency issues (63, 64). To achieve better efficacy compared to free drug, the current research would aim to optimize the DDS and test the same in *in-vitro* and *in-vivo* against an intracellular *Salmonella* infection model.

With a teamed approach in collaboration with the Department of Chemistry, Virginia Tech, our research aimed to develop a methodology for incorporating aminoglycosides into macromolecular complexes with anionic homo- and block copolymers via. cooperative electrostatic interactions between cationic drugs and anionic polymers. The ultimate goal of our research is to develop a DDS for treating intracellular pathogens. The rationale for choosing gentamicin, a member of aminoglycoside family, as the drug of choice for treating intracellular *Salmonella* in the present study is due to its broad activity against both Gram-negative and Gram-positive bacteria (21). Though gentamicin is well known for being cost effective and highly efficacious, yet its poor cell membrane permeability and loss in bioactivity at endosomal pH limits its clinical use, particularly in many intracellular bacterial infections (26). This is complicated further by its rapid clearance by the renal system resulting in a short plasma half-life (74). Moreover, their action is concentration dependent and requires a careful regimen of dosage (7). Inaccurate administrations of the drug may lead to potential problems of nephrotoxicity and ototoxicity which are dose-dependent effects (71). Thus, devising methodology to achieve cell specific delivery of gentamicin can potentially prevent many deleterious side effects in the patient. In addition, it may open new avenues for the pharmaceutical industry to use unapproved toxic antimicrobials. Furthermore, it will remove the source of infection for next generation of susceptible animals and human and the persistent infected carriers in the population.

Chapter 2 (sub-section 2.1) in the dissertation is focused on describing the general approach for improving encapsulation efficiency by incorporating gentamicin into anionic Poly(sodium acrylate) ($PAA^{-}\ ^{+}Na$) homo-polymer and block copolymers of poly(ethylene oxide-*b*-sodium

acrylate) (PEO-*b*-PAA^{-} $^{+}$Na) (N1). Since gentamicin is polycationic with net charge of +3.5 at pH 7.4 (1) and PAA^{-} $^{+}$Na is anionic in nature, they can electro-statically attract each other and can form nanostructure. Also, PAA^{-} $^{+}$Na has been utilized for oral, ophthalmic and associated biomedical applications; therefore its incorporation in DDS is highly favored (32). The rationale for the inclusion of PEO in the nanostructure is its ability to impart high water solubility and provide resistance to non-specific protein adsorption (58). Finally, the efficacy and drawback of this methodology in *in-vivo* clearance of intracellular *Salmonella* infection model is discussed.

Chapter 2 (sub-section 2.2) in the dissertation discusses a novel approach in improving the intracellular delivery of gentamicin. A methodology for the inclusion of pluronic-F68 $(PPO)_{68}$ in the block copolymers of the nanostructure is described. The pluronic block copolymers are composed of ethylene oxide (EO) and propylene oxide (PO) blocks arranged in a basic A-B-A structure: $EO_{x/2}$-PO_y-$EO_{x/2}$(37). This block arrangement results in an amphiphilic copolymer, in which the number of hydrophilic EO (x) and hydrophobic PO (y) units can be altered for a particular therapeutic application. It is noteworthy that pluronic copolymer $(PPO)_{68}$-PAA are non-biodegradable but biocompatible (8). The size-selective cut-off for efficient renal glomerular filtration is approximately 30 kD (upper limit: $\geq$ 60 kD); for molecular weight >30 kD, the glomerular filteration rate falls off sharply (17). The pluronic $(PPO)_{68}$-PAA in our drug delivery system are water soluble and have molecular weight of 10-20 kD, which is well below the glomerular filteration limit. Hence, we expect them to have efficient renal clearance. In addition, pluronics are in the Phase I & II studies in cancer chemotherapy and have been used as food additives and excipients in pharmaceutical industry for decades (18, 35, 85). Therefore, their inclusion in antimicrobial DDS is highly favored and needs intense investigation. Thus, this chapter investigates and establishes the techniques for preparing amphiphilic $(PPO)_{68}$-PAA core-shell nanostructures encapsulating gentamicin (N2), their rate and the route of uptake in the macrophages cells and the influence of amphiphilic surface in *in-vitro* intracellular Salmonella clearance.

Chapter 2 (sub-section 2.3) of the dissertation is focused on the *in-vivo* application of N2 against an intracellular *Salmonella* infection model. The concentration dependent toxicity of free gentamicin and the protective effects of encapsulated gentamicin in the nanostructures are

discussed in an *in-vivo* AJ-646 mouse model. The final section of this chapter will describe the efficacy and drawbacks of N2 in the clearance of intracellular *Salmonella.*

Chapter 3 (sub-section 3.1) of the dissertation will describe the synthesis and application of $(PPO)_{85}$-PAA core-shell nanostructures encapsulating gentamicin (N3). Pluronic P85 $(PPO)_{85}$ in the amphiphilic shell was incorporated to improve the stability of core-shell nanostructures at physiological pH of 7.4 and 0.1 NaCl. In addition, $(PPO)_{85}$ are relatively more lipophilic than $(PPO)_{68}$ which should favor more efficient uptake by macrophages (29). Research studies have shown that $(PPO)_{85}$ is protective against listeriosis in mice, through modulation of the host cell ATP's (50). Also, studies have shown that delivery of oligonucleotide (ODN) to liver can be selectively enhanced by formulating ODN's with PEO grafted to non-ionic amphiphilic block copolymer $(PPO)_{85}$ [$(PPO)_{85}$-g-PEI(2K)] (54). Therefore, it may be interesting to explore N3 for cell specific selective delivery to the target organ of *Salmonella* infection like the liver and spleen. This chapter will focus on understanding in detail the *in-vitro* characteristics of the N3 in terms of its uptake and efficacy. The rate and route of uptake of N3 will be studied by pathway inhibition studies. To investigate the role of sub-cellular localization of bacterium in influencing the efficacy of N3, two kinds of intracellular infection model system will be investigated namely vacuolar *Salmonella* and an intracytoplasmic *Listeria* model. The final section of this chapter will provide a detailed insight on the plausible mechanism of action of the N3.

Chapter 3 (sub-section 3.2) of the dissertation is focused on exploring the application of N3 against an *in-vivo* intracellular *Salmonella* model. Previous studies in cancer chemotherapy have reported that the $(PPO)_{85}$-PAA nanostructures can be effectively used via. an oral route to deliver anticancer agents. The effect of route of administration of N3 on intracellular *Salmonella* clearance is discussed in this chapter. The final section of this chapter discusses detailed toxicity in an *in-vivo* Balb/c mice model.

Chapter 4 in the dissertation summarizes the overall results of the proposed research. In this dissertation, we propose a new methodology for drug delivery against an intracellular pathogen particularly *Salmonella*. The knowledge gained in this study should provide us with critical information that enhances our understanding for optimizing DDS against intracellular pathogens. We believe that through this study, novel approaches to improve drug encapsulation and their enhanced delivery within the cells may be understood and applied for treatment of *Salmonella*.

Furthermore, we discuss the approaches to improve and optimize the DDS for future studies so that successful treatment of *Salmonella* may be achieved.

References

1. **Abraham, A. M., and A. Walubo.** 2005. The effect of surface charge on the disposition of liposome-encapsulated gentamicin to the rat liver, brain, lungs and kidneys after intraperitoneal administration. Int J Antimicrob Agents **25:**392-7.

2. **Abrahams, G. L., and M. Hensel.** 2006. Manipulating cellular transport and immune responses: dynamic interactions between intracellular Salmonella enterica and its host cells. Cell Microbiol **8:**728-37.

3. **Ahmad, Z., S. Sharma, and G. K. Khuller.** 2007. Chemotherapeutic evaluation of alginate nanoparticle-encapsulated azole antifungal and antitubercular drugs against murine tuberculosis. Nanomedicine **3:**239-43.

4. **Bakowski, M. A., V. Braun, and J. H. Brumell.** 2008. Salmonella-containing vacuoles: directing traffic and nesting to grow. Traffic **9:**2022-31.

5. **Balland, O., H. Pinto-Alphandary, S. Pecquet, A. Andremont, and P. Couvreur.** 1994. The uptake of ampicillin-loaded nanoparticles by murine macrophages infected with Salmonella typhimurium. J Antimicrob Chemother **33:**509-22.

6. **Balland, O., H. Pinto-Alphandary, A. Viron, E. Puvion, A. Andremont, and P. Couvreur.** 1996. Intracellular distribution of ampicillin in murine macrophages infected with Salmonella typhimurium and treated with (3H)ampicillin-loaded nanoparticles. J Antimicrob Chemother **37:**105-15.

7. **Barclay, M. L., E. J. Begg, and K. G. Hickling.** 1994. What is the evidence for once-daily aminoglycoside therapy? Clin Pharmacokinet **27:**32-48.

8. **Bromberg, L.** 2008. Polymeric micelles in oral chemotherapy. J Control Release **128:**99-112.

9. **Catron, D. M., M. D. Sylvester, Y. Lange, M. Kadekoppala, B. D. Jones, D. M. Monack, S. Falkow, and K. Haldar.** 2002. The Salmonella-containing vacuole is a major site of intracellular cholesterol accumulation and recruits the GPI-anchored protein CD55. Cell Microbiol **4:**315-28.

10. **CDC.** 2001. Control and Prevention. FDDB Epi, , Human **2001**.

11. **Chin, J.** 2000). Control of communicable diseases manual. American Public Health Association.

12. **Clift, M. J., B. Rothen-Rutishauser, D. M. Brown, R. Duffin, K. Donaldson, L. Proudfoot, K. Guy, and V. Stone.** 2008. The impact of different nanoparticle surface chemistry and size on uptake and toxicity in a murine macrophage cell line. Toxicol Appl Pharmacol **232:**418-27.

13. **Connor, B. A., and E. Schwartz.** 2005. Typhoid and paratyphoid fever in travellers. Lancet Infect Dis **5:**623-8.

14. **Cordeiro, C., D. J. Wiseman, P. Lutwyche, M. Uh, J. C. Evans, B. B. Finlay, and M. S. Webb.** 2000. Antibacterial efficacy of gentamicin encapsulated in pH-sensitive liposomes against an in vivo Salmonella enterica serovar typhimurium intracellular infection model. Antimicrob Agents Chemother **44:**533-9.

15. **Crump, J. A., K. Kretsinger, K. Gay, R. M. Hoekstra, D. J. Vugia, S. Hurd, S. D. Segler, M. Megginson, L. J. Luedeman, B. Shiferaw, S. S. Hanna, K. W. Joyce, E. D. Mintz, and F. J. Angulo.** 2008. Clinical response and outcome of infection with Salmonella enterica serotype Typhi with decreased susceptibility to fluoroquinolones: a United States foodnet multicenter retrospective cohort study. Antimicrob Agents Chemother **52:**1278-84.

16. **Crump, J. A., S. P. Luby, and E. D. Mintz.** 2004. The global burden of typhoid fever. Bull World Health Organ **82:**346-53.

17. **Daan J. A. Crommelin, R. D. S., Bernd Meibohm.** 2007. The size-selective cut-off for glomerular filtration is approximately 60 kD Pharmaceutical Biotechnology **3:**101-107.

18. **Danson, S., D. Ferry, V. Alakhov, J. Margison, D. Kerr, D. Jowle, M. Brampton, G. Halbert, and M. Ranson.** 2004. Phase I dose escalation and pharmacokinetic study of pluronic polymer-bound doxorubicin (SP1049C) in patients with advanced cancer. Br J Cancer **90:**2085-91.

19. **de Steenwinkel, J. E., W. van Vianen, M. T. Ten Kate, H. A. Verbrugh, M. A. van Agtmael, R. M. Schiffelers, and I. A. Bakker-Woudenberg.** 2007. Targeted drug delivery to enhance efficacy and shorten treatment duration in disseminated Mycobacterium avium infection in mice. J Antimicrob Chemother **60:**1064-73.

20. **Dillen, K., J. Vandervoort, G. Van den Mooter, and A. Ludwig.** 2006. Evaluation of ciprofloxacin-loaded Eudragit RS100 or RL100/PLGA nanoparticles. Int J Pharm **314:**72-82.

21. **Durante-Mangoni E, G. A., Utili R, Falagas ME.** 2008. Do we still need the aminoglycosides? Int J Antimicrob Agents. **33:**201-5.

22. **Ernst, R. K., T. Guina, and S. I. Miller.** 1999. How intracellular bacteria survive: surface modifications that promote resistance to host innate immune responses. J Infect Dis **179 Suppl 2:**S326-30.

23. **F, E. D.** 2005. Nanomedicine - prospective therapeutic and diagnostic application. Expert opin. Biol. Ther **5 [1]:**1-5.

24. **Feglo, P. K., E. H. Frimpong, and M. Essel-Ahun.** 2004. Salmonellae carrier status of food vendors in Kumasi, Ghana. East Afr Med J **81:**358-61.

25. **Fierer J, H. L., Lin JP, Estrella D, Mihalko P, Yau-Young A.** 1990. Successful treatment using gentamicin liposomes of Salmonella dublin infections in mice. Antimicrob Agents Chemother. **34:**343-8.

26. **Gamazo, C., M. C. Lecaroz, S. Prior, A. I. Vitas, M. A. Campanero, J. M. Irache, and M. J. Blanco-Prieto.** 2006. Chemical and biological factors in the control of Brucella and brucellosis. Curr Drug Deliv **3:**359-65.

27. **Gamazo, C., S. Prior, M. Concepcion Lecaroz, A. I. Vitas, M. A. Campanero, G. Perez, D. Gonzalez, and M. J. Blanco-Prieto.** 2007. Biodegradable gentamicin delivery systems for parenteral use for the treatment of intracellular bacterial infections. Expert Opin Drug Deliv **4:**677-88.

28. **Garcia-del Portillo, F., C. Nunez-Hernandez, B. Eisman, and J. Ramos-Vivas.** 2008. Growth control in the Salmonella-containing vacuole. Curr Opin Microbiol **11:**46-52.

29. **Gaymalov, Z. Z., Z. Yang, V. M. Pisarev, V. Y. Alakhov, and A. V. Kabanov.** 2009. The effect of the nonionic block copolymer pluronic P85 on gene expression in mouse muscle and antigen-presenting cells. Biomaterials **30:**1232-45.

30. **Gelperina, S., K. Kisich, M. D. Iseman, and L. Heifets.** 2005. The potential advantages of nanoparticle drug delivery systems in chemotherapy of tuberculosis. Am J Respir Crit Care Med **172:**1487-90.

31. **Geoffroy, C., J. L. Gaillard, J. E. Alouf, and P. Berche.** 1987. Purification, characterization, and toxicity of the sulfhydryl-activated hemolysin listeriolysin O from Listeria monocytogenes. Infect Immun **55:**1641-6.

32. **Gupta, K., M. Ganguli, S. Pasha, and S. Maiti.** 2006. Nanoparticle formation from poly(acrylic acid) and oppositely charged peptides. Biophys Chem **119:**303-6.

33. **Haraga, A., M. B. Ohlson, and S. I. Miller.** 2008. Salmonellae interplay with host cells. Nat Rev Microbiol **6:**53-66.

34. **Hope, B. K., R. Baker, E. D. Edel, A. T. Hogue, W. D. Schlosser, R. Whiting, R. M. McDowell, and R. A. Morales.** 2002. An overview of the Salmonella enteritidis risk assessment for shell eggs and egg products. Risk Anal **22:**203-18.

35. **Hsu, S. H., Y. L. Leu, J. W. Hu, and J. Y. Fang.** 2009. Physicochemical characterization and drug release of thermosensitive hydrogels composed of a hyaluronic acid/pluronic f127 graft. Chem Pharm Bull (Tokyo) **57:**453-8.

36. **K, K.** 2006. Nanomedicine. Future medicine **1(1):**1-3.

37. **Kabanov, A. V., and V. Y. Alakhov.** 2002. Pluronic block copolymers in drug delivery: from micellar nanocontainers to biological response modifiers. Crit Rev Ther Drug Carrier Syst **19:**1-72.

38. **Layton, A. N., and E. E. Galyov.** 2007. Salmonella-induced enteritis: molecular pathogenesis and therapeutic implications. Expert Rev Mol Med **9:**1-17.

39. **Lecaroz, C., C. Gamazo, and M. J. Blanco-Prieto.** 2006. Nanocarriers with gentamicin to treat intracellular pathogens. J Nanosci Nanotechnol **6:**3296-302.

40. **Lee, K. D., Y. K. Oh, D. A. Portnoy, and J. A. Swanson.** 1996. Delivery of macromolecules into cytosol using liposomes containing hemolysin from Listeria monocytogenes. J Biol Chem **271:**7249-52.

41. **Lutwyche, P., C. Cordeiro, D. J. Wiseman, M. St-Louis, M. Uh, M. J. Hope, M. S. Webb, and B. B. Finlay.** 1998. Intracellular delivery and antibacterial activity of gentamicin encapsulated in pH-sensitive liposomes. Antimicrob Agents Chemother **42:**2511-20.

42. **Magallanes, M., J. Dijkstra, and J. Fierer.** 1993. Liposome-incorporated ciprofloxacin in treatment of murine salmonellosis. Antimicrob Agents Chemother **37:**2293-7.

43. **Mainardes RM, G. M., Brunetti IL, da Fonseca LM, Khalil NM.** 2008, Apr. Zidovudine-loaded PLA and PLA-PEG blend nanoparticles: Influence of polymer type on phagocytic uptake by polymorphonuclear cells. J Pharm Sci. **98:**257-67.

44. **Miki T, O. N., Shimada Y, Danbara H.** 2004. Characterization of Salmonella pathogenicity island 1 type III secretion-dependent hemolytic activity in Salmonella enterica serovar Typhimurium. Microb Pathog. **37:**65-72.

45. **Monack, D. M., D. M. Bouley, and S. Falkow.** 2004. Salmonella typhimurium persists within macrophages in the mesenteric lymph nodes of chronically infected Nramp1+/+ mice and can be reactivated by IFNgamma neutralization. J Exp Med **199:**231-41.

46. **Moon, C., Y. M. Kwon, W. K. Lee, Y. J. Park, and V. C. Yang.** 2007. In vitro assessment of a novel polyrotaxane-based drug delivery system integrated with a cell-penetrating peptide. J Control Release **124:**43-50.

47. **Mugabe, C., A. O. Azghani, and A. Omri.** 2005. Liposome-mediated gentamicin delivery: development and activity against resistant strains of Pseudomonas aeruginosa

isolated from cystic fibrosis patients. Journal of Antimicrobial Chemotherapy **55:**269-271.

48. **Murata, T., W. Tseng, T. Guina, S. I. Miller, and H. Nikaido.** 2007. PhoPQ-mediated regulation produces a more robust permeability barrier in the outer membrane of Salmonella enterica serovar typhimurium. J Bacteriol **189:**7213-22.

49. **Nasti TH, K. M., Owais M., .** 2006. Enhanced efficacy of pH-sensitive nystatin liposomes against Cryptococcus neoformans in murine model. J Antimicrob Chemother **57:**349-52.

50. **Neudeck, B. L., T. D. Alford, N. G. Faith, and C. J. Czuprynski.** 2008. The poloxamer P85 is protective against Listeria monocytogenes invasion. Foodborne Pathog Dis **5:**859-65.

51. **Nix, R. N., S. E. Altschuler, P. M. Henson, and C. S. Detweiler.** 2007. Hemophagocytic macrophages harbor Salmonella enterica during persistent infection. PLoS Pathog **3:**e193.

52. **Nobili, S., I. Landini, B. Giglioni, and E. Mini.** 2006. Pharmacological strategies for overcoming multidrug resistance. Curr Drug Targets **7:**861-79.

53. **Ochiai, R. L., C. J. Acosta, M. C. Danovaro-Holliday, D. Baiqing, S. K. Bhattacharya, M. D. Agtini, Z. A. Bhutta, G. Canh do, M. Ali, S. Shin, J. Wain, A. L. Page, M. J. Albert, J. Farrar, R. Abu-Elyazeed, T. Pang, C. M. Galindo, L. von Seidlein, and J. D. Clemens.** 2008. A study of typhoid fever in five Asian countries: disease burden and implications for controls. Bull World Health Organ **86:**260-8.

54. **Ochietti, B., N. Guerin, S. V. Vinogradov, Y. St-Pierre, P. Lemieux, A. V. Kabanov, and V. Y. Alakhov.** 2002. Altered organ accumulation of oligonucleotides using polyethyleneimine grafted with poly(ethylene oxide) or pluronic as carriers. J Drug Target **10:**113-21.

55. **Ong, G., I. Wilson, B. Smyth, and P. Rooney.** 2007. Antimicrobial resistance in non-typhoidal salmonellas from humans in Northern Ireland, 2001-2003: standardization needed for better epidemiological monitoring. Epidemiol Infect **135:**675-80.

56. **Page-Clisson, M. E., H. Pinto-Alphandary, E. Chachaty, P. Couvreur, and A. Andremont.** 1998. Drug targeting by polyalkylcyanoacrylate nanoparticles is not efficient against persistent Salmonella. Pharm Res **15:**544-9.

57. **Page-Clisson, M. E., H. Pinto-Alphandary, M. Ourevitch, A. Andremont, and P. Couvreur.** 1998. Development of ciprofloxacin-loaded nanoparticles: physicochemical study of the drug carrier. J Control Release **56:**23-32.

58. **Pan, J., M. Zhao, Y. Liu, B. Wang, L. Mi, and L. Yang.** 2008. Development of a new poly(ethylene glycol)-graft-poly(D,L-lactic acid) as potential drug carriers. J Biomed Mater Res A **89:**160-7.

59. **Pasmans, F., K. Baert, A. Martel, A. Bousquet-Melou, R. Lanckriet, S. De Boever, F. Van Immerseel, V. Eeckhaut, P. de Backer, and F. Haesebrouck.** 2008. Induction of the carrier state in pigeons infected with Salmonella enterica subspecies enterica serovar typhimurium PT99 by treatment with florfenicol: a matter of pharmacokinetics. Antimicrob Agents Chemother **52:**954-61.

60. **Perrett, C. A., and M. A. Jepson.** 2007. Applications of cell imaging in Salmonella research. Methods Mol Biol **394:**235-73.

61. **Piddock, L. J.** 2006. Multidrug-resistance efflux pumps - not just for resistance. Nat Rev Microbiol **4:**629-36.

62. **Pinto-Alphandary, H., O. Balland, M. Laurent, A. Andremont, F. Puisieux, and P. Couvreur.** 1994. Intracellular visualization of ampicillin-loaded nanoparticles in peritoneal macrophages infected in vitro with Salmonella typhimurium. Pharm Res **11:**38-46.

63. **Prior, S., C. Gamazo, J. M. Irache, H. P. Merkle, and B. Gander.** 2000. Gentamicin encapsulation in PLA/PLGA microspheres in view of treating Brucella infections. Int J Pharm **196:**115-25.

64. **Prior, S., B. Gander, J. M. Irache, and C. Gamazo.** 2005. Gentamicin-loaded microspheres for treatment of experimental Brucella abortus infection in mice. J Antimicrob Chemother **55:**1032-6.

65. **Prost, L. R., S. Sanowar, and S. I. Miller.** 2007. Salmonella sensing of anti-microbial mechanisms to promote survival within macrophages. Immunol Rev **219:**55-65.

66. **Rajashekar, R., D. Liebl, A. Seitz, and M. Hensel.** 2008. Dynamic remodeling of the endosomal system during formation of Salmonella-induced filaments by intracellular Salmonella enterica. Traffic **9:**2100-16.

67. **Reddy, J. A., and P. S. Low.** 2000. Enhanced folate receptor mediated gene therapy using a novel pH-sensitive lipid formulation. J Control Release **64:**27-37.

68. **Ristuccia, A. M., and B. A. Cunha.** 1982. The aminoglycosides. Med Clin North Am **66:**303-12.

69. **Rosenberger, C. M., R. L. Gallo, and B. B. Finlay.** 2004. Interplay between antibacterial effectors: a macrophage antimicrobial peptide impairs intracellular Salmonella replication. Proc Natl Acad Sci U S A **101:**2422-7.

70. **Rotomskis, R., G. Streckyte, and V. Karabanovas.** 2006. [Nanoparticles in diagnostics and therapy: towards nanomedicine]. Medicina (Kaunas) **42:**542-58.

71. **Rougier, F., D. Claude, M. Maurin, A. Sedoglavic, M. Ducher, S. Corvaisier, R. Jelliffe, and P. Maire.** 2003. Aminoglycoside nephrotoxicity: modeling, simulation, and control. Antimicrob Agents Chemother **47:**1010-6.

72. **Rudt S, M. R.** 1993. In vitro phagocytosis assay of nano- and microparticles by chemiluminescence. III. Uptake of differently sized surface-modified particles, and its correlation to particle properties and in vivo distribution. European journal of pharmaceutical sciences **1:31-39.**

73. **Sanhai, W. R., J. H. Sakamoto, R. Canady, and M. Ferrari.** 2008. Seven challenges for nanomedicine. Nat Nanotechnol **3:**242-4.

74. **Silva, J. G., and I. Carvalho.** 2007. New insights into aminoglycoside antibiotics and derivatives. Curr Med Chem **14:**1101-19.

75. **Solnik-Isaac, H., M. Weinberger, M. Tabak, A. Ben-David, D. Shachar, and S. Yaron.** 2007. Quinolone resistance of Salmonella enterica serovar Virchow isolates from humans and poultry in Israel: evidence for clonal expansion. J Clin Microbiol **45:**2575-9.

76. **Swenson CE, S. K., Hammett JL, Fitzsimmons WE, Ginsberg RS.** 1990. Pharmacokinetics and in vivo activity of liposome-encapsulated gentamicin. Antimicrob Agents Chemother **34:**235-40.

77. **Tanaka, M., H. Nakayama, M. Haraoka, T. Nagafuji, T. Saika, and I. Kobayashi.** 1998. Analysis of quinolone resistance mechanisms in a sparfloxacin-resistant clinical isolate of Neisseria gonorrhoeae. Sex Transm Dis **25:**489-93.

78. **Vakulenko, S. B., and S. Mobashery.** 2003. Versatility of aminoglycosides and prospects for their future. Clin Microbiol Rev **16:**430-50.

79. **Vazquez-Boland, J. A., M. Kuhn, P. Berche, T. Chakraborty, G. Dominguez-Bernal, W. Goebel, B. Gonzalez-Zorn, J. Wehland, and J. Kreft.** 2001. Listeria pathogenesis and molecular virulence determinants. Clin Microbiol Rev **14:**584-640.

80. **Vitas, A. I., R. Diaz, and C. Gamazo.** 1996. Effect of composition and method of preparation of liposomes on their stability and interaction with murine monocytes infected with brucella abortus. Antimicrobial Agents and Chemotherapy **40:**146-151.

81. **Walsh, C., and S. Fanning.** 2008. Antimicrobial resistance in foodborne pathogens--a cause for concern? Curr Drug Targets **9:**808-15.

82. **Wasungu, L., and D. Hoekstra.** 2006. Cationic lipids, lipoplexes and intracellular delivery of genes. J Control Release **116:**255-64.

83. **Webb MS, B. N., Wiseman DJ, Saxon D, Sutton K, Wong KF, Logan P, Hope MJ.** 1998 Jan;. Antibacterial efficacy against an in vivo Salmonella typhimurium infection model and pharmacokinetics of a liposomal ciprofloxacin formulation. Antimicrob Agents Chemother **42(1):**:45-52.

84. **WR., W.** 1977. Tetracyclines, chloramphenicol, erythromycin, and clindamycin. Mayo Clin Proc. **52(10):**635-40.

85. **Yang, T., M. K. Choi, F. D. Cui, S. J. Lee, S. J. Chung, C. K. Shim, and D. D. Kim.** 2007. Antitumor effect of paclitaxel-loaded PEGylated immunoliposomes against human breast cancer cells. Pharm Res **24:**2402-11.

86. **Zuhorn, I. S., U. Bakowsky, E. Polushkin, W. H. Visser, M. C. Stuart, J. B. Engberts, and D. Hoekstra.** 2005. Nonbilayer phase of lipoplex-membrane mixture determines endosomal escape of genetic cargo and transfection efficiency. Mol Ther **11:**801-10.

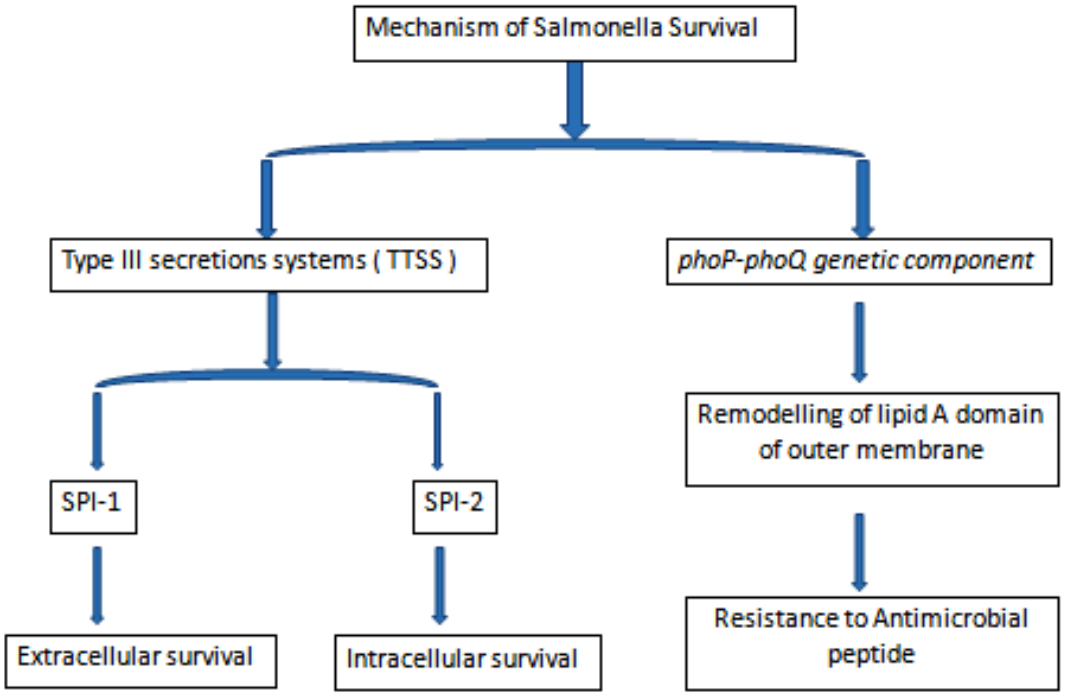

Fig. 1.1.1: Schematic diagram of mechanisms of intracellular survival of *Salmonella*

SPI-1: Salmonella Pathogenicity Island-1

SPI-2: Salmonella Pathogenicity Island-2

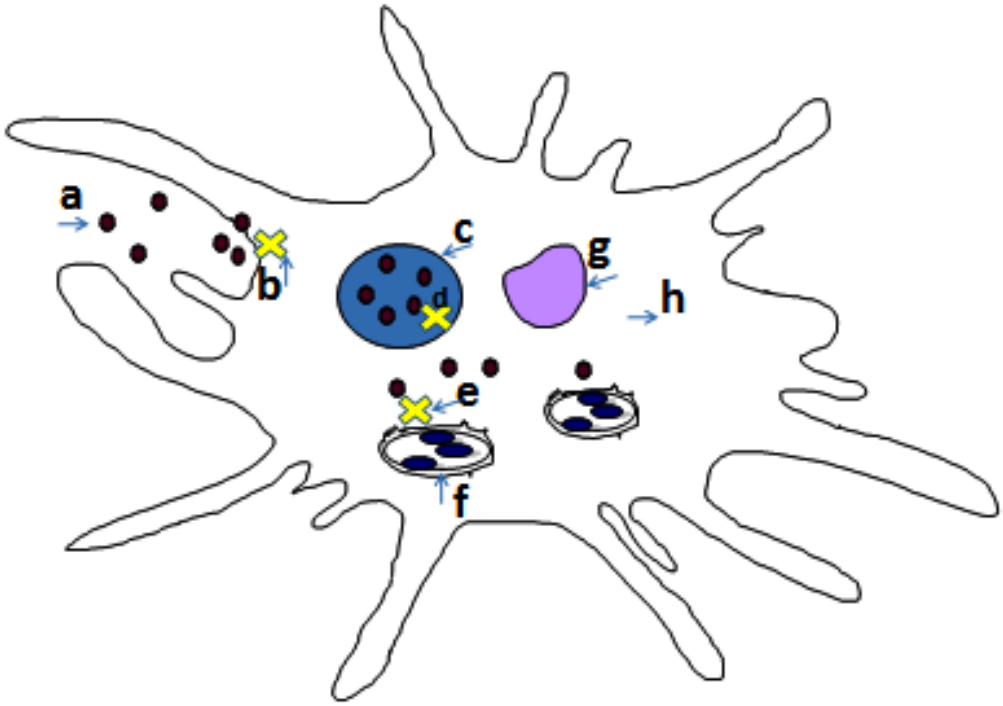

Fig. 1.1.2: Barriers to drug transport: a. Drug ; b. Cell membrane barrier ; c. Endosome ; d. Endosomal membrane barrier ; e. SCV membrane barrier ; f. SCV ; g. Nucleus ; h. Macrophages

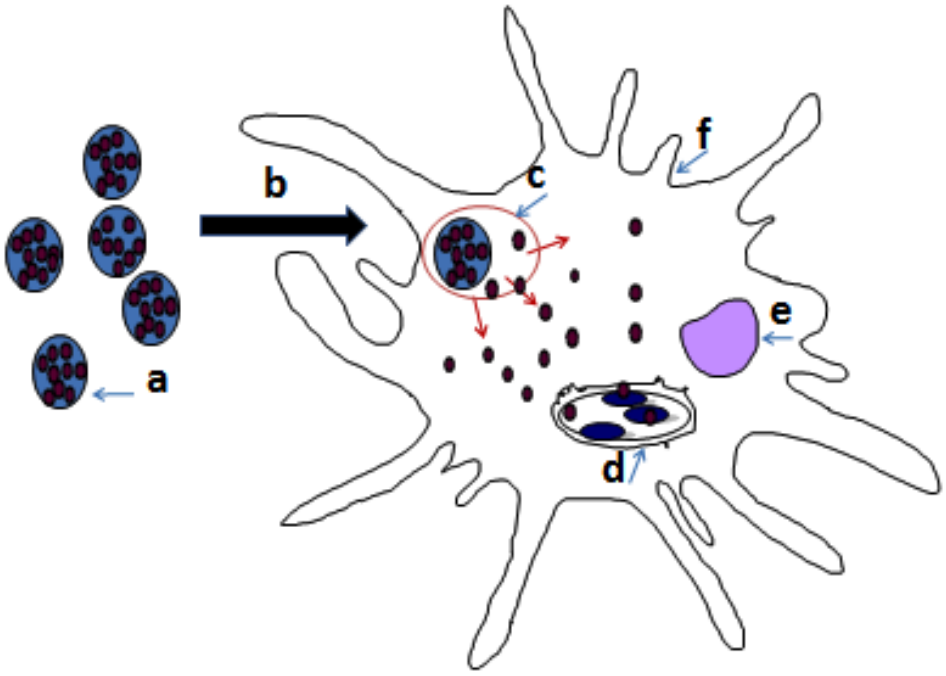

Fig.1.1.3: Nanoparticle based drug delivery system; **a**. Drug (Brown) encapsulated in nanocarrier; **b.** Phagocytosis of nano-drug carrier; **c.** Endosome; **d.** Drug inside SCV; **e.** Nucleus; **f**. macrophages

Chapter 2

Development of drug delivery approach for intracellular *Salmonella*

Chapter 2.1

Drug delivery using novel nanoplexes against a *Salmonella* mouse infection model

(Journal of nanoparticle Research, in press- May 2009)

Abstract:

A novel methodology for incorporating gentamicin into macromolecular complexes with anionic homo- and block copolymers via cooperative electrostatic interactions is described. Block copolymers of poly(ethylene oxide-*b*-sodium acrylate) (PEO-*b*-PAA^- ^+Na) or poly(ethylene oxide-*b*-sodium methacrylate) (PEO-*b*-PMA^- ^+Na) were blended with PAA^- Na^+ and complexed with the polycationic antibiotic gentamicin. Gentamicin nanoplexes made with PEO-*b*-PMA^- ^+Na/PAA^- ^+Na (PMPG) and analogous nanoplexes with PEO-*b*-PAA^- ^+Na/PAA^- ^+Na (PAPG) had mean intensity average diameters of 120 and 90 nm, zeta potentials of -17 and -11 mv, and incorporated 26 and 23% by weight of gentamicin, respectively. Gentamicin release rates at physiological pH from nanoplexes were relatively slow. PAPG and PMPG as drug delivery systems for treating murine salmonellosis at doses similar to the free gentamicin experiments resulted in reduced numbers of viable bacteria in the liver and spleen. Polymeric nanoplexes developed by this methodology can potentially improve targeting of intracellular pathogens.

Introduction:

Gentamicin is an antimicrobial in the aminoglycoside class that is used to treat bacterial infections caused primarily by Gram negative bacteria. Chronic intracellular infections caused by Gram negative bacteria such as *Brucella spp., Salmonella spp.* or *Mycobacterium spp*. are difficult to treat due to their ability to evade the mammalian host phagocytic killing mechanism and establish specialized intracellular niches sequestered from the host immune system (12, 20, 22). Polar polycationic antimicrobials like gentamicin sulfate cannot traverse the mammalian cell membrane efficiently after parenteral administration. Hence, the desired intracellular antimicrobial levels for complete clearance of bacteria residing in these specialized niches are

not achieved. This results in antimicrobial treatment failure, high incidence of relapse and associated organ toxicity with prolonged treatment (10). Thus, drugs like gentamicin sulfate which are highly active in-vitro are ineffective in-vivo due to extracellular localization in the mammalian host (6).

Drug encapsulation in liposomes and polymeric carriers has been reported to be an effective method to increase drug accumulation at the site of infection with reduced toxicity and side effects after parenteral or oral administration (2, 5, 7, 16) Despite initial success, however, the desired clinical outcomes have not yet been met (11, 14). The main pitfalls against achieving bacterial clearance include slow (or no) drug release inside the cells, and lack of a mechanism whereby the desired concentration of antimicrobial can be maintained in circulation without systemic toxicity. To control/eradicate intracellular infection, the therapeutic agents should avoid inactivation within phagolysosomal compartments, and ideally, should also deliver antimicrobials within the cells to the compartment where the intracellular pathogens replicate. Additionally, the capacity of a polymeric drug carrier should be engineered to incorporate high concentrations of gentamicin to achieve the required dosage, yet avoid side effects that may be associated with higher amounts of carriers.

In this chapter, we report a novel methodology for incorporating gentamicin into macromolecular complexes with anionic homo- and block copolymers via cooperative electrostatic interactions between cationic drugs and anionic polymers (Figure 1 [A-C]**).** Poly(sodium acrylate) ($PAA^{-}\ ^{+}Na$) has been utilized for oral, ophthalmic and associated biomedical applications (8). In this study, we designed and synthesized $PAA^{-}\ ^{+}Na$-based polyanions that form stable nanoplexes at physiological pH with gentamicin. Nuclear Magnetic Resonance spectroscopy (^{1}H NMR) and particle characterization showed stable electrostatic interactions with nanoplex formation. In addition, poly(ethylene oxide) (PEO) was added to the system as a component of a block copolymer due to its high water solubility and resistance to non-specific protein adsorption (15). Block copolymers of poly(ethylene oxide-*b*-sodium acrylate) (PEO-*b*-$PAA^{-}\ ^{+}Na$) were prepared utilizing a PEO macroinitiator to initiate a living free radical polymerization of t-butyl acrylate, then the t-butyl protecting groups were removed. These block copolymers were blended with $PAA^{-}\ ^{+}Na$ and the blends were complexed with the

polycationic antibiotic gentamicin. The resulting nanoplexes were investigated as drug delivery systems for treating intracellular *Salmonella.*

Materials and Methods:

All chemicals were purchased from Sigma-Aldrich unless otherwise noted. *t*-Butyl acrylate (tBA) was fractionally distilled under vacuum prior to polymerization. Tetrahydrofuran (THF) was dried over sodium containing benzophenone as an indicator and distilled immediately prior to use. Poly(ethylene oxide-*b*-methacrylic acid) (PEO-*b*-PMA) was purchased from Polymer Sources Inc. (Canada) and was converted to the sodium salt by titrating with 1N NaOH. 2-Mercaptoethanol (60 μL) was added to incomplete o-phthalaldehyde solution (12 mL) to prepare the reagent for gentamicin derivatization and subsequent detection. Other chemicals were used as received.

Synthesis of Anionic Polymers for Complexation with Gentamicin

Synthesis of α-methoxy-ω-bromoisobutyrate-PEO

In a 100-mL round-bottom flask, 6.0 g of α-methoxy-ω-hydroxy-PEO (3.0×10^{-3} mol, M_n 2000 g mol^{-1} by NMR) was dissolved in 50 mL of distilled THF. To this, 0.88 mL of triethylamine (6.2×10^{-3} mol) and then 0.75 mL of 2-bromoisobutyryl bromide (6.1×10^{-3} mol) was added dropwise at room temperature. After 24 h, the reaction mixture was filtered and concentrated. The polymer was isolated by precipitation into cold diethyl ether twice and dried under vacuum.

Synthesis of PEO-*b*-PtBA diblock copolymer by Atom Transfer Radical Polymerization (ATRP)

PEO-*b*-PtBA diblock copolymers were synthesized according to a previously reported procedure (Hou 2003). Briefly, 1.0 g of α-methoxy-ω-bromoisobutyrate-PEO (4.65×10^{-4} mol), 4.2 mL of *t*-butyl acrylate (2.9×10^{-2} mol), 210 μL of pentamethyldiethylenetriamine (PMDETA, 1×10^{-3} mol) and 8 mL dry toluene were added into a Schlenk flask. After degassing, 72 mg of cuprous bromide (CuBr, 5×10^{-4} mol) was added quickly under nitrogen. The reaction mixture was deoxygenated with 3 freeze-thaw cycles, and then polymerized at 80 ^{o}C for 8 h. After the polymerization, the catalyst was removed by filtering the reaction mixture through basic alumina

using dichloromethane as the eluent. The solvent was evaporated and the block copolymer was dried under vacuum at 50 ^{o}C overnight. Target = 10,000 M_n. Gel permeation chromatography (GPC) showed 10,200 M_n and NMR showed 9,200 M_n.

Synthesis of PEO-*b*-PAA sodium salt

PEO-*b*-PtBA diblock copolymer (1.0 g) was dissolved in 25 mL of dichloromethane. Trifluoroacetic acid (5 mL) was slowly added and the reaction mixture was stirred at room temperature overnight. The solvent was evaporated at 40 ^{o}C under vacuum and the residue was dissolved in deionized (DI) water with adjustment to a pH of 8 using 1N NaOH. The copolymer was recovered by freeze-drying. In the acid form, ^{1}H NMR showed the block molecular weights to be 2000 g mol^{-1} M_n PEO and 3600 g mol^{-1} M_n PAA.

Formation of Polymer-Antibiotic Nanoplexes

A schematic procedure for forming the gentamicin-polymer nanoplexes is provided in figure 1(C). In a 100-mL round-bottom flask, 25 mg of PAA^{-} $^{+}$Na (4.16 x 10^{-6} mol, 2.4 x 10^{-4} eq of anions) and 26 mg of PEO-*b*-PAA^{-} $^{+}$Na (10^{-6} mol, 1.3 x10^{-4} eq of anions) were dissolved in 50 mL of DI water to prepare a 1 mg mL^{-1} polymer solution. The solution was placed in a sonication bath and 5 mL of gentamicin sulfate solution (10 mg mL^{-1} gentamicin sulfate, equal to 30 mg gentamicin, 3.6 x 10^{-4} eq of cations) was added via syringe to form a turbid dispersion with sonication. Any non-complexed free gentamicin sulfate was removed by dialysis against 4 L of DI water at 4 ^{o}C for 24 h and the nanoplex was recovered by freeze-drying. Similar methodology was adopted to synthesize nanoplexes with a poly(ethylene oxide-*b*-sodium methacrylate) diblock copolymer (PEO-*b*-PMA^{-} $^{+}$Na). The gentamicin nanoplex made with the PEO-*b*-PMA^{-} $^{+}$Na/PAA^{-} $^{+}$Na blend is named PMPG and the analogous nanoplex with the PEO-*b*-PAA^{-} $^{+}$Na/PAA^{-} $^{+}$Na blend is named PAPG in this study.

Characterization of nanoplexes

The solute sizes, polydispersity and zeta potentials of the PAPG and PAMG nanoplexes were characterized by dynamic light scattering with a Zetasizer 1000 HS with laser diffractometry (Malvern Instruments, Malvern, UK). Each nanoplex (1 mg) was dispersed in one

mL of water and analyzed. Measurements were done in triplicate for each batch of particles. The results were taken as the average of three measurements.

Gentamicin concentration in the nanoplexes

The amount of gentamicin loaded into the nanoplexes was determined via an *o*-phthalaldehyde assay (Lecaroz *et al.* 2006b). Initially, standard concentrations of gentamicin sulfate were prepared by serial dilution with borate buffer (0.4M, pH 9.7) at concentrations of 250, 125, 62.5, 31.3, 15.7 and 7.8 μg mL^{-1}. Then, 0.5 mL of *o*-phthalaldehyde solution and 0.2 mL of isopropanol were added to 0.5 mL of each of the gentamicin solutions. The volume was adjusted to 3 mL by adding borate buffer and the mixtures were reacted for 1 h. The amount of free gentamicin was evaluated by measuring the absorptions at 340 nm (UV-Visible Spectrophotometer, Shimadzu Scientific instruments, USA) to construct a standard UV absorption curve relative to gentamicin concentration. The concentrations of gentamicin in the nanoplexes were measured by first dispersing the nanoplexes in the borate buffer (1 mg mL^{-1}). The basic pH causes the electrostatically-bound nanoplexes to dissociate to free gentamicin. Each nanoplex dispersion (0.5 mL) was mixed with 0.5 mL of *o*-phthalaldehyde solution and 0.2 mL of isopropanol, and the volume was adjusted to 3 mL with the borate buffer and reacted for 1 h. The absorbance of each solution was measured at 340 nm and the concentrations of gentamicin that were in each nanoplex were determined by comparison to the standard curve.

Characterization of drug release

Free gentamicin sulfate (16.6 mg containing 10 mg gentamicin) or 40 mg of a nanoplex containing 10 mg gentamicin was dissolved in 10 mL of DI Millipore water. The solution was transferred to a dialysis bag (MW cutoff 3500 g mol^{-1}) and dialyzed against 300 mL of PBS (pH 7.4) at 37 ^{o}C. At prescribed times, 0.3 mL aliquots were taken from the receptor medium and stored at 4 ^{o}C. To quantify the amount of released gentamicin, the aliquot was mixed with 0.5 mL of the *o*-phthalaldehyde reagent and 0.2 mL isopropanol. The volume was adjusted to 3 mL with 0.4M borate buffer, pH 9.7. The mixture was reacted at room temperature for 1 h and the absorbance at 340 nm was measured. The percentage of the drug that was released relative to the total amount of gentamicin in the nanoplex was calculated from the absorbance of the aliquot divided by the absorbance corresponding to complete diffusion of the free gentamicin through

the dialysis membrane (eq. 1). The release profile of free gentamicin (the control) was compared with the nanoplex at the respective time points using the standardized curve.

% gentamicin release = (Abs due to release from the nanoplex/Abs of all of the free gentamicin) x 100

eq. 1

***In- vivo* efficacy of nanoplexes against *Salmonella* Typhimurium.**

Salmonella enterica Typhimurium χ4665, a reference strain (23) responsible for chronic infection in mice was provided by Roy Curtiss III, Department of Biology, Washington University, St. Louis, MO. *S.* enterica Typhimurium χ4665 was grown overnight in Luria-Bertani (LB) broth, centrifuged, washed in PBS and serially diluted to achieve a final suspension containing 5,000 colony forming units (CFU) per mL. Twenty female AJ 646 mice (5 to 6 months old) were injected intraperitoneally (I.P.) with 100 µL of inocula containing 500 CFUs per mouse. Subsequently, the mice were observed for development of clinical symptoms of Salmonellosis. After day five of infection, five AJ 646 mice/group were treated with either free gentamicin sulphate (in PBS) or the PAPG or PMPG nanoplexes I.P. at a dosage of 5µg g^{-1} of body weight. The dosage was repeated again 48 h post administration of the first dose, I.P. At day 3 (post second I.P. injection), the mice were euthanized, spleens and livers were removed aseptically, and organs were crushed and homogenized for 1-2 min in the presence of 2 mL of LB broth. Aliquots (500 µL) of the organ suspensions were serially diluted in 4.5 mL of LB broth to a maximum of 10^5-fold dilution. Subsequently, the dilutions were plated on tryptic soy agar plates, incubated overnight at 37 °C, and the resulting grey mucoid, discrete colonies were counted for plates containing between 30 and 300 colonies. The colonies were initially screened using *Salmonella* polyvalent anti 'O' antibodies in a slide agglutination test. Any colony that agglutinated within 30-45 s at room temperature was considered a *Salmonella* species. Later, the strain was confirmed with biochemical fingerprinting using API20E strips.

Results:

Block copolymer synthesis

PEO-*b*-PtBA was successfully synthesized via ATRP. The narrow molecular weight distribution and the control over molecular weight of the PtBA block signify the living nature of this ATRP polymerization. The PtBA units were deprotected and the resultant carboxylic acids were neutralized with base to form PEO-*b*-PAA^{-} $^{+}$Na. ^{1}H NMR (Figure 2) confirmed the expected copolymer structure. The molecular weights of the blocks in the copolymer derived from ^{1}H NMR were 2,000 g mol^{-1} PEO and 3,600 g mol^{-1} PAA.

Properties of the nanoplexes

DLS showed that the PAPG and PMPG nanoplexes had mean intensity average diameters of 90 and 120 nm, respectively (Table 1). Also, the polydispersity indexes of PAPG and PMPG were 0.118 and 0.112 indicating the narrow size distribution of these nanoplexes (Table 1). Both the PAPG and PMPG nanoplexes had small negative zeta potentials, -11 and -17 mV respectively, suggesting that the PEO in the copolymer was effectively screening the charges in the core from the physiological environment. The gentamicin loading in the nanoplexes based on the *o*-phthalaldehyde assay was 23 (PAPG) and 26% (PMPG) by weight.

Drug release from the nanoplexes

Release of gentamicin from the nanoplexes at the physiological pH was relatively slow (Figure 2.1.3). A burst release occurred during the first five hours comprising approximately 15-20% of the total amount of drug, and 25-30% had been released at 24 hours. In addition, the release profiles from both nanoplexes were similar, signifying that the more hydrophobic nature of the PMPG did not appreciably inhibit the rate.

***In vivo* antibacterial efficacy of free gentamicin sulfate relative to the nanoplexes**

The antibacterial activities of free gentamicin and the nanoplexes were compared in a *S.* Typhimurium infection model in AJ 646 mice. In our first set of *in-vivo* experiments, PAPG and PMPG were tested to evaluate effects of the molecular and nanoplex parameters on *in-vivo* bacterial clearance. Free gentamicin, administered at 5 μg g^{-1} body weight I.P. in AJ 646 mice infected with 500 CFUs of *S.* Typhimurium, yielded comparable numbers of viable bacteria recovered from the livers and spleens to those recovered from controls (Table 2.1.1). Nanoplexes administered at doses similar to the free gentamicin experiments resulted in reduced

numbers of viable bacteria in the liver and spleen by approximately one log compared to the number reduced by free gentamicin (Table 2.1.1). Similar efficacies were observed with PMPG and PAPG nanoplexes at the same dose, though the reduction in viable numbers of bacteria were slightly better for the mice treated with PMPG. At 5 μg g^{-1}, the numbers of viable bacteria remaining in the livers and spleens of infected AJ 646 mice treated with PMPG were 0.72 and 0.55 log lower than those of the control (untreated) or AJ 646 mice treated with similar doses of free gentamicin respectively. Similarly, PAPG resulted in 0.37 and 0.17 log lower numbers of viable bacteria than those of the control (untreated). Statistical analyses conducted after two dosages post I.P. administration showed significant differences in the bacterial counts in the livers of the mice treated with PMPG compared to those treated with free gentamicin ($P < 0.05$, Kruskal Wallis non parametric test).

Discussion:

Eradication of intracellular bacterial pathogens by conventional therapeutic regimens is challenging because of the inability of antimicrobials to traverse cell membranes. Clinical utility can also be reduced by limitations in dosage administration caused by drugs such as ciprofloxacin having poor solubilities at the physiological pH (4). Similarly, aminoglycosides and in particular gentamicin, in spite of being highly efficacious *in-vitro*, shows variable effects *in-vivo* (9, 16, 21). Extended treatments with these drugs can also lead to nephrotoxicity and ototoxicity. Thus, to prevent treatment failures and relapse, nanotechnology-based approaches are being explored wherein nanoparticles are fabricated to favor their ionic (physical) crosslinking to a variety of antimicrobials. Though such approaches have resulted in improved drug efficacy, previous nanoparticle drug delivery systems (DDS) based primarily on liposomes or polymers have shown poor *in-vivo* stability and drug loading efficiency (9, 21). This is in contrast to *in-vitro* experiments where the results have been far better. Thus, in order to realize effective delivery, the nanoparticle DDS should have controlled physico-chemical properties in terms of size, zeta potential and pH sensitivity (24). Herein, we report preliminary results for a novel method of drug incorporation into nanoparticles through cooperative electrostatic attractions.

One goal has been to create nanoplexes with high concentrations of gentamicin. Nanoplexes formed between gentamicin and $PAA^{-}\,^{+}Na$ with a cation to anion ratio of 1:1 were

insoluble in aqueous media, and formed agglomerates that sedimented out of solution. Since the cation to anion ratio was equalized, there were no net charges available for producing electrostatic repulsive forces between particles to avoid agglomeration. In the work reported herein, PEO-*b*-PAA^{-} $^{+}$Na and PEO-*b*-PMA^{-} $^{+}$Na block copolymers were included in the nanoplexes. Thus, the polyelectrolyte blocks complexed with the polycationic antibiotic and the non-ionic, water-soluble PEO blocks were free to protrude into the aqueous medium to afford steric repulsion between particles and prevent agglomeration (Fig. 2.1.1C). This is consistent with previous findings where the PEO blocks aided in forming uniform particles in aqueous dispersions (1, 26). Thus, even with equal anion to cation ratios, stable dispersions were obtained by employing the block copolymers blended with the PAA^{-} $^{+}$Na homopolymer. Moreover, it was discovered that the nanoplexes obtained by this novel technique can incorporate up to ~25% by weight of gentamicin (Table 1). The remarkable loading was a result of strong interactions between the cationic gentamicin and the anionic polymer. This high loading is 20-25 folds higher than the values reported by Lecaroz *et al.*, where gentamicin was loaded into hydrophobic microspheres or nanospheres. This is of great potential benefit in parenteral administration of drugs where dosage is a limiting factor in efficacy (17).

It is critically important that the solute sizes and charge characteristics of the nanoplexes be controlled to optimize their efficacy. For example, it is postulated that as the surface of a particle becomes more positive, it's recognition by macrophages should be enhanced (3). In addition, a drug delivery vehicle engineered to deliver a therapeutic molecule inside a macrophage cell should be within the appropriate size limits to be recognized by the cell. Recognition of the particle by the macrophages may be delayed if the diameter is smaller than ~85 nm (19). The sizes of the PAPG and PMPG nanoplexes were 90 nm and 120 nm respectively in diameter. The relative concentrations of block copolymers and homopolymers used in our experiments were 50% by weight and the "as-synthesized" anion to cation ratio was maintained at 1:1. It should be noted, however, that the nanoplexes were dialyzed to remove any free gentamicin sulfate that may not have been incorporated, and that this may have modified the anion to cation ratio to be slightly net anionic. This is likely since the PAPG and PMPG nanoplexes had small but negative zeta potentials of -11 and -17 mV, respectively (Table 1).

The low charge characteristics of these nanoplexes likely reflect the fact that the non-ionic PEO component of the block copolymer shields the inner ionic core from the external environment.

The drug release profiles of free gentamicin and the nanoplexes were distinctly different at pH 7.4. About 25-30% of the total gentamicin was released from the nanoplexes over 24 hours in PBS at pH 7.4 (Figure 3). This indicates that the nanoplexes remain intact under physiological conditions (pH 7.4) for long times, and this may be helpful for enhancing phagocytosis by the reticulendothelial system (RES) and reducing nephrotoxicity associated with the use of free aminoglycosides (18). We believe that the relatively slow release rates from the nanoplexes are due to the cooperativity of multiple charge associations between the multifunctional homo- and copolymers and the drug. The nanoplexes initially had equal ratios of anionic and cationic charges. As the gentamicin begins to leave the complex, the net anionic character of the complexes increases. As this occurs, greater electrostatic attraction between the polymer and gentamicin may slow the release. Therefore, we hypothesize that the nanoplexes may act as depot systems, releasing gentamicin slowly and continuously in the target organ of infection, viz. liver and spleen. Longer-term release experiments will undoubtedly shed more light on these aspects.

The *in-vivo* antibacterial activity of the nanoplexes achieved comparatively better reductions in the numbers of *S.* Typhimurium organisms residing in the spleen and liver (Table 2.1.1) than the controls under our experimental protocol. Since a strain that causes chronic Salmonellosis was utilized in these experiments, the reductions in numbers of viable bacteria are highly encouraging. PMPG treated groups of mice showed significant reduction in viable numbers of bacteria in the livers compared to the free gentamicin group. The reduction, however, was not statistically significant between the PAPG and free gentamicin groups of mice. Variable CFUs with low numbers of mice per group lead to relatively high standard deviations, which compromised the statistical significance in these cases. Several research groups have investigated biodegradable aliphatic polyesters such as poly(lactide)s and poly(lactide-*co*-glycolide)s or liposomes as carriers for gentamicin in efforts to provide sustained release with improved treatment efficacies (Lecaroz *et al.* 2007; Cordeiro *et al*. 2000). In an *in-vivo* chronic *Brucella* model, poly(lactide) microspheres reportedly reduced the number of viable organisms by 0.41 log to 0.72 log in the spleen. Similarly, pH sensitive liposomes in an *in-vivo Salmonella enterica*

Typhimurium model were shown to significantly reduce the number of viable bacteria in the spleen by 10^3 CFUs. Unfortunately, only low concentrations of about 1-4 wt% of the polar cationic gentamicin sulfate salt could be incorporated into these otherwise-desirable carriers, and this is attributed to the inherent incompatibility of the very polar drug with the relatively hydrophobic drug carriers. Similar results are reported in *in-vitro* Salmonella models wherein greater than 75% reduction in vacuole resistant *S.* Typhimurium was observed with pH dependent liposomes encapsulating gentamicin (Lutwyche *et al.* 1998).

The PEO component and concentration in the nanoplexes may hinder uptake by the macrophages. For example, uptake of PEGylated liposomes has been reported to be reduced by 50% because of an inability of macrophages to recognize and phagocytose them (25). PEO is used frequently in cancer chemotherapy to promote evasion of the drug delivery system by the RES and increase circulation time in the blood stream (13). Thus, for targeted drug delivery to the infected liver and spleen, it is of paramount importance that PEO be sufficiently regulated to achieve recognition by the RES.

To our knowledge, this is the first report of gentamicin nanoplexes containing very high loadings of aminoglycoside antibiotics. Future studies will address the effects of molecular parameters on size and charge and correlate these aspects with uptake into macrophages, longer-term release, and therapeutic efficacy *in-vivo*.

Acknowledgements

The authors are grateful to NSF DMR-0312046 and to Virginia Tech's Institute for Critical Technologies and Applied Sciences (ICTAS) for funding.

References

1. **Azamian, B. R., K. S. Coleman, J. J. Davis, N. Hanson, and M. L. Green.** 2002. Directly observed covalent coupling of quantum dots to single-wall carbon nanotubes. Chem Commun (Camb)**:**366-7.

2. **Cordeiro, C., D. J. Wiseman, P. Lutwyche, M. Uh, J. C. Evans, B. B. Finlay, and M. S. Webb.** 2000. Antibacterial efficacy of gentamicin encapsulated in pH-sensitive liposomes against an in vivo Salmonella enterica serovar typhimurium intracellular infection model. Antimicrob Agents Chemother **44:**533-9.

3. **Davaran, S., M. R. Rashidi, B. Pourabbas, M. Dadashzadeh, and N. M. Haghshenas.** 2006. Adriamycin release from poly(lactide-coglycolide)-polyethylene glycol nanoparticles: synthesis, and in vitro characterization. Int J Nanomedicine **1:**535-9.

4. **Ellbogen, M. H., K. M. Olsen, M. J. Gentry-Nielsen, and L. C. Preheim.** 2003. Efficacy of liposome-encapsulated ciprofloxacin compared with ciprofloxacin and ceftriaxone in a rat model of pneumococcal pneumonia. J Antimicrob Chemother **51:**83-91.

5. **Galdiero, F., C. R. Carratelli, I. Nuzzo, C. Bentivoglio, L. De Martino, A. Folgore, and M. Galdiero.** 1995. Enhanced cellular response in mice treated with a Brucella antigen-liposome mixture. FEMS Immunol Med Microbiol **10:**235-43.

6. **Gamazo, C., M. C. Lecaroz, S. Prior, A. I. Vitas, M. A. Campanero, J. M. Irache, and M. J. Blanco-Prieto.** 2006. Chemical and biological factors in the control of Brucella and brucellosis. Curr Drug Deliv **3:**359-65.

7. **Gaspar, M. M., A. Cruz, A. F. Penha, J. Reymao, A. C. Sousa, C. V. Eleuterio, S. A. Domingues, A. G. Fraga, A. L. Filho, M. E. Cruz, and J. Pedrosa.** 2008. Rifabutin encapsulated in liposomes exhibits increased therapeutic activity in a model of disseminated tuberculosis. Int J Antimicrob Agents **31:**37-45.

8. **Gupta, K., M. Ganguli, S. Pasha, and S. Maiti.** 2006. Nanoparticle formation from poly(acrylic acid) and oppositely charged peptides. Biophys Chem **119:**303-6.

9. **Lecaroz, C., M. J. Blanco-Prieto, M. A. Burrell, and C. Gamazo.** 2006. Intracellular killing of Brucella melitensis in human macrophages with microsphere-encapsulated gentamicin. J Antimicrob Chemother **58:**549-56.

10. **Lecaroz, C., C. Gamazo, and M. J. Blanco-Prieto.** 2006. Nanocarriers with gentamicin to treat intracellular pathogens. J Nanosci Nanotechnol **6:**3296-302.

11. **Lecaroz, M. C., M. J. Blanco-Prieto, M. A. Campanero, H. Salman, and C. Gamazo.** 2007. Poly(D,L-lactide-coglycolide) particles containing gentamicin: pharmacokinetics and pharmacodynamics in Brucella melitensis-infected mice. Antimicrob Agents Chemother **51:**1185-90.

12. **Monack, D. M., D. M. Bouley, and S. Falkow.** 2004. Salmonella typhimurium persists within macrophages in the mesenteric lymph nodes of chronically infected Nramp1+/+ mice and can be reactivated by IFNgamma neutralization. J Exp Med **199:**231-41.

13. **Oskay-Oezcelik, G., D. Koensgen, H. J. Hindenburg, P. Klare, B. Schmalfeldt, W. Lichtenegger, R. Chekerov, S. E. Al-Batran, U. Neumann, and J. Sehouli.** 2008. Biweekly pegylated liposomal doxorubicin as second-line treatment in patients with relapsed ovarian cancer after failure of platinum and paclitaxel: results from a multi-center phase II study of the NOGGO. Anticancer Res **28:**1329-34.

14. **Page-Clisson, M. E., H. Pinto-Alphandary, E. Chachaty, P. Couvreur, and A. Andremont.** 1998. Drug targeting by polyalkylcyanoacrylate nanoparticles is not efficient against persistent Salmonella. Pharm Res **15:**544-9.

15. **Pan, J., M. Zhao, Y. Liu, B. Wang, L. Mi, and L. Yang.** 2008. Development of a new poly(ethylene glycol)-graft-poly(D,L-lactic acid) as potential drug carriers. J Biomed Mater Res A.

16. **Pandey, R., and G. K. Khuller.** 2007. Nanoparticle-based oral drug delivery system for an injectable antibiotic - streptomycin. Evaluation in a murine tuberculosis model. Chemotherapy **53:**437-41.

17. **Prior, S., B. Gander, J. M. Irache, and C. Gamazo.** 2005. Gentamicin-loaded microspheres for treatment of experimental Brucella abortus infection in mice. J Antimicrob Chemother **55:**1032-6.

18. **Ristuccia, A. M., and B. A. Cunha.** 1982. The aminoglycosides. Med Clin North Am **66:**303-12.

19. **Rudt S, M. R.** 1993. In vitro phagocytosis assay of nano- and microparticles by chemiluminescence. III. Uptake of differently sized surface-modified particles, and its correlation to particle properties and in vivo distribution. European journal of pharmaceutical sciences **1:31-39.**

20. **Seleem, M. N., S. M. Boyle, and N. Sriranganathan.** 2008. Brucella: a pathogen without classic virulence genes. Vet Microbiol **129:**1-14.

21. **Smyth Templeton, N.** 2003. Cationic liposomes as in vivo delivery vehicles. Curr Med Chem **10:**1279-87.

22. **Steinberg, B. E., and S. Grinstein.** 2008. Pathogen destruction versus intracellular survival: the role of lipids as phagosomal fate determinants. J Clin Invest **118:**2002-11.

23. **Sukupolvi, S., A. Edelstein, M. Rhen, S. J. Normark, and J. D. Pfeifer.** 1997. Development of a murine model of chronic Salmonella infection. Infect Immun **65:**838-42.

24. **Vonarbourg, A., C. Passirani, P. Saulnier, and J. P. Benoit.** 2006. Parameters influencing the stealthiness of colloidal drug delivery systems. Biomaterials **27:**4356-73.

25. **Yang, T., F. D. Cui, M. K. Choi, J. W. Cho, S. J. Chung, C. K. Shim, and D. D. Kim.** 2007. Enhanced solubility and stability of PEGylated liposomal paclitaxel: in vitro and in vivo evaluation. Int J Pharm **338:**317-26.

26. **Yang, T., F. D. Cui, M. K. Choi, H. Lin, S. J. Chung, C. K. Shim, and D. D. Kim.** 2007. Liposome formulation of paclitaxel with enhanced solubility and stability. Drug Deliv **14:**301-8.

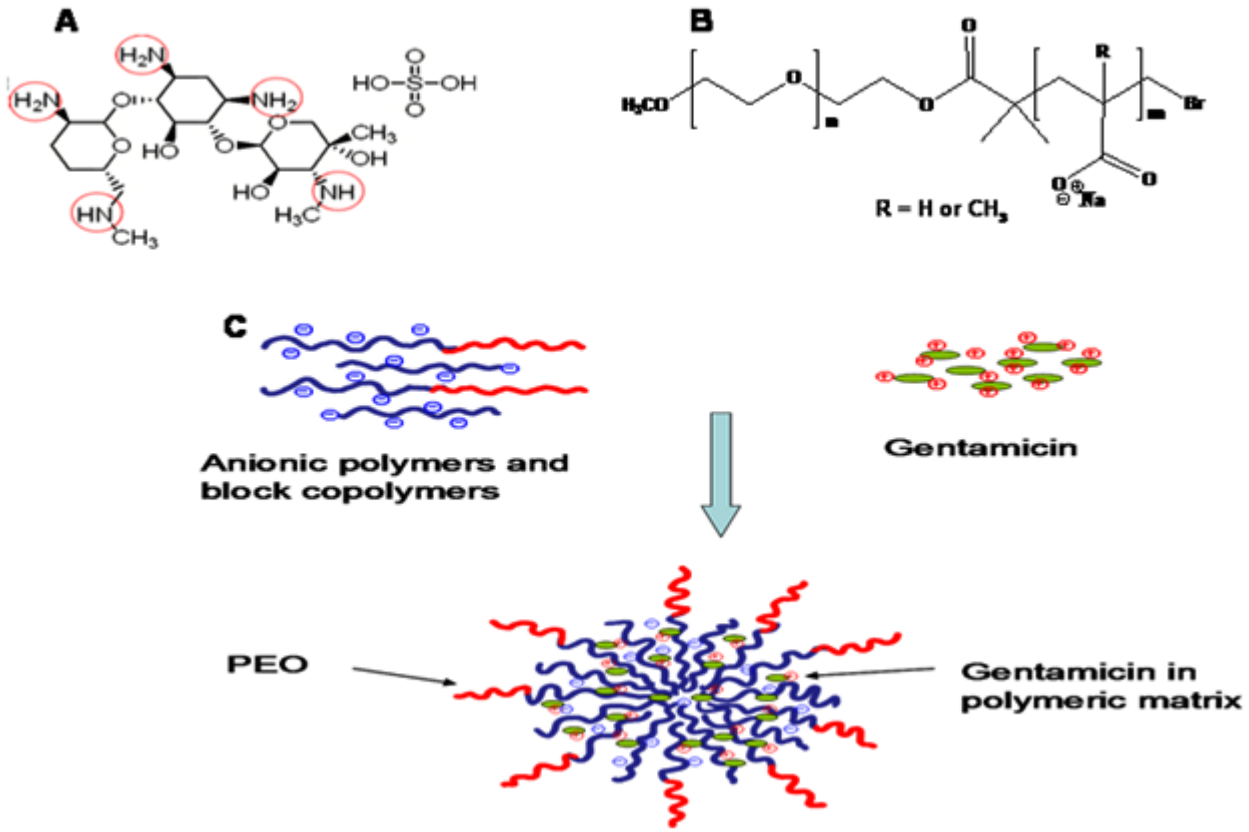

Fig. 2.1.1: Gentamicin incorporation in polymeric carrier (A-C): 1A. Gentamicin are polycationic aminoglycosides with five amino groups; 1B. Anionic block copolymers for electrostatic complexation to gentamicin, 1C. Strategy to incorporate gentamicin into the cores of the polymeric carrier

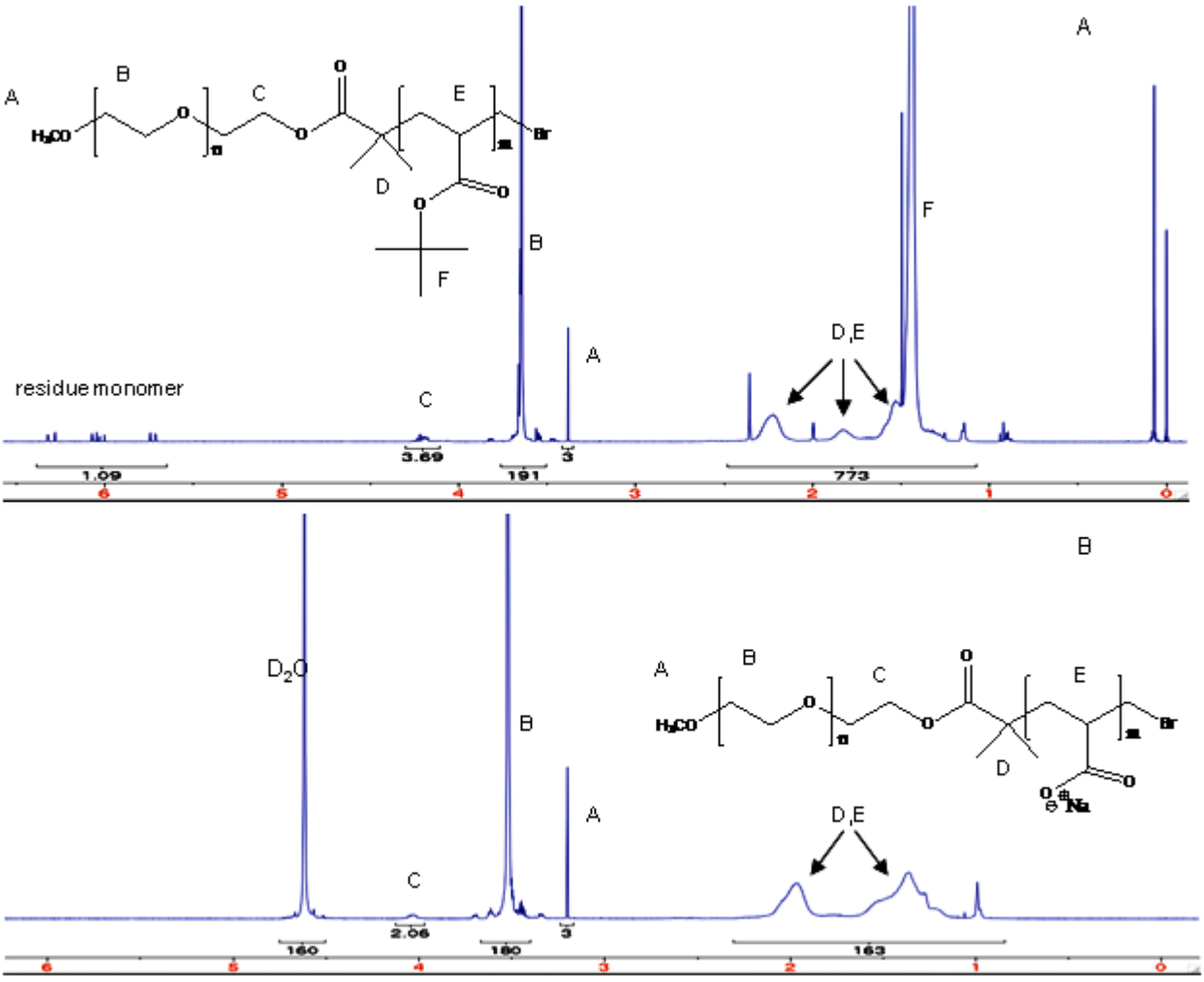

Fig. 2.1.2: ^{1}H NMR of A) PEO-b-PtBA and B) PEO-b-PAA show complete removal of t-butyl groups

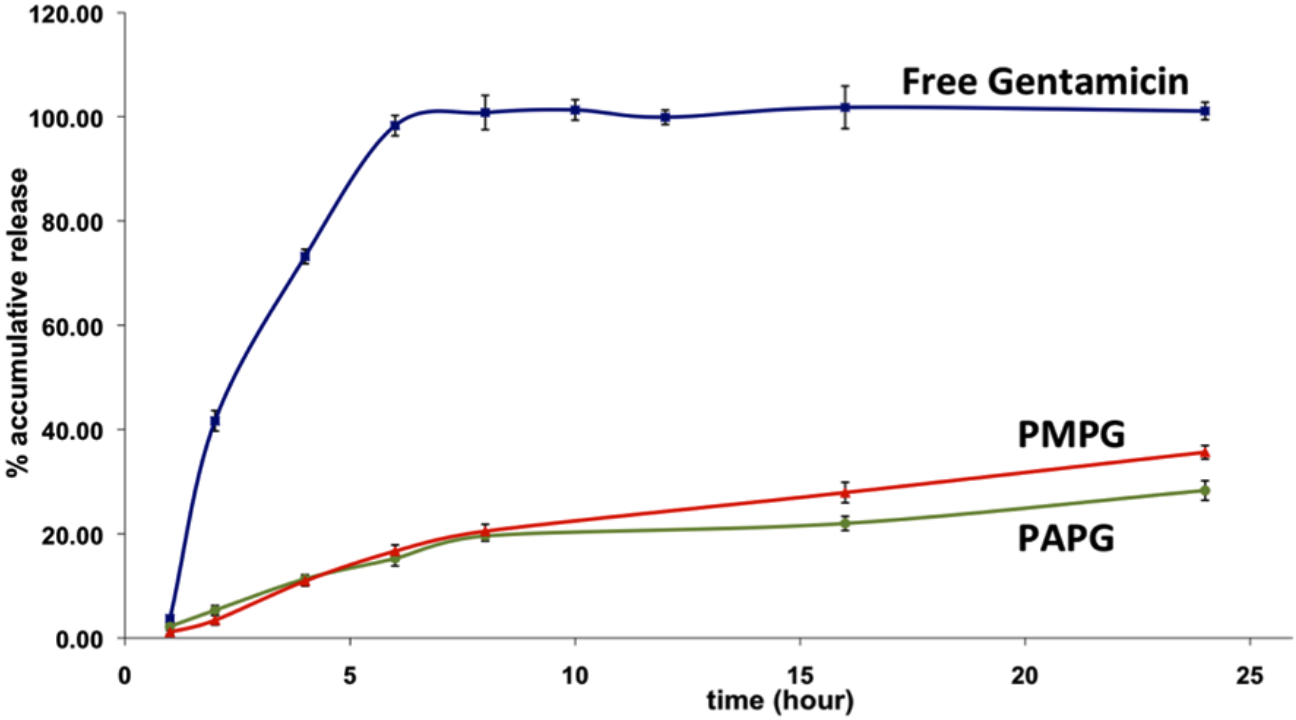

Fig. 2.1.3: Drug Releasing profile of PAPG, PMPG and Free gentamicin at pH 7.4 and 37 °C; all the values represent mean of three measurements and are shown with SD bars

Table 2.1.1: Size and gentamicin content of the PAPG and PMPG nanoplex

Nanoplex	**Hydrodynamic diameter (nm)**	**Zeta Potential (mV)**	**Gentamicin content (mg mg^{-1} complex)***
PAA-gentamicin	Particles agglomerate	n/a	n/a
PMPG	120 (0.112)[a]	-17	0.26
PAPG	90 (0.118)[a]	-11	0.23

* Drug loading content post dialysis

[a]Polydispersity index of nanoplexes

Table 2.1 2: Efficacy of free gentamicin and the nanoplexes against intracellular Salmonella infection

Treatment	**Liver cfu (log) (CI)**	**Liver cfu (log) reduction**	**Spleen cfu (log) (CI)**	**Spleen cfu (log) reduction**
Control	5.85 (5.05, 6.64)	0.00 [ab]	5.86 (4.99, 6.73)	0.00 [a]
Free gentamicin	6.00 (5.19, 6.79)	+0.14 [a]	5.56 (4.70, 6.43)	0.30 [a]
PAPG	5.48 (4.68, 6.27)	0.37 [ab]	5.71 (4.84, 6.57)	0.17 [a]
PMPG	5.13 (4.33, 5.92)	0.72 [b]	5.31 (4.44, 6.18)	0.55 [a]

* a and b superscripts indicate significant difference at $P<0.05$

Chapter 2

Development of drug delivery approach for intracellular *Salmonella*

Chapter 2.2

In-vitro trafficking and efficacy of core-shell nanostructures for treating intracellular *Salmonella*

(Antimicrobial Agents and Chemotherapy, Vol. 53, No. 9, p. 3985-3988, September 2009)

Abstract

The research objectives of this work are to develop core-shell nanostructures containing antimicrobials for improving their transport into cells, understand pathway(s) of uptake, and determine their therapeutic efficacies in *Salmonella* infected J774A.1 macrophage cells *in-vitro*. Block copolymer nanostructures encapsulating gentamicin via cooperative electrostatic interactions, and having predominantly either amphiphilic (N1) or hydrophilic (N2) surfaces were designed. The rate of cellular uptake and sub-cellular localization were studied by flow cytometry and confocal microscopy. The influence of chemistry of the nanostructures in clearing intracellular *Salmonell*a infections was determined. Flow cytometry demonstrated a higher rate of uptake for nanostructures having amphiphilic surfaces (N1) in comparison to those having hydrophilic surfaces (N2), and the data was consistent with confocal microscopy observations. The majority of N1 were localized in the cytoplasm of macrophage cells, whereas N2 localized with the endosomes/lysosomes. Intracellular green fluorescent protein-expressing *Salmonella* did not appear to colocalize with rhodamine-labeled N1 or N2 after 2 h of incubation. However, significant *in-vitro* reductions in bacterial counts were observed after incubation with the N1 structures, but not with N2. Gentamicin encapsulation in N1 nanostructures having amphiphilic surfaces enhances the rate and modulates the route of uptake into macrophages, thus promoting significant reduction in the intracellular *Salmonella*. Thus, the hydrophilic/hydrophobic nature of the surfaces of aminoglycoside drug delivery vehicles affects both the intracellular localization and therapeutic efficacy *in-vitro*.

Introduction

Aminoglycosides comprise a group of antibiotics that exhibit antimicrobial activities against Gram-positive and Gram-negative bacteria (i.e., *Salmonella* spp.), mycobacteria and protozoa. In the last few decades, emergence of drug resistant bacterial strains of *Mycobacteriun* spp. and *Salmonella* spp. have increasingly become a source of global health concern, thereby creating new challenges in finding effective therapeutic strategies [1]. Many of the intracellular bacteria that cause chronic infections develop drug resistance. These bacteria can evade the phagocytic killing mechanism of mammalian host cells by establishing specialized intracellular niches sequestered from the immune system [2]. The antimicrobial activities of aminoglycosides such as streptomycin, gentamicin, tobramycin and amikacin are concentration dependent [3]. In spite of their efficacy against bacterial and protozoal pathogens *in-vitro*, clinical uses of aminoglycosides are limited by their inabilities to transport through cell membranes, and reduced intracellular drug accumulation leading to poor bacterial clearance. In addition, repeated administration of aminoglycosides can lead to drug-induced ototoxicity and nephrotoxicity [4,5].

The intracellular localization of bacteria, mainly in macrophages, requires novel therapeutic strategies. In this regard, liposomal and polymeric nanocarriers have been investigated to control intracellular infections [6,7]. Encapsulating drugs within nanoparticles has the potential to reduce toxicity by providing slow, sustained release, and to enhance delivery to the intracellular compartments where the bacteria reside. Drugs encapsulated in nanoparticle carriers are recognized as foreign materials and are taken up by cells of the reticulo-endothelial system (RES). The nanoparticles are thus taken up by blood monocytes and macrophages of the liver, spleen and bone marrow [8]. This behavior can potentially be exploited for delivering drugs to infected phagocytic cells of the RES. To improve the transport of antimicrobials into macrophages, it is important that the mechanism(s) of uptake and fate(s) of nanoparticle drug carriers inside the cells be understood.

Pluronic™ triblock copolymers comprised of poly(ethylene oxide) (PEO) terminal blocks with a poly(propylene oxide) (PPO) central block (i.e., PEO-*b*-PPO-*b*-PEO) are currently being evaluated for chemotherapy of multidrug resistant tumors [9]. The PPO segments are more hydrophobic than the water-soluble PEO blocks, and this results in increased incorporation into cells. In this study, we designed and synthesized core-shell nanostructures with PEO-*b*-PPO-*b*-

PEO shells, and cores containing gentamicin complexed with polyacrylate anions. The weakly lipophilic nature of the shells increases interactions with macrophages relative to analogous nanostructures with only PEO shells, while the anionic cores bind the cationic aminoglycoside well. These nanostructured drug carrier systems carrying gentamicin disperse in aqueous media at physiological pH. The gentamicin-polymer nanostructures were investigated *in-vitro* as drug delivery systems for treating intracellular *Salmonella.*

Materials and Methods

Materials

All chemicals were purchased from Sigma-Aldrich unless otherwise noted. 5-(and 6-)-Carboxyfluorescein succinimidyl ester (fluorescein-NHS) and 5-(and 6-)carboxytetramethyl rhodamine succinimidyl ester (rhodamine-NHS) were purchased from Thermo Scientific (IL, USA). Pluronic F68™ (PEO-*b*-PPO-*b*-PEO) was kindly provided by BASF. The composition was established by NMR as 19 wt% PPO and 81 wt% PEO. Monomethoxy PEO (Aldrich) and Pluronic F68™ were dried under vacuum at 70 °C before copolymerization. Poly(sodium acrylate) ($PAA^-\ ^+Na$) with a molecular weight of 6000 was purchased from Polysciences Inc. Gentamicin sulfate was obtained from Sigma-Aldrich with ~60 wt% of gentamicin. Other solvents and chemicals were analytical grade and used as received.

Preparation of core-shell nanostructures loaded with gentamicin

Block copolymers of poly(sodium acrylate)-(PEO-*b*-PPO-*b*-PEO)-poly(sodium acrylate) ($PAA^-\ ^+Na$-(PEO-*b*-PPO-*b*-PEO)-$PAA^-\ ^+Na$) and PEO-$PAA^-\ ^+Na$ were prepared according to a previously published procedure [10]. Briefly, PEO-*b*-PPO-*b*-PEO (Pluronic F68™) with hydroxyl terminal groups was derivatized with 2-bromoisobutyryl bromide to provide bromoalkyl functional end groups, and then t-butyl acrylate was polymerized by controlled free radical polymerization (ATRP). The protective t-butyl groups were subsequently removed with trifluoroacetic acid and the polymer was neutralized with NaOH to form the sodium salt ($PAA^-\ ^+Na$-(PEO-*b*-PPO-*b*-PEO)-$PAA^-\ ^+Na$). The diblock PEO (2000 MW)-$PAA^-\ ^+Na$ (8900 MW) was prepared in an analogous manner utilizing monomethoxy PEO as the starting material. Fluorescein-NHS (10 mg, 2.10×10^{-5} mol) was dissolved in 0.5 mL dimethylsulfoxide. The solution was then slowly added to a solution of 22 mg of gentamicin sulfate (5.15×10^{-5} mol) in

2 mL of phosphate buffer, pH 7.4. The mixture was reacted in the dark at room temperature overnight. The solution of fluorescein-labeled gentamicin (1 mL, 8.8 mg gentamicin sulfate) was added into 4 mL of gentamicin sulfate solution (10 mg mL^{-1} gentamicin sulfate, 30 mg gentamicin, ~3.5 x 10^{-4} eq of cations) to prepare the labeled drug mixture for incorporation into the nanostructures. Core-shell nanostructures containing gentamicin wherein pentablock copolymers of $PAA^{-}{}^{+}Na$ (5,300 MW) -*b*-PEO (3,300 MW)-*b*-PPO (1,600 MW)-*b*-PEO (3,300 MW)-*b*-$PAA^{-}{}^{+}Na$ (5,300 MW) were mixed with polymers of $PAA^{-}{}^{+}Na$ (4,200 MW) and condensed with gentamicin. In a 100-mL round bottom flask, 34 mg of $PAA^{-}{}^{+}Na$-(PEO-*b*-PPO-*b*-PEO)-$PAA^{-}{}^{+}Na$ (1.90 x 10^{-4} eq of anions) and 16 mg of $PAA^{-}{}^{+}Na$ (1.6 x 10^{-4} eq of anions) were dissolved in 50 mL of deioinized (DI) water with adjustment to pH 7 with NaOH (1 N). The solution was placed in a sonication bath and 5 mL of fluorescein-gentamicin/gentamicin sulfate solution was added via syringe to form a turbid dispersion. The dispersion was stirred overnight. Any non-complexed free fluorescein-gentamicin or free gentamicin salts were removed by ultra-centrifugation at 20,000 rpm for 15 min (Optima ™ L-XP Ultracentrifuge, Beckman Coulter Inc.). The supernatant was removed and the sedimented nanostructures were washed twice with sterile DI water, and then recovered by freeze-drying. Nanostructures labeled with rhodamine were prepared in a similar manner utilizing rhodamine-NHS. The nomenclature describing these nanostructures adopted for this study is N1 (N1F labeled with fluorescein and N1R labeled with rhodamine). Similar methodology was utilized to prepare nanostructures with a PEO-$PAA^{-}{}^{+}Na$/$PAA^{-}{}^{+}Na$ blend. These nanostructures are designated N2 (N2F labeled with fluorescein and N2R labeled with rhodamine). The amount of gentamicin loaded into the nanoplexes was determined via an o-phthalaldehyde assay by derivatization of the gentamicin to make it UV-active, then by measuring the intensity of UV light absorption at 335 nm [11,12].

Characterization of drug release

Either the free aminoglycoside sulfate salt (16 mg) or a delivery complex (N1 and N2) containing 10 mg of the aminoglycoside was dissolved in 10 mL of DI water. The solution was transferred to a dialysis bag (MW cutoff 3,500 g mol^{-1}) and dialyzed against 300 mL of PBS (pH 7.4) at 37 ^{o}C. At prescribed times, 0.3 mL aliquots were taken from the receptor medium and stored at 4 ^{o}C. To quantify the amount of released gentamicin, the aliquot was mixed with 0.5 mL of the *o*-phthalaldehyde reagent and 0.2 mL isopropanol. The volume was adjusted to 3 mL

with 0.4M borate buffer, pH 9.7. The mixture was incubated at room temperature for 1 h and the absorbance at 340 nm was measured. The percentage of the drug that was released relative to the total amount of gentamicin in the nanostructures was calculated from the absorbance of the aliquot divided by the absorbance corresponding to complete diffusion of the free gentamicin through the dialysis membrane (eq. 1). The release profile of free gentamicin (the control) was compared with the nanoplex at the respective time points using the standardized curve.

% gentamicin release = (Abs due to release from the nanoplex/Abs of all of the free gentamicin) x 100

eq. 1

J774A.1 murine macrophage cell line

J774A.1 cells (murine macrophage cell line from American Type Culture Collection) were routinely grown as monolayers in 75 cm^2 tissue culture flasks (Corning, Inc.) in a humidified incubator with 5% CO_2 atmosphere at 37 °C. The cells were cultured and maintained in Dulbecco's modified Eagle's medium (Sigma-Aldrich) supplemented with 10% fetal bovine serum (FBS), L-glutamine, $NaHCO_3$, pyridoxine-HCl, and 45,000 mg/L glucose and preserved with 1% penicillin-streptomycin solution (Mediatech, Inc.).

Uptake of the nanostructures into the cells by flow cytometry

Cultured J774A.1 cells at 80-90% confluency were gently scraped, seeded onto 12-well plates at 1 x 10^6 cells/well and incubated in a humidified incubator with 5% CO_2 atmosphere at 37 °C for 24 h to allow for attachment. The culture media was discarded from each well, 200 µL (1 mg nanostructures/mL in DI water) of either N1F or N2F were added into each well. One mL of DMEM supplemented with 10% FBS were added to each well. The plates were incubated for 1 h or 4 h in a 5% CO_2 atmosphere at 37 °C. After incubation, the supernatants were removed, the wells were washed twice with PBS (without divalent calcium or magnesium ions), then 1 mL of PBS was added to each well and the cells were gently scraped from the wells. The contents of each well were transferred into a 15-mL falcon tube, resuspended in 10 mL of PBS (without Ca^{2+} and Mg^{2+} ions), and centrifuged at 3000 rpm for 10 min to remove any non-phagocytosed nanostructures. The supernatants were discarded and the recovery procedure was repeated twice. The sedimented cell populations were resuspended in 500 µL PBS (without Ca^{2+} and Mg^{2+} ions) and transferred into 10-mL falcon tubes. The fluorescence intensity of each sample was analyzed

by FACS flow cytometry (BD FACS Aria) with an excitation wavelength of 488 nm and analyzed with a 530/30 nm emission filter.

Imaging uptake of nanostructures into the cells by confocal microscopy

For microscopic examinations, 1 x 10^5 J774A.1 cells suspended in 250 µL of DMEM with 10% FBS were seeded into the 10-mm diameter microwell of 35 mm petridishes (Mat-tek Corporation, USA) and incubated for 1 h at 37 °C in a humidified 5% CO_2 atmosphere to allow the cells to attach onto the glass surface. After incubation, the remainder of the dish was gently filled with 2 mL of DMEM medium containing 10% FBS and the dishes were incubated for 48 h at 37 °C in a humidified 5% CO_2 atmosphere. The cells in each microwell were washed twice with 2 mL of PBS each, 100 µL of N1F or N2F (concentration of the nanostructures in the wells was 100 µg/well) was added to each well, then each petridish was gently filled with DMEM supplemented with 10% FBS, and the contents were incubated for 2 h or 4 h at 37 °C in a humidified 5% CO_2 atmosphere. The wells were examined using a 63x oil-immersion objective on a Zeiss LSM 510 META confocal microscope.

Live cell lysosomal/endosomal and nuclear staining for confocal microscopy

An Image-iT live lysosomal and nuclear labeling kit (Invitrogen, USA) was used to stain the lysosome/endosome and nuclear compartments of the cells. After incubation with the nanostructures for 4 h, the cells were washed twice with PBS. Hoechst 33342 (excitation/emission maxima ~350/461 nm) was added to the microwells (2.0 µg/mL Hanks balanced salt solution (HBSS)) and the contents were incubated for 5 min at 37 °C in a 5% CO_2 atmosphere to stain the nuclei (blue). Later, the cells were washed three times with 1 mL each of HBSS and incubated with LysoTracker Red DND-99 (excitation/emission maxima ~577/590 nm) for 1 min at room temperature. The LysoTracker Red DND-99 dye was used at a concentration of 100 nM/well for staining acidic cell organelles such as endosomes and lysosomes. Following incubation, the cells were washed twice with 1 mL each of HBSS and mounted on the microscope slide.

Preparation of Green Fluorescent Protein-expressing (GFP) *Salmonella* for macrophage infection and imaging

GFP constructs

A promoterless Green Fluorescent Protein gene (GFP) was excised from a pGFPuv vector (BD Biosciences Clonetech) and cloned inframe and downstream of the TrcD promoter with the UP stream element in the multiple cloning site (MCS) of a pNSTrcD vector [13] to form pNSTrcD/GFP.

Preparation and transformation of competent cells with *Salmonella* for GFP expression

To prepare *Salmonella enterica* spp serotype Typhimurium *(S. typimurium)* competent cells, 300 µL of bacterial culture OD_{600} = 1 was spread on TSA plates, and incubated overnight at 37 °C. The bacteria were gently scraped from the plates and washed twice with ice-cold 10% glycerol. The cells were resuspended to a density of approximately 10^{11} cells/mL in ice-cold 10% glycerol. The pNSTrcD/GFP plasmid was transformed into *S. typhimurium* by electrotransformation with a Gene Pulser (BTX) set at 2.7 KV, 25 µF and 200 Ω using 1-mm gap cuvettes (Eppendorf). After electroporation, the cells were transferred to SOC medium (Invitrogen) and incubated at 37 °C with shaking at 200 rpm for 2 h to allow expression of the antibiotic resistant gene. The transformation mixture was plated on several TSA plates containing 30 µg/mL of chloramphenicol. The pNSTrcD/GFP expression vector with GFP expressed under the TrcD promoter was transformed into *S. typhimurium* as described earlier. Discrete colonies were isolated, transferred into 10 mL of trypticase soy broth (TSB) supplemented with 30 µg/mL of chloramphenicol, and incubated for 16-18 h at 37 °C with shaking. The bacterial suspension was adjusted to 75 Klett units by dilution in TSB, centrifuged at 3000 rpm for 10 min, the supernatant was discarded, and the cells were washed twice with PBS and adjusted to a concentration of 1 x 10^8 CFU/mL.

J774A.1 macrophage infection with GFP *S. typhimurium*

J774A.1 murine macrophages (1 x 10^5 cells) suspended in 150 µL of DMEM supplemented with 10% FBS were seeded into 10-mm diameter microwells of 35 mm petridishes and cultured for 48 h as described previously. Before infection, the media from each petridish was discarded, and the contents of the microwells were washed twice with PBS to remove dead and unattached cells. Then, 100 µL of GFP *S. typhimurium* suspended in DMEM supplemented with 10% FBS was added to the macrophages adjusted at a multiplicity of infection (MOI) of 20 bacteria per cell and incubated at 37 °C for 45 min. After incubation, the culture medium was discarded, and the infected cells were carefully washed three times to remove extracellular bacteria. They were

incubated with 2 mL of fresh DMEM supplemented with 10% FBS containing 5μg/mL gentamicin for 15 min to kill remaining extracellular bacteria, then washed twice with PBS and further incubated with 2 mL of fresh DMEM supplemented with 10% FBS for 4 h. The number of colony forming units (CFU)/microwell was determined after lysing the macrophages with cold 1% Triton X-100 for 5 min at 37 °C and plating the serial dilutions of the lysates onto TSA plates.

Treatment of GFP *S. typhimurium* infected macrophages with nanostructures and imaging

J774A.1 macrophage cells infected with GFP *S. typhimurium* at a MOI of 1:20 in each microwell were treated with 25 μg of gentamicin sulfate (15 μg gentamicin) in solution, or N1R or N2R complexes (each containing ~15 μg of gentamicin) for 4 h. A control group of cells without drug or nanostructures was compared. The capacity of the nanostructures to treat intracellular *Salmonella* was measured by plating serial dilutions of lysed macrophages and counting the number of CFUs. For each treatment and control, triplicate samples were used. The results were expressed as an average reduction in intracellular *Salmonella* in the treatment and appropriate control groups. Infected macrophages expressing GFP, treated with the nanostructures for 2 h, were imaged by confocal microscopy to visualize any co-localization of bacteria with nanostructures.

Statistical analysis

Comparisons were made between groups by student *t* tests. The statistical significance level for the experiments was defined as $P < 0.05$.

Results

Uptake of the nanostructured delivery systems into macrophage cells

The nanostructures containing gentamicin were incubated with J774A.1 murine macrophages and their uptakes into the cells were analyzed by flow cytometry after one and four hours. At both time points, the cells that had been incubated with the somewhat hydrophobic N1F nanostructures had significantly more particles incorporated relative to the cells that were exposed to the hydrophilic N2F nanostructures. This is depicted in fig. 2.2.1 using fluorescence histograms of nanostructure uptake that distinguish the two types of nanoparticle delivery systems.

Confocal micrographs of the J774.1 macrophages after incubation for two hours with the N1F or N2F nanostructures show more uptake of these delivery systems with the hydrophobic N1F relative to the hydrophilic N2F structures (fig. 2.2.2 a and 2.2.2 b). Thus, the flow cytometry and confocal microscopy results show good correlation.

Intracellular localization of the nanostructured delivery systems

The acidic lysosomes and endosomes of the J774A.1 cells were stained red with a lysotracker dye and the cells were incubated with N1F or N2F nanostructures (stained green) for two hours (figure 3). An orange-to-yellow color is produced in cases where the nanostructures co-localize with the lysosomes/endosomes inside the cells, whereas distinct regions of red and green signify minimal co-localization. For the more hydrophobic N1F nanostructures, the particles appeared to be in the cytoplasm (figure 2.2.3 a), whereas for N2F, the majority of the particles co-localized with the red endosomes/lysosomes (figure 2.2.3b).

After incubation of the GFP *Salmonella*-infected cells with the N1R and N2R nanostructures for four hours, confocal micrographs were taken in efforts to determine whether the nanostructure delivery systems co-located with the bacteria inside the cells (fig. 2.2.4a and 2.2.4b). We did not observe any significant co-location of the nanostructures with the intracellular bacteria.

Drug release from the nanoplexes

The release of gentamicin from the complexes (N2 and N3) at the physiological pH 7.4 was relatively slow and sustained. (Figure 2.2.5). A burst release occurred during the first five hours comprising approximately 15-20% of the total amount of drug, and 25-30% had been released at 24 hours.

Treatment of GFP *S. typhimurium* infected macrophages with nanostructures

J774A.1 macrophages were infected with GFP-expressing *Salmonella*, and incubated with N1R and N2R nanostructures. The results were compared to infected cells incubated with free gentamicin and control cells. The N1R hydrophobic gentamicin delivery systems resulted in significant reductions of intracellular GFP *Salmonella* after four hours, as compared to cells that were treated with the hydrophilic N2R systems and both controls ($P < 0.05$). At a dose of 15 µg of gentamicin per well, N1R nanoparticles reduced the intracellular bacteria compared to free gentamicin or N2R complexes by 0.44 log (Table 2.2.1). By contrast, treatments with the N2R

systems were statistically similar to the infected control cells and those that were treated with free gentamicin.

Discussion

Uptake of the nanostructure delivery systems into the macrophage cells

Antimicrobials in the aminoglycoside class such as gentamicin are cationic and polar, and the permeability of gentamicin across nonpolar lipophilic cell membranes is very low [14]. The activities of aminoglycosides are also pH-dependent due to their propensity to become protonated at low pH. For example, a 64-fold increase in MIC has been observed for gentamicin at pH 5 [15]. Due to low intracellular penetration and acid-inactivation of free gentamicin, bactericidal clearance of intracellular *Salmonellae* does not occur efficiently. To minimize pH dependent loss in bioactivity of gentamicin in the late endosomes, intracellular pathways that either avoid or allow escape from endosomes may be desirable.

Encapsulating or conjugating drug molecules to nanoparticles can potentially improve internalization into mammalian cells [16]. Drug encapsulation in hydrophilic delivery vehicles can improve dispersion in physiological media, decrease aggregation and improve efficacy. In this study, we report the development of two types of nanostructures that encapsulate gentamicin within their cores, but differ in their surface chemistries. The N1 nanostructures have shells comprised of amphiphilic copolymers that have both hydrophobic and hydrophilic segments, and thus those delivery vehicles are somewhat more hydrophobic than the N2 structures. In contrast, the N2 nanostructures have only hydrophilic shells. The natures of the nanostructure shells result in different cell uptake patterns. The consequent effects on *in-vitro* bacterial clearance are reported herein.

Previous work has shown that the rate of nanoparticle uptake by macrophages depends on the surface structures of polymeric carriers [17]. For example, phagocytosis of polylactide (PLA) nanoparticles by polymorphonuclear cells has been observed to be more efficient than for a blend of PLA and poly(ethylene oxide) (PEO) (1:0.25). This was explained by the relative hydrophobicity of PLA having a stimulatory effect on both adhesion and internalization by the cells. Hence, controlling the parameters that influence the particle surface chemistry is crucial for eliciting desirable particle recognition and uptake by *Salmonella* infected macrophage cells.

In this study, we designed block copolymer nanostructures encapsulating gentamicin, and containing predominantly either amphiphilic (N1) or hydrophilic (N2) surfaces and studied their influence on particle uptake. The polycationic gentamicin was incorporated via cooperative electrostatic interactions to study its capacity for clearing intracellular bacteria. Our results show that the surface chemistry of the nanostructures influences the cell uptake. Flow cytometry conducted after co-incubation of J774A.1 macrophage cells for one and four hours with either N1 or N2 demonstrated a higher rate of uptake for N1 in comparison to N2 (Fig. 2.2.1). These findings may be attributable to the increased hydrophobic character of the N1 surfaces that might promote positive interactions with lipophilic cell membranes. In addition, the data is consistent with previous observations wherein the effect of block copolymers comprised of PEO and poly(propylene oxide) (PPO) is fundamentally dependent on the relative hydrophobicity [18]. Greater potency of such copolymers in mediating multi-drug resistance in cancer cells through interactions with the cell membranes was observed at intermediate hydrophobic PPO and relatively short hydrophilic PEO segment lengths. Interestingly, after two hours of co-incubation of N1F with J774A.1 cells, confocal micrographs indicate that the cells had taken up significantly more N1F nanostructures relative to N2F (Fig. 2.2.2). Thus, our current findings that nanostructures with PEO-PPO block copolymer surfaces (N1) enter cells more rapidly than the N2 structures having only the PEO hydrophilic surfaces seem plausible.

Intracellular localization of the nanostructured delivery systems

Sub-cellular localization of the nanostructures with the different surfaces was also investigated by confocal microscopy. The majority of the N2F hydrophilic nanostructures appeared to reside in endosomes. This was indicated by distinct yellow-to-orange spots formed by co-localization of green nanoparticles and red endosomes/lysosomes inside the cells (figure 2.2.3). In contrast, the majority of the N1F nanostructures with amphiphilic surfaces were found in the cell cytoplasm, suggesting that these particles may have been taken up by a different mechanism. To our knowledge, this is the first report that the hydrophilic/hydrophobic nature of aminoglycoside drug delivery vehicles can make a distinct difference in intracellular localization. The means by which such materials enter the cells as functions of their surface chemistry will require considerable further examination.

It is also important to understand whether the nanostructures can reach the compartments where the bacteria reside and replicate within the cells. Upon phagocytosis, it has been reported that *Salmonella* are found in membrane bound vacuoles, also referred to as *Salmonella* containing vacuoles (SCV) [19,20]. Thus, we attempted to analyze any co-localization of N1R or N2R nanostructures with GFP expressing *Salmonella* by incubating rhodamine-labeled (red) nanoparticles with green bacteria for four hours (fig 2.2.4). We could not distinguish significant co-localization in the confocal micrographs under these conditions. Longer-term incubation experiments may shed more light on this phenomenon since flagellated *Salmonella* bacilli escape intermittently from the host cell over extended periods and could possibly interact directly with the nanostructures in different locations during this process [21]. Previous studies have reported that intracellular flagellation of *Salmonella* is partially dependent on duration of infection. *Salmonella* may be flagellum negative until two hours of infection and up-regulate genes required for flagellum synthesis promoting exit from host cells eight hours after infection.

Treatment of GFP *S. typhimurium* infected macrophages with nanostructures

Finally, we assessed the relative effectiveness of the N1R and N2R nanostructures labeled with rhodamine in reducing intracellular *Salmonella*. Significant reductions in bacterial counts were observed with the N1 structures, but not with N2. These results suggest that delivery of the N1 nanostructures into the cell cytoplasm has a positive effect on reducing the intracellular bacterial population. It is noteworthy that the release of gentamicin from the nanostructures at the physiological pH of 7.4 was relatively slow and sustained (Fig. 2.3.5). However, the release profiles from both nanostructures were similar, signifying that the more-hydrophobic N1 did not appreciably inhibit the release rate relative to the release rate of the more-hydrophilic N2 nanostructures. Thus, the enhanced activity may be either due to higher bioactivity of the drug in the cell cytoplasm or increased intra-cytoplasmic gentamicin concentration due to greater nanostructure uptake by the macrophage cells. Studies reported previously have shown that gentamicin delivery into cells by hydrophobic microspheres correlates directly with intracellular bacterial killing [22]. This is supported by findings of *in-vitro* efficacy of poly(lactide-co-glycolide) (PLGA) microspheres in clearing intracellular *Brucella*. Transmission electron micrographs of gold-labeled microspheres in those studies showed no evidence of fusion of endosomes harboring *Brucella* and microspheres, yet transmembrane transfer of gentamicin to the Brucellas' niches occurred [23]. It is possible that the N1 nanostructures release gentamicin

within the cells and somehow distribute the drugs not only to the cell cytoplasm but also to the S*almonella*'s SCV. Clearly, the release profiles over time and with conditions, and the effects of these issues on bacterial clearance need further investigation. N2 nanostructures did not show any difference in killing efficiency in comparison to free gentamicin or the infected controls. It is plausible that at a concentration of 15 μg, endosomal uptake of the N2 structures may have lead to inactivation of gentamicin in the acidic environment, consequently resulting in poor bacterial clearance.

Previous investigations have been conducted with drugs encapsulated in polymeric or liposomal carriers to probe endosomal trafficking inside macrophage cells [24]. For example, uptake of ampicillin-loaded polycyanoacrylate nanoparticles was studied by transmission electron and confocal microscopy. The nanoparticles were endocytosed, and were mostly concentrated in phagosomes or phagolysosomes. Similarly, lipid-based cationic and anionic drug carriers with gentamicin have also been studied [6]. The cationic carriers were efficiently internalized by cells via an endosomal route. Such a pathway may result in poor intracellular activity of gentamicin due to drug inactivation at the relatively low endosomal pH. By contrast, gentamicin encapsulated in anionic liposomal vesicles showed increased activity in killing intracellular *Salmonella*. This was mainly attributed to the ability of lipid components of the anionic carriers to perturb the endosomal membrane integrity promoting cytoplasmic delivery of gentamicin.

Summary

In summary, our studies show that gentamicin encapsulation in nanostructures having PEO-PPO amphiphilic surfaces enhances the rate and modulates the route of uptake into macrophages. This phenomenon may have an influence on the therapeutic activity against intracellular bacterial clearance. In conclusion, therapeutic efficacy of cell impermeable antimicrobials can be augmented by intra-cytoplasmic delivery of nanostructures.

Acknowledgements

The authors are grateful to NSF DMR-0312046 and to Virginia Tech's Institute for Critical and Applied Technologies (ICTAS) for funding.

References:

1. Bush K: **Antibacterial drug discovery in the 21st century**. *Clin Microbiol Infect* 2004, **10 Suppl 4**:10-17.

2. Monack DM, Mueller A, Falkow S: **Persistent bacterial infections: the interface of the pathogen and the host immune system**. *Nat Rev Microbiol* 2004, **2**:747-765.

3. Durante-Mangoni E GA, Utili R, Falagas ME.: **Do we still need the aminoglycosides?** *Int J Antimicrob Agents.* 2008.

4. Lecaroz C, Gamazo C, Blanco-Prieto MJ: **Nanocarriers with gentamicin to treat intracellular pathogens**. *J Nanosci Nanotechnol* 2006, **6**:3296-3302.

5. Ristuccia AM, Cunha BA: **The aminoglycosides**. *Med Clin North Am* 1982, **66**:303-312.

6. Lutwyche P, Cordeiro C, Wiseman DJ, St-Louis M, Uh M, Hope MJ, Webb MS, Finlay BB: **Intracellular delivery and antibacterial activity of gentamicin encapsulated in pH-sensitive liposomes**. *Antimicrob Agents Chemother* 1998, **42**:2511-2520.

7. Fattal E, Rojas J, Youssef M, Couvreur P, Andremont A: **Liposome-entrapped ampicillin in the treatment of experimental murine listeriosis and salmonellosis**. *Antimicrob Agents Chemother* 1991, **35**:770-772.

8. Prior S, Gamazo C, Irache JM, Merkle HP, Gander B: **Gentamicin encapsulation in PLA/PLGA microspheres in view of treating Brucella infections**. *Int J Pharm* 2000, **196**:115-125.

9. Batrakova EV, Li S, Li Y, Alakhov VY, Elmquist WF, Kabanov AV: **Distribution kinetics of a micelle-forming block copolymer Pluronic P85**. *J Control Release* 2004, **100**:389-397.

10. Tian Y, Bromberg L, Lin SN, Hatton TA, Tam KC: **Complexation and release of doxorubicin from its complexes with pluronic P85-b-poly(acrylic acid) block copolymers**. *J Control Release* 2007, **121**:137-145.

11. Lecaroz C, Campanero MA, Gamazo C, Blanco-Prieto MJ: **Determination of gentamicin in different matrices by a new sensitive high-performance liquid chromatography-mass spectrometric method**. *J Antimicrob Chemother* 2006, **58**:557-563.

12. Virto MR, Elorza B, Torrado S, Elorza Mde L, Frutos G: **Improvement of gentamicin poly(D,L-lactic-co-glycolic acid) microspheres for treatment of osteomyelitis induced by orthopedic procedures**. *Biomaterials* 2007, **28**:877-885.

13. Seleem M, Ali M, Abd Al-Azeem MW, Boyle SM, Sriranganathan N: **High-level heterologous gene expression in Ochrobactrum anthropi using an A-rich UP element**. *Appl Microbiol Biotechnol* 2007, **73**:1123-1127.

14. Lecaroz C, Gamazo C, Renedo MJ, Blanco-Prieto MJ: **Biodegradable micro- and nanoparticles as long-term delivery vehicles for gentamicin**. *J Microencapsul* 2006, **23**:782-792.

15. Gamazo C, Lecaroz MC, Prior S, Vitas AI, Campanero MA, Irache JM, Blanco-Prieto MJ: **Chemical and biological factors in the control of Brucella and brucellosis**. *Curr Drug Deliv* 2006, **3**:359-365.

16. Gelperina S, Kisich K, Iseman MD, Heifets L: **The potential advantages of nanoparticle drug delivery systems in chemotherapy of tuberculosis**. *Am J Respir Crit Care Med* 2005, **172**:1487-1490.

17. Mainardes RM GM, Brunetti IL, da Fonseca LM, Khalil NM.: **Zidovudine-loaded PLA and PLA-PEG blend nanoparticles: Influence of polymer type on phagocytic uptake by polymorphonuclear cells**. *J Pharm Sci.* 2008, Apr.

18. Batrakova E, Lee S, Li S, Venne A, Alakhov V, Kabanov A: **Fundamental relationships between the composition of pluronic block copolymers and their hypersensitization effect in MDR cancer cells**. *Pharm Res* 1999, **16**:1373-1379.

19. Bakowski M, Braun V, Brumell JH: **Salmonella-containing vacuoles: directing traffic and nesting to grow**. *Traffic* 2008.

20. Garcia-del Portillo F, Nunez-Hernandez C, Eisman B, Ramos-Vivas J: **Growth control in the Salmonella-containing vacuole**. *Curr Opin Microbiol* 2008, **11**:46-52.

21. Sano G, Takada Y, Goto S, Maruyama K, Shindo Y, Oka K, Matsui H, Matsuo K: **Flagella facilitate escape of Salmonella from oncotic macrophages**. *J Bacteriol* 2007, **189**:8224-8232.

22. Prior S, Gander B, Irache JM, Gamazo C: **Gentamicin-loaded microspheres for treatment of experimental Brucella abortus infection in mice**. *J Antimicrob Chemother* 2005, **55**:1032-1036.

23. Lecaroz MC, Blanco-Prieto MJ, Campanero MA, Salman H, Gamazo C: **Poly(D,L-lactide-coglycolide) particles containing gentamicin: pharmacokinetics and pharmacodynamics in Brucella melitensis-infected mice**. *Antimicrob Agents Chemother* 2007, **51**:1185-1190.

24. Pinto-Alphandary H, Balland O, Laurent M, Andremont A, Puisieux F, Couvreur P: **Intracellular visualization of ampicillin-loaded nanoparticles in peritoneal macrophages infected in vitro with Salmonella typhimurium**. *Pharm Res* 1994, **11**:38-46.

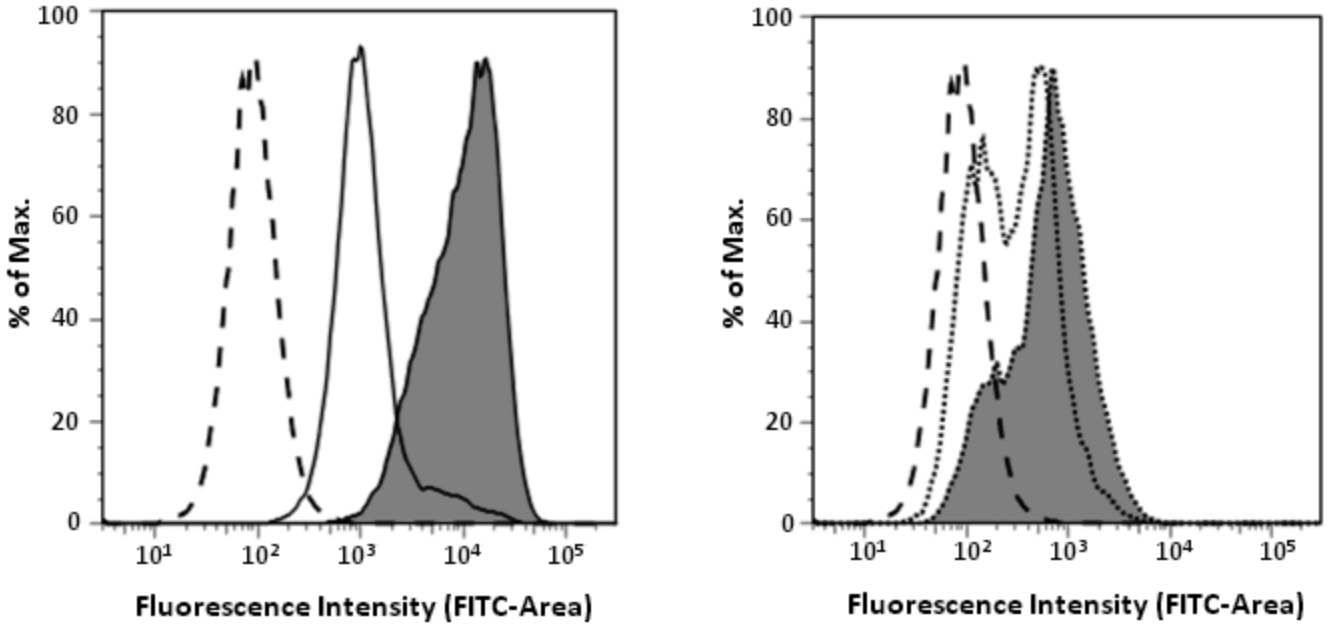

FIG. 2.2.1. Fluorescence histogram from flow cytometry depicting the uptake of nanostructures labeled with fluorescein isothiocyanate (FITC) into J774A.1 cells. Left histogram shows uptake of N1F: cells without nanostructures (dashed line), uptake after incubation with N1F for 1 h (solid line without shading), and uptake after incubation with N1F for 4 h (solid line with shading). Right histogram shows uptake of N2F: cells without nanostructures (dashed line), uptake after incubation with N2F for 1 h (dotted line without shading), and uptake after incubation with N2F for 4 h (dotted line with shading)

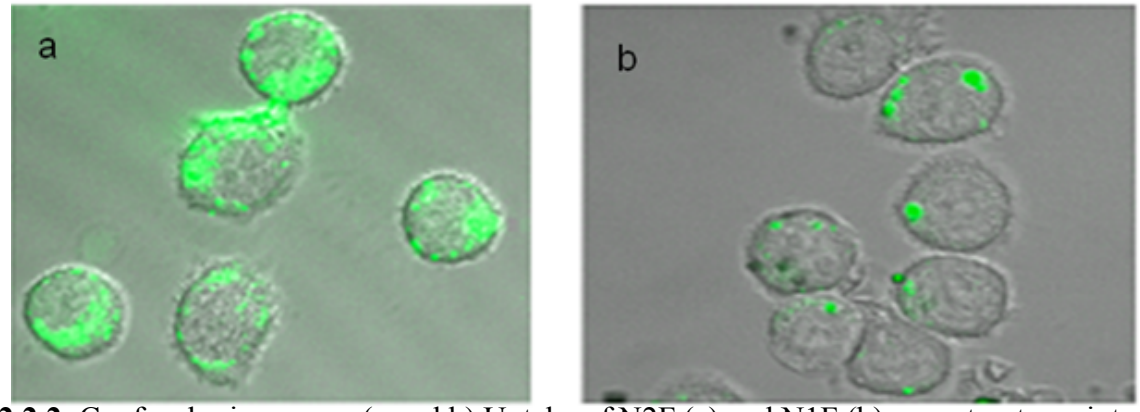

Fig. 2.2.2: Confocal microscopy (a and b) Uptake of N2F (a) and N1F (b) nanostructures into J774A.1 cells

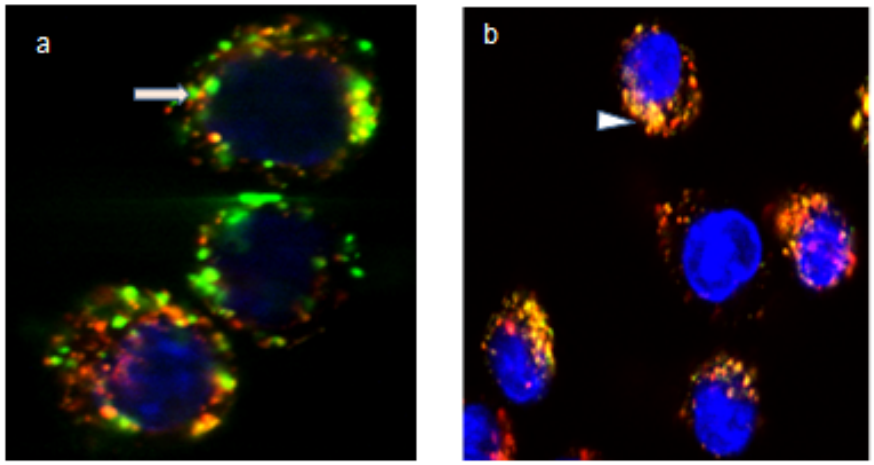

FIG. 2.2.3: Confocal microscopy (a and b) Colocalization of nanostructures with endosome/lysosome after incubation for 2 h. N1F (arrow) (a) and N2F (arrowhead) (b) nanostructures is shown by yellow-to-orange spots formed by green nanoparticles and red endosomes/lysosomes, showing that a majority of the N2F hydrophilic nanostructures appear to reside in endosomes.

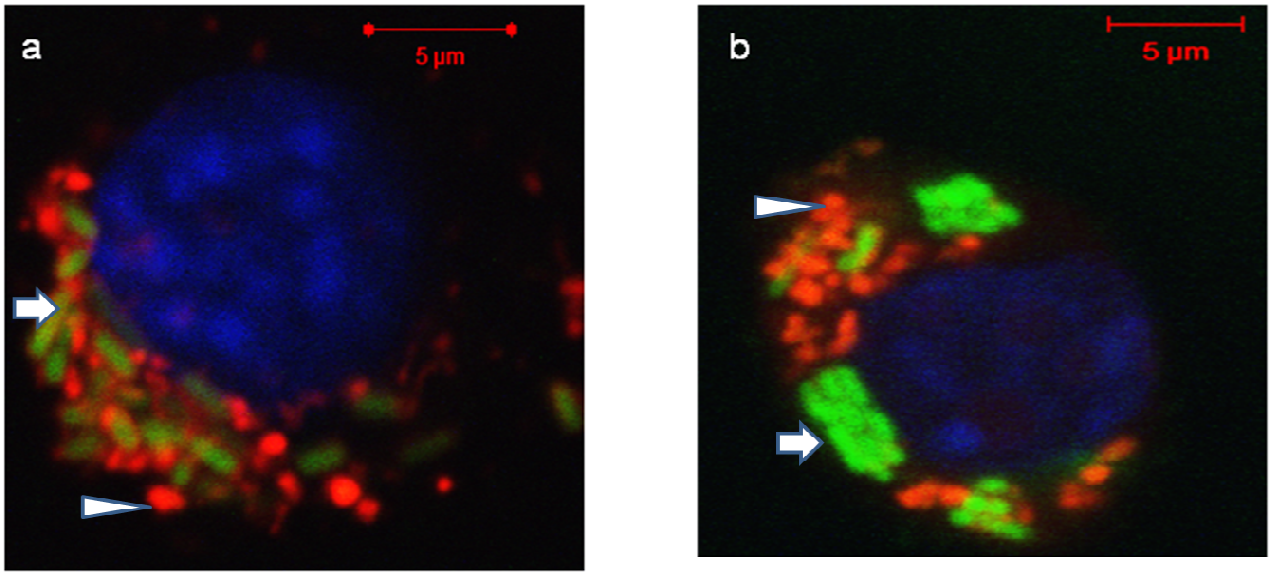

Fig.2.2.4: Confocal microscopy showing *Salmonella* (arrow) infected J774A.1 macrophage cells incubated for 4 h with two kinds of nanostructures (arrowheads). Left (a) and right (b) panels showing macrophage cells incubated with N1R and N2R nanostructures, respectively.

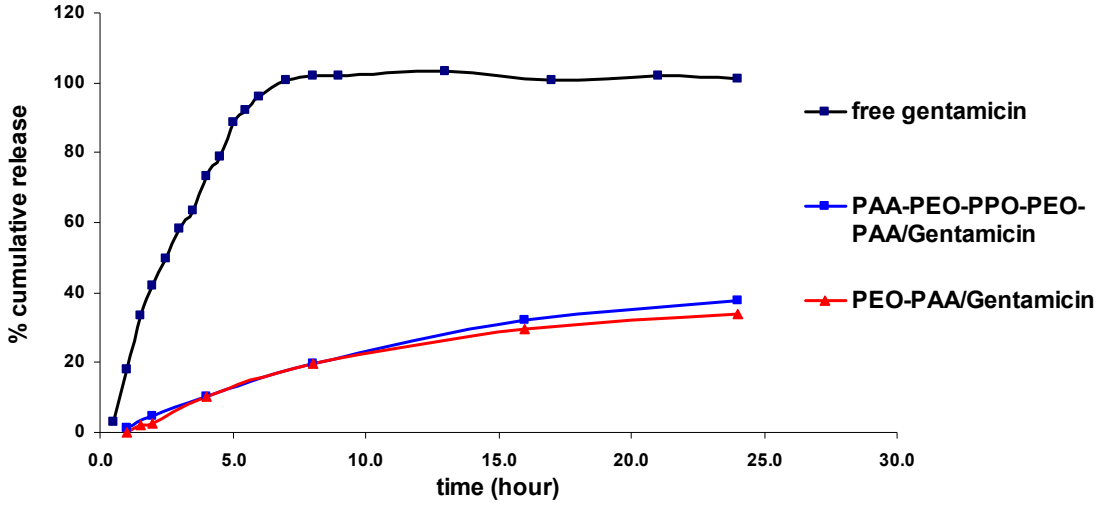

Fig. 2.2.5: Release rates of gentamicin from N1, N2 in PBS, pH 7.4 at 37 °C

Table2.2.1: Drug delivery efficacy of nanoplexes in comparison to appropriate controls

Groups	CFU ± SD	log CFU reduction
Control	7.68 ± 0.07	0.00
Free gentamicin	7.70 ±0.19	+ 0.02
N1R **	7.24 ± 0.03	0.44**
N2R	7.67 ± 0.08	0.01

** Significant at P< 0.05

Chapter 2

Development of drug delivery approach for intracellular *Salmonella*

Chapter 2.3

Antibacterial efficacy of core-shell nanostructures encapsulating gentamicin against an *in-vivo* intracellular *Salmonella* model

(Int. Journal of Nanomedicine, in press September 2009)

Abstract

Pluronic based core-shell nanostructures encapsulating gentamicin were designed in this study. Block copolymers of ($PAA^{-+}Na$-*b*-(PEO-*b*-PPO-*b*-PEO)-b-$PAA^{-+}Na$) were blended with $PAA^{-}Na^{+}$ and complexed with the polycationic antibiotic gentamicin to form nanostructures. Synthesized nanostructure had a hydrodynamic diameter of 210 nm, zeta potentials of -0.7 (±0.2), and incorporated ~20% by weight of gentamicin. Nanostructures upon co-incubation with J774A.1 macrophage cells showed no adverse toxicity *in-vitro*. Nanostructures administered *in-vivo* either at multiple dosage of 5µg g^{-1} mice body weight or single dosage of 15µg g^{-1} in AJ-646 mice infected with *Salmonella* resulted in significant reduction of viable bacteria in the liver and spleen. Histopathological evaluation for concentration dependent toxicity at a dosage of 15µg g^{-1} revealed mineralized deposits in 50 % kidney tissues of free gentamicin treated mice which in contrast was absent in nanostructure treated mice. Thus, encapsulation of gentamicin in nanostructures may reduce toxicity and improve *in-vivo* bacterial clearance.

Introduction

Delivery systems capable of transferring cell-impermeable drugs into cells have tremendous potential for improving therapeutic efficacies *in-viv*o (12). In the last few decades, nanotechnology has been increasingly employed in new drug delivery systems (DDS). DDS developed through nanotechnology may allow for reductions in dosage and dosage frequency and may also prevent toxicity associated with conventional therapy. This may be especially beneficial for chronic intracellular infections which now require long-duration combination therapies (2). For example, aminoglycosides are a common class of antibiotics utilized clinically

for treating bacterial infections. They have broad activities against both Gram-negative and Gram-positive bacteria (26). However, the action of aminoglycosides is concentration dependent and free gentamicin filters rapidly through the renal system, thus necessitating high dosages. Administration of high dosages of aminoglycosides may result in nephrotoxicity and ototoxicity, which may be prevented with nanomedicine based therapy (24).

To achieve intracellular delivery of aminoglycosides, several drug delivery strategies have been utilized including liposomes and polymeric carriers (9, 17). These drug delivery systems have improved the intracellular delivery of aminoglycosides, but suffer from low drug incorporation. Core-shell drug delivery systems have recently attracted considerable attention due to their unique ability in encapsulating charged therapeutic molecules (2). The unique ability is conferred to the core-shell structures mainly by fabricating the core to contain high amounts of ionic species and tailoring shell with specific hydrophobic/hydrophilic chemistry as shown schematically in fig. 1. This may result in encapsulation of high payload of oppositely charged ionic species like gentamicin inside the cores and successful interaction of the shell's hydrophobic segment with the cell membranes.

We previously reported synthesis of core-shell nanostructure with amphiphilic shell containing pluronic F68 (PPO) which can incorporate up to ~25% by weight of gentamicin and their *in-vitro* trafficking and efficacy in infected macrophage cells (22). Pluronics have widely been used as excipients in pharmaceutics (13). Pluronic™ triblock copolymers are comprised of hydrophilic poly(ethylene oxide) (PEO) terminal blocks with a hydrophobic poly(propylene oxide) (PPO) central block (i.e., PEO-*b*-PPO-*b*-PEO) in a basic A-B-A structure: $EO_{x/2}$-PO_y-$EO_{x/2}$ (14). Different pluronic copolymers are characterized distinctly by their hydrophilic-lipophilic balance (HLB). For example, the HLB of pluronic F68 is 29 whereas that of pluronic P85 is 16. Therefore, pluronic F68 is relatively less hydrophobic than pluronic P85. Pluronics have been investigated extensively for cancer chemotherapy of multidrug resistant (MDR) tumors (5). By varying the lengths of the hydrophobic propylene oxide (y) and hydrophilic ethylene oxide (x) segments, increased potency and intracellular uptake of the DDS were seen in the tumor cells (3). Studies on KBv cell lines have shown that the accumulation of pluronics inside the cells is dependent on HLB. In general, pluronics with HLB of 20-29 had minimal effect on drug transport. In contrast, pluronics with HLB less than 20 exhibited varying degree of activity

against MDR cells (14). Thus, the triblock arrangement provides an advantage of altering the hydrophilic/hydrophobic balance to suit a particular therapeutic application (21). Therefore, its incorporation in DDS for cell specific therapy may be highly favorable (34), especially for intracellular infections.

Preclinical studies conducted previously with biodegradable DDS made from a combination of poly(ε-caprolactone) (PCL) and Pluronic F68 did not cause any adverse toxicological response in rats or dogs (18). In this study, we designed core-shell nanostructure by synthesizing $PAA^{-+}Na$-*b*-PEO-*b*-PPO-*b*-PEO-b-$PAA^{-+}Na$ block copolymers and complexed them with gentamicin to form nanostructures with PEO-*b*-PPO-*b*-PEO shells, and PAA cores containing the antibiotic shown schematically in fig.1. The efficacies of these core-shell nanostructures were investigated in an *in-vivo* intracellular *Salmonella* mouse infection model. Our objectives also included an evaluation of the observed reduction in gentamicin toxicity that resulted from encapsulation in the cores.

Materials and Methods:

Materials

All chemicals were purchased from Sigma-Aldrich unless otherwise noted. *t*-Butyl acrylate (tBA) was distilled from calcium hydride under vacuum prior to polymerization. Pluronic F68™ (M_n ~ 8,300 g mol^{-1}) was kindly provided by BASF (NJ, USA). Pluronic F68 and polyethylene oxide monomethyl ether (M_n ~ 2,000 g mol^{-1}) were dried under vacuum at 70 ^oC for 48 hours prior to any polymerizations.

Preparation of core-shell nanostructures loaded with gentamicin

Block copolymers of poly(sodium acrylate)-(PEO-*b*-PPO-*b*-PEO)-poly(sodium acrylate) ($PAA^{-}{}^{+}Na$-(PEO-*b*-PPO-*b*-PEO)-$PAA^{-+}Na$) and PEO-$PAA^{-+}Na$ were prepared according to a previously published procedure(30). Briefly, PEO-*b*-PPO-*b*-PEO (Pluronic F68™) with hydroxyl terminal groups was derivatized with 2-bromoisobutyryl bromide to provide bromoalkyl functional endgroups and then t-butyl acrylate was polymerized by controlled Atom Transfer Radical Polymerization (ATRP). The protective t-butyl groups were subsequently removed with trifluoroacetic acid and the polymer was neutralized with NaOH to form the sodium salt (PAA^{-}

$^{+}$Na-(PEO-*b*-PPO-*b*-PEO)-PAA^{-+}Na). Core-shell nanostructures containing gentamicin wherein pentablock copolymers of PAA^{-+}Na (5300 MW) -*b*-PEO (3300 MW)-*b*-PPO (1600 MW)-*b*-PEO (3300 MW)-*b*-PAA^{-+}Na (5300 MW) were mixed with polymers of PAA^{-+}Na (4200 MW) and condensed with gentamicin. In a 100-mL round-bottom flask, 34 mg of PAA^{-+}Na-(PEO-*b*-PPO-*b*-PEO)-PAA^{-+}Na (1.90 x10^{-4} eq of anions) and 16 mg of PAA^{-+}Na (1.6 x10^{-4} eq of anions) were dissolved in 50 mL of DI water and the pH was adjusted to 7 with NaOH (1 N). The solution was placed in a sonication bath and 5 mL of gentamicin sulfate solution (10 mg mL^{-1} gentamicin sulfate, equal to 30 mg gentamicin, 3.5 x 10^{-4} eq of cations) was added via syringe to form a turbid dispersion. Any non-complexed free gentamicin sulfate was removed by dialysis against 4 L of Deionised (DI) water at 4 ^{o}C for 24 h and the core-shell nanostructures were recovered by freeze-drying. Core-shell nanostructure prepared by this methodology was later utilized for *in-vivo* treatment efficacy studies at dosage of 5µg g^{-1} and 15µg g^{-1} respectively. The nomenclature describing the mice treated at 5µg g^{-1} adopted for this paper is D1 (D1N for the group treated with core-shell nanostructure and D1G for the group treated with free gentamicin alone). Similarly, the mice administered with 15 µg are designated as D2 (D2N for the group treated with the core-shell nanostructure and D2G for mice group treated with free gentamicin alone).

Characterization of complexes

The solute sizes and zeta potentials of the complexes were characterized by DLS with a Zetasizer 1000 HS with laser diffractometry (Malvern Instruments, Malvern, UK) at a scattering angle of 90^{o}. Each complex (1 mg) was dispersed in one mL of DI water and analyzed. Measurements were done in triplicate for each batch of particles. The results were taken as the average of three measurements.

Gentamicin concentration in the nanostructure

The amount of gentamicin loaded into the core-shell nanostructures was determined via an *o*-phthalaldehyde assay according to a previously published procedure (22). To quantify the amount of encapsulated gentamicin, the complexes were dissolved in borate buffer at pH 9.7 to disintegrate the particles and release the drug in the free amine form. The primary amine on gentamicin was then reacted with an excess of phthalaldehyde in the presence of mercaptoethanol to produce a derivative that was quantified via UV-visible spectroscopy. For

derivatisation, gentamicin solution, phthalaldehyde reagent containing mercaptoethanol, and isopropanol (to avoid precipitation of the products) were reacted for 30 minutes at room temperature, and the absorbance of the product was measured at 335 nm.

In-vitro MTS toxicity assessment

An in-vitro homogeneous, colorimetric CellTiter 96® AQueous Non-Radioactive Cell Proliferation MTS (3-(4,5-dimethylthiazol-2-yl)-5-(3-carboxymethoxyphenyl)-2-(4-sulfophenyl)-2H-tetrazolium) Assay (Promega) for determining the numbers of viable J774A.1 cells was utilized to determine any cytotoxicity of the polymers and the nanostructures. Briefly, ~2 x 10^4 J774A.1 cells suspended in 200 µL of DMEM supplemented with 10% fetal bovine serum (FBS), L-glutamine, $NaHCO_3$, pyridoxine-HCl, and 4.5% glucose and preserved with 1% penicillin-streptomycin solution were seeded in 96-well plates and incubated for 24 h at 37 °C in a 5% CO_2 atmosphere. The J774A.1 cells were further incubated with 250 µg/mL of free gentamicin, copolymer, core-shell nanostructures encapsulating gentamicin along with the appropriate untreated control for 24 h. The culture media was discarded, and the cells in each well were washed with PBS and re-suspended with 100 µL of cell culture media. Then 20 µL of CellTiter 96® AQ_{ueous} reagent solution was pipetted into each well, and the plates were incubated for 4 h at 37 °C in a humidified 5% CO_2 atmosphere. The absorbance at 490 nm was recorded using a 96-well Elisa plate reader (SoftMax Pro inc. USA). Results were expressed as the percentage mean absorbance by cells upon incubation with various treatments (nanostructure, copolymer or free gentamicin) with respect to incubation in untreated control.

In-vivo toxicity

To assess concentration/dose dependent toxicity, kidney tissue from the untreated, D2N or D2G treated mice group were harvested and assessed for histopathological changes. The kidneys were fixed in 10% neutral buffered formalin, routinely processed into paraffin blocks, and 5 micron sections were stained with haematoxylin and eosin on glass slides (Virginia-Maryland Regional College of Veterinary Medicine, Veterinary Teaching Hospital). Tissue samples were examined independently by light microscopy and scored by two veterinary pathologists. The pathologists were blinded to obtain unbiased assessment. The kidneys were scored on a scale of 0-4 based on the degree of inflammation as reported before (4, 11). Briefly, a semi-quantitative scale

consisting of whole numbers with scores from 0-4 was being given as (0) =unremarkable, (1) = minimum, (2) =mild, (3) =moderate, and (4) =marked with regard to changes. Changes include inflammation (infiltration of inflammatory cells), necrosis (morphologic changes of renal parenchyma cells consistent with degeneration and necrosis) and vascular disruptions (hemorrhage, edema and other signs of vascular leakage). The percentage of affected section of tissue being affected is what was used to score any change viz. 0% = unremarkable (0), 0-5% = minimal (1), 6-10%= mild (2), 11-20%= moderate (3),> 20% =marked (4). Furthermore, any samples with the presence of mineral deposits associated with regions of inflammation were assigned an additional 0.5 points to take mineralization into account for final analysis.

Treatment efficacy of core-shell nanostructures against against *Salmonella* Typhimurium

Salmonella enterica typhimurium (wild type) was grown overnight in Luria-Bertani (LB) broth, centrifuged, washed in PBS and serially diluted to achieve a final suspension containing 10,000 colony forming units (CFU) per mL. Twenty five AJ 646 mice (6-8 weeks old) were injected intraperitoneally (I.P.) with 100 µL of inocula containing 1000 CFUs per mouse. After 48 h of infection, five AJ 646 mice/group were treated with either D1G (in PBS) or the D1N I.P. at a recommended dosage of 5µg g^{-1} of body weight (32). The dosage was repeated twice at intervals of 24 h, I.P for a total of 3 doses. At day 2 (post third I.P. injection), the mice were euthanized, the spleens and livers were removed aseptically, and the organs were crushed and homogenized for 1-2 min in the presence of 2 mL of LB broth. Aliquots (500 µL) of the organ suspensions were serially diluted in 4.5 mL of LB broth to a maximum of 10^5-fold dilution. Subsequently, the dilutions were plated on tryptic soy agar plates, incubated overnight at 37 °C, and the resulting grey mucoid, discrete colonies were counted for plates containing between 30 and 300 colonies. Also, two groups of *Salmonella* infected mice (5mice/group) were administered with either D2G or the D2N at a single I.P. dosage of 15 µg g^{-1} of body weight to determine any concentration-dependent toxicity on the kidneys. The mice were euthanized at Day 5 of the study along with the normally administered dosed mice.

Statistical Analysis

The mean absorbance in the MTS assay was compared between the groups using analysis of variance. The kidney scores were compared between the three groups using the Kruskal-Wallis

Test followed by Dunn's procedure for multiple comparisons. Statistical significance was set to alpha = 0.05. Analyses were performed using JMP (ANOVA and Kruskal-Wallis test) and SAS (Dunn's procedure for multiple comparisons).

Results:

Core-shell nanostructures

DLS showed that polymer-gentamicin core-shell nanostructures had a mean intensity average diameter of 210 (±17) nm and had negligible zeta potentials, ranging from -0.7 (±0.2) mv. The amount of gentamicin encapsulation based on a UV spectroscopic analyis of an *o*-phthalaldehyde-mercaptoethanol derivative of the drug showed an encapsulation of ~25%. The rather high drug concentration of ~25% by weight is attributed to strong interactions between the cationic gentamicin and the anionic polymer.

***In-vitro* MTS assay**

MTS assays conducted on the free gentamicin, copolymer, core-shell nanostructure and untreated control showed no significant differences in percentage mean absorption between various treatments (Fig. 2), indicating that the polymers at doses similar to that of the free gentamicin or untreated control were non-toxic *in-vitro*.

***In-vivo* toxicity assessment**

Based on degrees of inflammation and mineralization of kidney tissues, D2N had a median score of 0 (range 0 to 0.50), untreated control 0 (range 0 to 0.75) and D2G 0.75 (range 0 to 2.50), determined by compiling the individual data scored by the pathologists (Table 1). The Kruskal-Wallis statistical test showed that various treatments had a statistically significant effect on kidney scores (p=0.0288). Moreover, Dunn's procedure for multiple comparisons showed that the median kidney score for D2G was significantly greater than the median kidney score for D2N (p=0.0223). The other two comparisons (D2G vs the untreated control, and the untreated control vs D2N) did not differ significantly. Histopathologically, the D2G-treated kidney tissues revealed minimal to mild lymphocytic inflammation associated with mineralized deposits (Figure 2). In contrast, the untreated or D2N tissues typically showed unremarkable to rare small peri-glomerular aggregates of mononuclear cells.

***In-vivo* efficacy**

The antibacterial activities of free gentamicin and the core shell nanostructures were compared in a *S. typhimurium* infection model in AJ 646 mice. The gentamicin nanostructures were tested at two different dosages - viz. 5 and 15 μg g^{-1} to evaluate the efficacy in *in-vivo* bacterial clearance (Table 2). D1N resulted in significant reduction of viable bacteria both in the liver (0.46 log10) and in the spleen (0.25 log10) compared to the untreated control. However, D1G yielded significant reductions of viable bacteria in the liver (0.48 log10) but not in the spleen relative to those recovered from the controls. In contrast, statistically significant reductions in the numbers of viable bacteria in the liver (1.03 log10) and spleen (0.29 log10) were observed for the D2N in comparison to the D2G and infected control ($P < 0.05$).

Discussion

Aminoglycosides are one of the most commonly used classes of antimicrobials against Gram-negative bacteria due to their high efficacy and low costs, but they have the potential to produce nephrotoxic and ototoxic side effects (19, 20). Basically, aminoglycosides are low protein binding drugs that can freely filter in the kidney glomeruli upon parenteral administration without metabolization in the body. However, around 10% of an administered aminoglycoside such as gentamicin can selectively accumulate in kidney tissue and may cause structural and functional damage to the renal tubular cells. Thus, development of new strategies aiming to prevent their accumulation in the renal tissues is highly desirable for reducing toxicity. Also, though aminoglycosides are highly efficacious *in-vitro,* their *in-vivo* activity is limited by an inability to traverse through the phagocytic cell membrane. This is because intracellular penetration of a drug molecule depends on its polarity, and polar drugs cannot permeate readily across non-polar, lipophilic cell membranes. Hence, aminoglycosides such as gentamicin which are cationic and polar have relatively low permeabilities across cell membranes (16).

One means to reduce toxicity and improve efficacy is to favor delivery of drugs to the infected organs. In the case of systemic infection with S. typhimurium, the target organs of infection are the spleen and liver (15). By encapsulating drug molecules in polymeric core-shell nanostructures where the physico-chemical characteristics of the shell have been designed to interact with lipid membranes, internalization by the tissue macrophage cells can be improved.

This reduces transport of free gentamicin to renal tissues and enhances targeting to the liver or spleen. In this research, we utilized an amphiphilic Pluronic F-68 copolymer as the shell, and gentamicin was incorporated into the nanoparticle cores through cooperative electrostatic attractions. To fabricate the nanostructured complexes, a polyanionic $PAA^{-}{}^{+}Na$ homopolymer (10) and $PAA^{-}{}^{+}Na$-*b*-PEO-*b*-PPO-*b*-PEO-*b*-$PAA^{-}{}^{+}Na$ block copolymer were co-dissolved and a polycationic gentamicin sulfate solution (1) was added with sonication to form a final one-to-one ratio of anions to cations. In general, the polyacrylate components formed the core of the complex while the nonionic blocks extended outward into the aqueous medium to form the shells, so the polyacrylate homopolymer was used to "build up" the sizes and drug loadings of the cores as shown schematically in Fig. 1. The non-ionic polyether shell afforded steric repulsion between particles and prevented macroscale agglomeration. The nanostructures prepared via this technique had a drug loading of ~25% by weight of the polymer. However, while the 25% drug loading is high, it is noteworthy to observe that a significant amount of the charged drug was not incorporated and better understanding of this issue will be topic for continuing research. Also, gentamicin releases from the core-shell nanostructure could be a function of cooperativity between the homo and block copolymers and drug. This is evidenced from our previous findings wherein rate of release of gentamicin from nanostructure with pluronic F68 shell was relatively slow compared to free gentamicin at physiological pH 7.4 and 37 °C (22, 23). Even though the overall complexes had a significant net negative charge, they had small zeta potentials in DI water, ranging from -0.7 (±0.2) mV. This suggests that the non-ionic PEO and PEO-*b*-PPO-*b*-PEO shells effectively screened the excess of anionic charges in the core from the environment (28). It has also been suggested that the rate of particle uptake by macrophage cells increases with an increase in size with the minimum recognizable size of ~70-85 nm (7, 25). In our experimental analysis, we observed that the size of the core-shell nanostructure was ~210 (±17) nm but a systematic study of the effect of size has not yet been conducted.

The core-shell nanostructures can be potentially realized in clinical situations by ruling out any toxicity associated with their use in biological systems. This was determined *in-vitro* via an MTS assay which measures mitochondrial activity through the formation of a soluble formazan product which is directly proportional to the number of live cells in culture (29). MTS assays conducted upon incubation of cells with the core-shell nanostructures containing gentamicin

showed no significant differences in absorption compared to untreated control, indicating that the polymers at doses similar to that of the free gentamicin or untreated control were non-toxic *in-vitro* (fig. 2). Further, *in-vivo* studies of renal histopathology were performed independently by two anatomic pathologists to screen for microscopic lesions. Each kidney was given a subjective score from 0 (unremarkable) to 4 (marked). Both evaluators noted minimal to mild increased inflammation in half of the kidneys in the mice group treated with free gentamicin. Additionally, both evaluators noticed mineral deposits within the renal cortex associated with inflammatory cells and these lesions were not present in kidneys from the untreated or core-shell nanostructure treated groups of mice. These lesions are consistent with either the deposition of a mineralized substance eliciting inflammation or chronic regions of inflammation with dystrophic mineralization. The inflammatory infiltrate in these kidneys were predominantly comprised of lymphocytes and macrophages, as has been similarly observed previously for gentamicin nephrotoxicity (6). However, the kidneys did not exhibit distended tubules, hyaline casts, tubular degeneration, glomerular basement membrane alterations or necrosis reported in gentamicin toxicity (27, 31). Plausibly, the single dose administration of gentamicin at 15 $\mu g\ g^{-1}$ body weight of mice may not have been enough to cause concentration dependent toxicity. Repeated administration for multiple times/days to the mice similar to previous studies may shed more light on the protective effects of gentamicin encapsulation against nephrotoxicty (27). Regardless, unremarkable to minimal renal lesions in untreated and core-shell nanostructure treated mice suggest that gentamicin encapsulation may be protective in preventing adverse effects in the kidney.

Finally, AJ-646 mice were infected with *S. typhimurium* and treated with the core-shell nanostructures. The results indicated that at a 15 $\mu g\ g^{-1}$ dose, free gentamicin was ineffective in bacterial clearance. In contrast *Salmonella* was reduced significantly in the liver and spleen tissues in the D2N treated group. Significant reductions in *Salmonella* were also observed on administration of multiple doses of D1N at 5 $\mu g\ g^{-1}$ in the spleen and liver and in the liver of D1G-treated mice respectively. Previous studies conducted with liposomes in an *in-vivo Salmonella* infection model have suggested that the gentamicin levels in plasma, liver and spleen are increased significantly upon encapsulation (8). This consequently has a favorable effect on the bacterial clearance as evidenced by 10(4) reductions in the CFU counts of spleen and liver tissue. In addition, encapsulation increases the circulation time of the drug, thereby enhancing

delivery to the target organ of infection and preventing the free drug from reaching the renal tissues (33). Furthermore, uptake studies in our laboratory have shown that increased amphiphilicity of the gentamicin-polymer core-shell nanostructure significantly improves the amount and rate of uptake by the macrophage cells (23). Thus, improved efficacy in *Salmonella* clearance by the D2N-treated mice could be an interplay of both enhanced delivery and increased uptake by the tissue macrophage cells.

Altogether, the current study shows that improved efficacy and delivery to the infected organs can be achieved by incorporating gentamicin in Pluronic-based core-shell structures. This has a protective effect in preventing adverse toxic effects on the kidney. Future studies aiming to improve the intracellular targeting to the niche where the *Salmonella* reside may enhance the suitability of the core-shell antimicrobial DDS systems.

5. Acknowledgements

The authors are grateful to NSF DMR-0312046 and to Virginia Tech's Institute for Critical and Applied Sciences (ICTAS) for funding.

References:

1. **Abraham, A. M., and A. Walubo.** 2005. The effect of surface charge on the disposition of liposome-encapsulated gentamicin to the rat liver, brain, lungs and kidneys after intraperitoneal administration. Int J Antimicrob Agents **25:**392-7.

2. **Ahmad, Z., S. Sharma, and G. K. Khuller.** 2007. Chemotherapeutic evaluation of alginate nanoparticle-encapsulated azole antifungal and antitubercular drugs against murine tuberculosis. Nanomedicine **3:**239-43.

3. **Alakhov, V., E. Klinski, P. Lemieux, G. Pietrzynski, and A. Kabanov.** 2001. Block copolymeric biotransport carriers as versatile vehicles for drug delivery. Expert Opin Biol Ther **1:**583-602.

4. **Bajema, I. M., E. C. Hagen, B. E. Hansen, J. Hermans, L. H. Noel, R. Waldherr, F. Ferrario, F. J. van der Woude, and J. A. Bruijn.** 1996. The renal histopathology in systemic vasculitis: an international survey study of inter- and intra-observer agreement. Nephrol Dial Transplant **11:**1989-95.

5. **Batrakova, E. V., and A. V. Kabanov.** 2008. Pluronic block copolymers: evolution of drug delivery concept from inert nanocarriers to biological response modifiers. J Control Release **130:**98-106.

6. **Bledsoe, G., S. Crickman, J. Mao, C. F. Xia, H. Murakami, L. Chao, and J. Chao.** 2006. Kallikrein/kinin protects against gentamicin-induced nephrotoxicity by inhibition of inflammation and apoptosis. Nephrol Dial Transplant **21:**624-33.

7. **Chono, S., and K. Morimoto.** 2006. Uptake of dexamethasone incorporated into liposomes by macrophages and foam cells and its inhibitory effect on cellular cholesterol ester accumulation. J Pharm Pharmacol **58:**1219-25.

8. **Cordeiro, C., D. J. Wiseman, P. Lutwyche, M. Uh, J. C. Evans, B. B. Finlay, and M. S. Webb.** 2000. Antibacterial efficacy of gentamicin encapsulated in pH-sensitive

liposomes against an in vivo Salmonella enterica serovar typhimurium intracellular infection model. Antimicrob Agents Chemother **44:**533-9.

9. **Fattal, E., J. Rojas, L. Roblot-Treupel, A. Andremont, and P. Couvreur.** 1991. Ampicillin-loaded liposomes and nanoparticles: comparison of drug loading, drug release and in vitro antimicrobial activity. J Microencapsul **8:**29-36.

10. **Gupta, K., M. Ganguli, S. Pasha, and S. Maiti.** 2006. Nanoparticle formation from poly(acrylic acid) and oppositely charged peptides. Biophys Chem **119:**303-6.

11. **Joss, N., S. Morris, B. Young, and C. Geddes.** 2007. Granulomatous interstitial nephritis. Clin J Am Soc Nephrol **2:**222-30.

12. **K, K.** 2006. The emergence of nanomedicine: a field in the making. Nanomedicine **1:**1-3.

13. **Kabanov, A. V., and V. Y. Alakhov.** 2002. Pluronic block copolymers in drug delivery: from micellar nanocontainers to biological response modifiers. Crit Rev Ther Drug Carrier Syst **19:**1-72.

14. **Kabanov, A. V., E. V. Batrakova, and V. Y. Alakhov.** 2002. Pluronic block copolymers as novel polymer therapeutics for drug and gene delivery. J Control Release **82:**189-212.

15. **Lahiri, A., P. Das, and D. Chakravortty.** 2009. Salmonella Typhimurium: Insight into the multi-faceted role of the LysR-type transcriptional regulators in Salmonella. Int J Biochem Cell Biol.

16. **Lecaroz, C., C. Gamazo, and M. J. Blanco-Prieto.** 2006. Nanocarriers with gentamicin to treat intracellular pathogens. J Nanosci Nanotechnol **6:**3296-302.

17. **Lutwyche, P., C. Cordeiro, D. J. Wiseman, M. St-Louis, M. Uh, M. J. Hope, M. S. Webb, and B. B. Finlay.** 1998. Intracellular delivery and antibacterial activity of gentamicin encapsulated in pH-sensitive liposomes. Antimicrob Agents Chemother **42:**2511-20.

18. **Ma, G., C. Song, H. Sun, J. Yang, and X. Leng.** 2006. A biodegradable levonorgestrel-releasing implant made of PCL/F68 compound as tested in rats and dogs. Contraception **74:**141-7.

19. **Nagai, J.** 2006. [Molecular mechanisms underlying renal accumulation of aminoglycoside antibiotics and mechanism-based approach for developing nonnephrotoxic aminoglycoside therapy]. Yakugaku Zasshi **126:**327-35.

20. **Nagai, J., and M. Takano.** 2004. Molecular aspects of renal handling of aminoglycosides and strategies for preventing the nephrotoxicity. Drug Metab Pharmacokinet **19:**159-70.

21. **Neudeck, B. L., T. D. Alford, N. G. Faith, and C. J. Czuprynski.** 2008. The poloxamer P85 is protective against Listeria monocytogenes invasion. Foodborne Pathog Dis **5:**859-65.

22. **Ranjan A, P. N., Seleem M, Jain J, Sriranganathan N , Riffle J. S. and Kasimanickam R.** 2009. Drug delivery using novel nanoplexes against a Salmonella mouse infection model J Nanopart Res **DOI 10.1007/s11051-009-9641-y**.

23. **Ranjan A, P. N., Seleem MN, Sriranganathan N, Kasimanickam R, Makris M, Riffle JS.** 2009. In-vitro trafficking and efficacy of core-shell nanostructures for treating intracellular Salmonella. **53**.

24. **Ristuccia, A. M., and B. A. Cunha.** 1982. The aminoglycosides. Med Clin North Am **66:**303-12.

25. **Rudt S, M. R.** 1993. In vitro phagocytosis assay of nano- and microparticles by chemiluminescence. III. Uptake of differently sized surface-modified particles, and its correlation to particle properties and in vivo distribution. European journal of pharmaceutical sciences **1:31-39.**

26. **Silva, J. G., and I. Carvalho.** 2007. New insights into aminoglycoside antibiotics and derivatives. Curr Med Chem **14:**1101-19.

27. **Stojiljkovic, N., S. Veljkovic, D. Mihailovic, M. Stoiljkovic, M. Radenkovic, G. Rankovic, and P. Randjelovic.** 2009. Protective effects of pentoxifylline treatment on gentamicin-induced nephrotoxicity in rats. Ren Fail **31:**54-61.

28. **Tang, G. P., J. M. Zeng, S. J. Gao, Y. X. Ma, L. Shi, Y. Li, H. P. Too, and S. Wang.** 2003. Polyethylene glycol modified polyethylenimine for improved CNS gene transfer: effects of PEGylation extent. Biomaterials **24:**2351-62.

29. **Theas, M. S., C. Rival, S. Jarazo-Dietrich, P. Jacobo, V. A. Guazzone, and L. Lustig.** 2008. Tumour necrosis factor-alpha released by testicular macrophages induces apoptosis of germ cells in autoimmune orchitis. Hum Reprod **23:**1865-72.

30. **Tian, Y., L. Bromberg, S. N. Lin, T. A. Hatton, and K. C. Tam.** 2007. Complexation and release of doxorubicin from its complexes with pluronic P85-b-poly(acrylic acid) block copolymers. J Control Release **121:**137-45.

31. **Ulutas, B., M. Sarierler, G. Bayramli, and K. Ocal.** 2006. Macroscopic findings of idiopathic congenital megaoesophagus in a calf. Vet Rec **158:**26.

32. **VV, T.** 1998. Drug therapy in pet rodents. Veterinary Medicine **93:**988-991.

33. **Webb MS, B. N., Wiseman DJ, Saxon D, Sutton K, Wong KF, Logan P, Hope MJ.** 1998 Jan;. Antibacterial efficacy against an in vivo Salmonella typhimurium infection model and pharmacokinetics of a liposomal ciprofloxacin formulation. Antimicrob Agents Chemother **42(1):**:45-52.

34. **Yang, Z., G. Sahay, S. Sriadibhatla, and A. V. Kabanov.** 2008. Amphiphilic block copolymers enhance cellular uptake and nuclear entry of polyplex-delivered DNA. Bioconjug Chem **19:**1987-94.

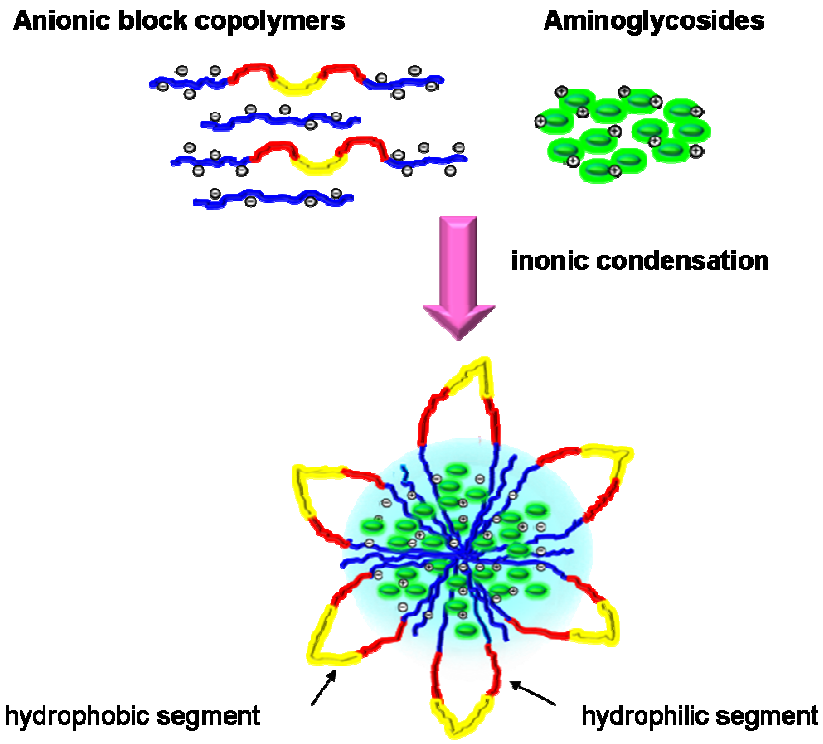

Fig.2.3.1: Schematic illustration of methodology for preparing core-shell nanostructure encapsulating Gentamicin

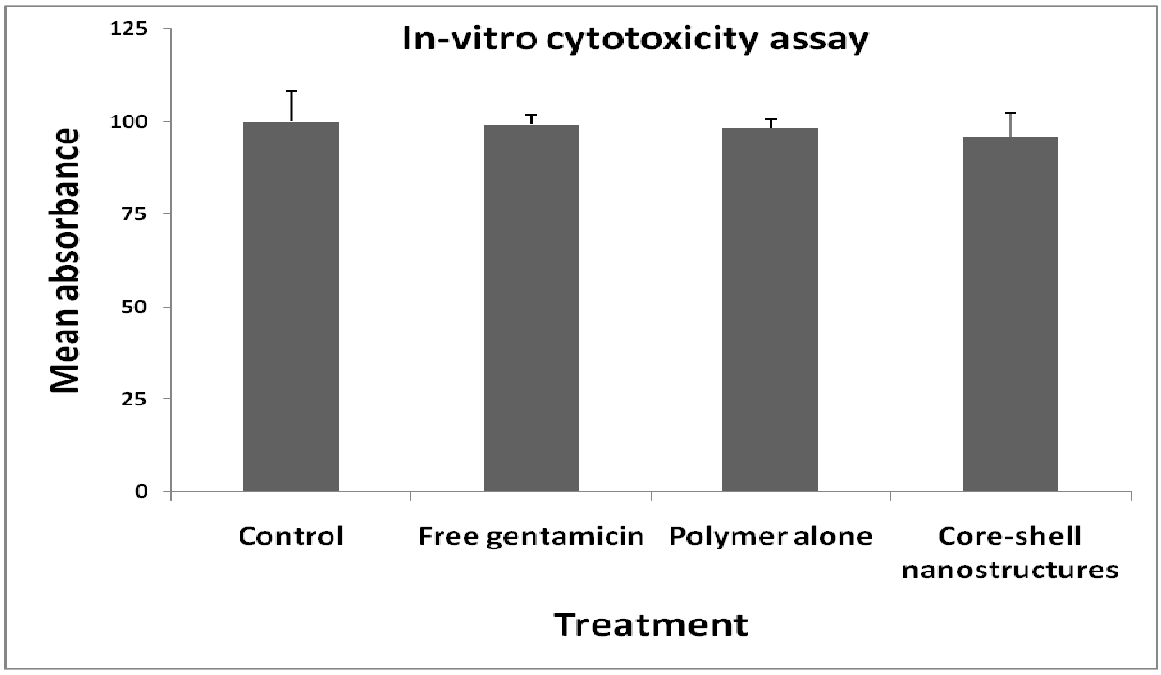

**No significant difference between treatments at $p< 0.05$

Fig. 2.3.2: MTS assay showing the percentage mean absorbance (depicted by % cell viability at wavelength of 490 nm) after incubating J774A.1 cells with 250 µg mL^{-1} of core-shell nanostructures along with appropriate controls. Results are expressed as means ± SD of six measurements. $^{**}P < 0.05$, ANOVA.

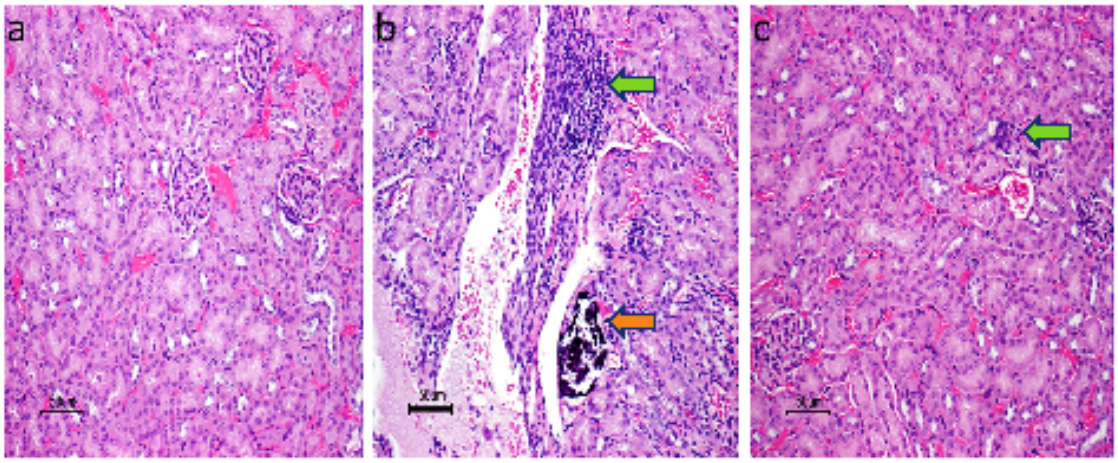

Fig.2.3.3: Histopathological microscopic images of kidney tissues of AJ-646 mice euthanized 5 days after intraperitoneal administration: (a) Untreated control group; (b) D2G treated group: Minimal to mild lymphocytic inflammation (green arrow) associated with mineralized deposits (orange arrows); (c) D2N treated group: Typically unremarkable to rare small peri-glomerular aggregates of mononuclear cells (arrow). The tissues were hematoxylin and eosin stained. Scale bar represents 50 µm.

Table 2.3.1: Kidney scoring by individual pathologist

Kidney #	Kidney score- D2N		Kidney Score- Untreated		Kidney Score- D2G	
	1st Pathologist	2nd Pathologist	1st Pathologist		1st Pathologist	2nd Pathologist
1	0	0	0	0	2***	2***
2	0	0	0	0	2***	2***
3	0	0	1	0	1	1
4	0	0	0*	0*	0	0
5	0	0	1*	0*	0	1
6	0	0	0	0*	1**	1
7	0	0	0	0	0	0
8	0	0	0	0	2***	0
9	1	0	0	0	0	0
10	0	0	0	0	0	0

* = mineralization of renal epithelium lining renal papilla collecting ducts.

** = mineralized deposits randomly scattered within the cortex and in medulla

*** = indicates mineralized deposits in the cortex associated with inflammatory cells

Kidney Scores:

0- normal

1 - minimal inflammation

2- mild inflammation

3- moderate inflammation

4- marked inflammation

Table 2.3.2: Efficacy cfu (log) reduction) of free gentamicin or core-shell nanostructure polymers in liver and spleen from Salmonella infected mouse.

Treatment	Liver cfu (log) (CI)	Liver cfu (log) reduction	Spleen cfu (log) (CI)	Spleen cfu (log) reduction
Infected control	4.18 (3.98, 4.29)	0.00	3.89 (3.76, 4.28)	0.00
D1N	3.72 (3.28, 3.88)	0.46 [a]	3.64 (3.50, 3.69)	0.25 [a]
D1G	3.70 (3.29, 3.75)	0.48 [a]	3.98 (3.83, 4.01)	-0.09
D2N	3.11 (2.99, 3.53)	1.07 [a]	3.60 (3.48, 4.02)	0.29 [a]
D2G	3.95 (3.92, 3.98)	0.23	4.23 (4.13, 4.32)	-0.34

[a]Significantly different from control ($P<0.05$)

Chapter 3

Improved drug delivery approach for intracellular *Salmonella*

Chapter 3.1

Efficacy of Pluronic P85 core-shell nanostructures encapsulating gentamicin against *in-vitro Salmonella* and *Listeria* intracellular infection model

(To be submitted)

Abstract

Intracellular pathogens like *Salmonella* evade host pathogenic killing by various mechanisms and requires cell specific delivery of antimicrobials. Core-shell nanostructures with amphiphilic pluronic shells and encapsulating gentamicin in the cores were designed to develop alternative therapy for intracellular pathogens. Flow cytometry, confocal microscopy, and specific inhibitors, were used to investigate the influence of shell chemistry on nanostructure uptake by cells. Flow cytometry and confocal microscopy determined that the rate of uptake of nanostructure with amphiphilic shells was significantly higher than nanostructures with hydrophilic shells and they entered cells mainly by fluid phase endocytosis and clathrin mediated pathway. The nanostructures were non-toxic *in-vitro* at a dose range of 50-250 μg/mL upon incubation with macrophages. Upon treatment of infected macrophages with nanostructure encapsulating gentamicin, bacterial clearance was shown to be dependent on the sub-cellular localization of bacteria. Nanostructure encapsulating gentamicin achieved significant reduction of vacuolar resident *Salmonella* (0.53 log) and intracytoplasmic *Listeria* (3.16 log) suggesting that targeting of *Salmonella* was less effective compared to *Listeria*. In conclusion, our study showed that encapsulation of gentamicin in the cores of nanostructure improves intracellular drug delivery and the efficacy was correlated with the sub-cellular localization of bacterium.

Introduction

Aminoglycosides are a group of antibiotics that exhibits antimicrobial activity against both Gram-positive and Gram-negative bacteria. Gentamicin like other aminoglycosides binds to ribosomal components in the bacterial cell, resulting in production of abnormal proteins and

subsequent killing of the bacterium (5). Though the efficacy of gentamicin is well known yet its poor cell membrane permeability limits their clinical use, particularly against many intracellular bacterial infections (6). Moreover, their action is concentration dependent and therefore requires a careful regimen of dosage (2). To favor better gentamicin delivery inside the cells, liposomal and polymeric drug delivery system (DDS) has been reported to improve intracellular bacterial clearance (12, 13). These DDS suffers from poor gentamicin incorporation and releasing efficiency. Thus novel tools are required to enhance the encapsulation efficiency and controlling the parameters influencing the intracellular release of antimicrobials. In this regards, pluronic based DDS may be highly efficient and requires further investigation.

Pluronics are a FDA approved polaxamer family of polyether with a triblock structure (PEO-b-PPO-b-PEO) and are used primarily as excipients in pharmaceutical industry (4, 27). Pluronic based core-shell nanostructures have already been formulated for anticancer drugs. For example, the synthesis of cores containing polyelectrolyte counterion for interaction with polyelectrolyte drugs is a significant development (4, 9). These nanostructures appear to provide a controlled and targeted delivery of drugs, alter pathways of bio-circulation, modify the cellular distribution, and improve the amount of intracellular delivery. Considering the polycationic nature of aminoglycosides like gentamicin, incorporation of such drugs in a mixed population of polyanionic homopolymeric cores with amphiphilic shells through cooperative electrostatic interaction is highly favored. We previously reported synthesis of core-shell nanostructure encapsulating gentamicin with amphiphilic shell containing pluronic F68 (21). In this study we aimed to enhance the *in-vitro* delivery of the gentamicin by encapsulating it in core-shell nanostructures; the cores constituted by polyacrylate homopolymers and shells made by block copolymer of pluronic P85 and polyacrylates. Pluronic P85 has been shown to enhance gene expression in the injection site of the myocytes/karyocytes in the muscle and macrophage and dendritic cells of the distant organs, especially the draining lymph nodes and spleen (7). Recently, pluronic P85 was reported to be protective against listeriosis in mice, through modulation of the host cell's ATP (17). Therefore, investigating the direct use of P85 by including them in the shell of core-shell nanostructure in control of intracellular infection may be highly interesting to explore.

Although core-shell nanostructure encapsulating gentamicin with amphiphilic shell containing pluronic F68 resulted in significant reduction in intracellular *Salmonella* in our previous studies, more studies are required to understand the mechanism of killing. It is noteworthy that intracellular bacteria evades killing by the phagocytic cells by virtue of their subcellular localization in niches sequestered from the immune system (15). For example, *Salmonella* and *Listeria* reside in different niche inside the cell viz. in *Salmonella* containing vacuole (SCV) and cytoplasm respectively (1, 24). An understanding of the influence of sub-cellular localization in intracellular bacterial clearance by DDS may be highly valuable in controlling nanostructure properties. The objective of this study was to synthesize pluronic P85 based core-shell nanostructures encapsulating gentamicin, study their uptake mechanism by the macrophages and *in-vitro* efficacy based on sub-cellular localization against intracellular *Salmonella* and *Listeria* as a control for cytoplasmic localization.

Materials and Methods

Synthesis of nanostructures:

All chemicals were purchased from Sigma-Aldrich unless otherwise noted. Pluronic P85™ (PEO-*b*-PPO-*b*-PEO) was kindly provided by BASF. Poly(tert-butyl acrylate-b-PEO-b-PPO-b-PEO-b-tert-butylacrylate) or (PtBA-b-PEO-b-PPO-b-PEO-b-PtBA) was synthesized via controlled Atom Transfer Radical Polymerization (ATRP) through a method adapted from the literature (8, 26). Initially, PtBA-*b*-PEO-*b*-PPO-*b*-PEO-*b*-PtBA copolymer (2.0 g, 1.09 x 10^{-2} eq of t-butyl ester groups) was dissolved in 30 mL of dichloromethane, then trifluoroacetic acid (5 mL, 6.50 x 10^{-2} mol) was added slowly over 30 min and the reaction mixture was stirred at room temperature overnight. The solvent was evaporated at 40 ^{o}C under vacuum and the residue was dissolved in TetraHydroFuran (THF) and subsequently dialyzed against 4 L of DI water through a cellulose acetate membrane (MWCO 3,500 g mol^{-1}) for 72 h. The poly(acrylic acid-*b*-PEO-*b*-PPO-*b*-PEO-*b*-acrylic acid) (PAA-*b*-PEO-*b*-PPO-*b*-PEO-*b*-PAA) was recovered by freeze-drying and followed by drying at 40 ^{o}C under vacuum. Core-shell nanostructures containing gentamicin wherein pentablock copolymers of $PAA^{-}{}^{+}Na$ (2500 MW)-*b*-PEO (1100 MW)-*b*-PPO (2300 MW)-*b*-PEO (1100 MW)-*b*-$PAA^{-}{}^{+}Na$ (2500 MW) were mixed with diblock copolymers of $PAA^{-}{}^{+}Na$ (7100 MW)-*b*-PEO (2000 MW) and condensed with gentamicin shown schematically in Fig. 3.1.1. To prepare the nanostructures, the P85PAA copolymer described

above (25 mg, 1.68 x 10^{-4} eq of anions) and 25 mg of PEOPAA (1.63 x10^{-4} eq of anions) were charged to a 100-mL round-bottom flask and dissolved in 25 mL PBS. The solution was placed in a sonication bath and 5 mL of gentamicin sulfate solution (5.2 mg mL^{-1} gentamicin sulfate equal to 31 mg gentamicin, 3.31 x 10^{-4} eq of cations) was added via syringe to form a turbid dispersion. The resulting complexes were collected by ultra-centrifugation of the solution at 20,000 rpm for 15 min (Optima™ L-XP Ultracentrifuge, Beckman Coulter Inc.). The supernatant was removed and the centrifugate was rinsed twice with DI water. Finally, the complex was recovered by freeze-drying.

Preparation of fluorescent nanostructures

Fluorescein-NHS (10 mg, 2.10 x 10^{-5} mol) dissolved in 0.5 mL DMF was slowly added to a gentamicin solution (37 mg gentamicin sulfate, 22 mg gentamicin, 5.15 x 10^{-5} mol, 1.55 x 10^{-4} mol primary amines) in 2 mL phosphate buffer, pH 7.4. The mixture was allowed to react in the dark at room temperature for 24 h and used without further purification. PNF was prepared by adding the solution of fluorescein-gentamicin (1 mL, 8.8 mg gentamicin) to 4 mL of the gentamicin sulfate solution (37 mg gentamicin sulfate, 22 mg gentamicin) in DI water. This mixture was subsequently added drop wise to the polymer solution (with sonication) to prepare the nanostructures. PNF was recovered as described above by ultracentrifugation.

Trafficking assay

J774A.1 macrophages were grown in tissue culture flasks using Dulbecco Modified Eagle Medium (DMEM) cell culture medium supplemented with 10% Fetal bovine serum (FBS) and 1% penicillin–streptomycin at 37℃ with 5% CO_2 in an incubator. Macrophages were harvested by gently scrapping in 5 mL of culture media at 70–90% confluency, resuspended in 45 mL of culture media and seeded with 2 mL of cell suspension at a rate of (1.25x10^5 cells/ml) onto 24 well cell culture plate. Prior to the experiment, culture medium was discarded from 24 wells and cells in the wells were incubated with fresh serum free DMEM medium. To study the effect of various inhibitors on the uptake of PN nanostructure, the cells were pre-incubated with the clathrin (chlorpromazine), caveolar (filipin) and fluid phase endocytosis (sucrose) inhibitors at the following concentrations: (i) 10 µg/ml of chlorpromazine for 30 min, (ii) 5 µg/ml of filipin for 30 min, (iii) 450mM of sucrose for 30 min as described previously (18). Following this, the

cells were incubated with 15 µg/mL of PNF for 2 h, then the culture media was discarded, and the cells were recovered by gentle scrapping in 2mL of cold Hanks Balanced Salt solution (HBBS) in 15 mL falcon tubes. The cell suspension was centrifuged at 1500 rpm for 5 min to obtain a cell pellet, rinsed with HBBS buffer, spun down, resuspended in 100 µL of HBBS, and subsequently the fluorescence intensity of each sample was analyzed by FACS flow cytometry (BD FACS Aria, USA) with an excitation wavelength of 488 nm and analyzed with a 530/30 nm emission filter by counting 5,000 single cell events. Only the viable cells were gated for fluorescence analysis. The geometric mean fluorescence intensity of the cells was computed from the histogram plot calculated from triplicate data. Also, to study rate of uptake of PNF in comparison to hydrophilic nanostructures (HNF), the J774A.1 cells were co-incubated with 15 µg of PNF and HNF for 2 h in a 5% CO2 atmosphere at 37 °C and processed for flow cytometry as explained previously.

Confocal Experiment

For microscopic examinations, 1 x 10^5 J774A.1 cells suspended in 250 µL of DMEM with 10% FBS were seeded into the 10-mm diameter microwell of 35 mm petridishes (Mat-tek Corporation, USA) and incubated for 1 h at 37 °C in a humidified 5% CO_2 atmosphere to allow the cells to attach onto the glass surface. After incubation, the remainder of the dish was gently filled with 2 mL of DMEM medium containing 10% FBS and the dishes were incubated for 48 h at 37 °C in a humidified 5% CO_2 atmosphere. Prior to the experiment, the cells in each microwell were washed with 2 mL of PBS, added with 10 µg/well of either PNF or Alexa fluor 488 (positive control for endosomal pathway) in each well, then each petridish was gently filled with DMEM supplemented with 10% FBS, and the contents were incubated for 2 h at 37 °C in a humidified 5% CO_2 atmosphere. In addition, an Image-iT live lysosomal and nuclear labeling kit (Invitrogen, USA) was used to stain the lysosome/endosome and nuclear compartments of the cells. After incubation with the nanostructures for 2 h, the cells were washed twice with PBS. Hoechst 33342 (excitation/emission maxima ~350/461 nm) was added to the microwells (2.0 µg/mL Hanks balanced salt solution (HBSS) and the contents were incubated for 5 min at 37 °C in a 5% CO_2 atmosphere to stain the nuclei (blue). Later, the cells were washed three times with 1 mL each of HBSS and incubated with LysoTracker Red DND-99 (excitation/emission maxima ~577/590 nm) for 1 min at room temperature. The LysoTracker Red DND-99 dye was used at a

concentration of 100 nM/well for staining acidic cell organelles such as endosomes and lysosomes. Following incubation, the cells were washed twice with 1 mL each of HBSS and mounted on the microscope slide. The wells were examined using a 63x oil-immersion objective on a Zeiss LSM 510 META confocal microscope (Thornwood, USA).

***In-vitro* toxicity assessment**

An *in-vitro* homogeneous, colorimetric method for determining the number of viable J774A.1 cells using the CellTiter 96® AQ_{ueous} Non-Radioactive Cell Proliferation Assay (Promega, USA) was used to determine any cytotoxic effects of P85 pluronic and core-shell nanostructures. Briefly, ~2 x 10^4 J774A.1 cells suspended in 200 µL of DMEM supplemented with 10% fetal bovine serum (FBS), L-glutamine, $NaHCO_3$, pyridoxine-HCl, and 45,000 mg/L glucose and preserved with 1% penicillin-streptomycin solution were seeded in 96-well plates and incubated for 24 hours at 37 °C in a 5% CO_2 atmosphere. Later, the J774A.1 cells were incubated with a dose range of 5- 50 µg/well of free gentamicin, pluronic P85 (PEO-*b*-PPO-*b*-PEO), copolymers (PAA-*b*-PEO-*b*-PPO-*b*-PEO-*b*-PAA), core-shell nanostructure PN along with untreated control for 24 hours. Following this, the culture media was discarded, and the cells in each well were washed with PBS and re-suspended with 100 µL of cell culture media. Then 20 µL of CellTiter 96® AQ_{ueous} reagent solution was pipetted into each well, and the plates were incubated for 4 hours at 37 °C in a humidified 5% CO_2 atmosphere. The absorbance at 490 nm was recorded using a 96-well Elisa plate reader.

***In-vitro* cell culture experiment**

The ability of the PN to kill intracellular bacteria was evaluated in an intracellular *Salmonella typhimurium* strain LT2 (14) and *Listeria monocytogenes (wild type)* infection model. Initially, J774A.1 cells were seeded at 2×10^5 cells/well in 24-well plates and grown at 37°C in 5% CO_2 in DMEM plus 10% FBS for 48 h. Then, stock cultures of *S. typhimurium* and *L. monocytogenes* adjusted to a multiplicity of infection (MOI) of 10 bacteria per macrophage in DMEM supplemented with 10% FBS was added to the macrophages and incubated at 37°C in 5% CO_2 for 30 min. After incubation, the culture medium was discarded, each well was incubated with 2 mL of fresh DMEM supplemented with 10% FBS containing 25 µg/mL gentamicin for 30 min to kill extracellular bacteria, then washed twice with PBS containing Ca^{++} and Mg^{++} and further

incubated with 2 mL of fresh DMEM supplemented with 10% FBS. At this stage, infected cells were treated with 25 µg/mL of gentamicin in solution or PN, then uptake and treatment was allowed to proceed for 6 h at 37°C in 5% CO_2. A control group of cells without drug or nanostructures was compared. Finally, the wells were washed with PBS containing Ca^{++} and Mg^{++}, the number of colony forming units (CFU)/well was determined after lysing the macrophages with cold 1% Triton X-100 for 15-20 min at 37 °C and plating the serial dilutions of the lysates onto Tryptic soy agar (TSA) plates at 37°C for 24 h. For each treatment and control, triplicate assays were performed for statistical analysis. For statistics, groups were compared for differences in mean CFU using ANOVA followed by Tukey's procedure for multiple comparisons.

Results

Trafficking Assay

Based on the median fluorescence intensity of PNF, flow cytometry study suggests that the uptake of PNF nanostructures is significantly reduced in the presence of chlorpromazine (~ 46%) and sucrose (~40%) compared to PNF alone. In contrast, filipin is not significant in inhibiting particle uptake when compared to PNF alone (Fig. 3.1.2). Also, the rate of uptake of PNF was significantly higher than HNF at 2 h of incubation ($p< 0.05$) (Fig. 3.1.3).

Confocal microscopy

The PNF were phagocytosed successfully upon incubation with the macrophage cells (Fig 3.1.4 a). In agreement with flow cytometry, PNF uptake by macrophage cells is through multiple mechanisms. Co-localization studies showed PNF in the endosomes/lysosome indicated by distinct yellow-to-orange spots formed by co-localization of green particles and red lysotracker inside the cells (Fig 3.1.4b). In addition, green PNF nanostructures were also observed in cell cytoplasm suggesting uptake by a different mechanism. In contrast, majority of Alexa fluor-488 appeared to reside in endosomes (Fig. 3.1.4c - Positive control for endosomal pathway).

MTS assay

Co-incubation of J774A.1 cells with PN did not result in significant difference in absorbance compared to free gentamicin, pluronic, copolymer or untreated control in the dose range of 5-50

μg/well ($p<0.05$). For all dose ranges, the absorbance was comparable or higher than untreated control indicating lack of toxicity (Fig. 3.1.5).

In-vitro cell culture experiment

The efficacy of PN to augment intracellular bacterial reduction based on sub-cellular location was determined in infected J774A.1 cells. Free gentamicin, copolymer alone or infected control did not show significant difference in their ability to clear intracellular *Salmonella* or *Listeria*. In contrast, PN resulted in a significant reduction of intracellular *Salmonella* (0.53 log) and Listeria (3.16log) ($p\leq0.05$) as shown in Table 3.1.1 and Table 3.1.2.

Discussion

Gentamicin inspite of being highly efficacious *in-vitro* is poorly permeable across the cell membrane (11). Due to its high solubility and polarity, gentamicin upon parenteral administration at the maximum tolerated doses remains largely in the extracellular location and is filtered rapidly by the kidney (13, 16). We had previously reported that the surface properties of DDS has an influence on the rate of uptake and efficacy of the core-shell nanostructures encapsulating gentamicin (22). In this study, similar to our previous finding, laboratory results indicate that the rate of uptake of amphiphilic PNF nanstructures is higher than that of hydrophilic HNF nanostructures (Fig. 3.1.3). Also, PNF core-shell nanostructures appears to enter the cells by multiple pathways. Inhibition studies using flow cytometry showed that the particle follows both clathrin mediated and an alternative pathway mediated mainly by fluid phase endocytosis (Fig. 3.1.2). Though the inhibitor of fluid phase endocytosis (sucrose) can also inhibit clathrin-dependent receptor internalization by blocking clathrin-coated pit formation (25), previous research studies have shown that the inhibition is largely non-specific and affects multiple pathways (18). This was verified by confocal micrographs in our study which were in agreement with the flow cytometry analysis (Fig. 3.1.4). The P85 nanostructures appeared to colocalize within the endosomes and were also observed in the cytoplasm. Previous studies with FITC labelled P85 upon incubation with bovine brain microvessel endothelial cell have similarly shown that the block copolymer spreads/distributes throughout the cell and interacts with various intracellular targets, including mitochondria (3). Additionally, inhibition of caveolar mediated pathway (filipin) did not result in any decrease in uptake compared to control. Thus, it is

plausible that the improved intracellular delivery of PNF could be an interplay of straight delivery of nanostructures by fluid phase endocytosis into the cytosol or an escape of PNF from the endosome upon uptake by clathrin mediated pathway. Live cell time scale microsopy tracking the movement of nanostructures inside cells may shed more light on this phenomenon.

In-vitro MTS assay results suggested that the viability of the macrophage is not affected after incubation with the P85 nanostructures encapsulating gentamicin, copolymer, free gentamicin or P85 alone (Fig. 3.1.5). In agreement with previous results, under optimum incubation conditions of 37℃, P85 did not affect cell viability (10). However, pluronic P85 alone at a sublethal temperatuture of 43℃ in synergy with time can affect tumor cell viability by depleting intracellular ATP to fatal levels. Also, in some cases, higher values of absorbance were observed for various treatments compared to untreated control signifying higher mitochondrial activity and an enhanced metabolic state of the cells.

We had previously reported that treatment with polyacrylate based nanoplex encapsulating gentamicin significantly reduces the viable number of intracellular bacteria *in-vitro* and *in-vivo* (19, 20). *In-vitro* treatment efficacy studies showed similar findings with P85 nanostructures. In addition we also observed that the percentage log reduction compared to control is dependent on the intracellular localization of bacteria (Table 3.1.1 and 3.1.2). Upon treatment with gentamicin, the log reduction achieved for *Salmonella* and *Listeria* was 0.53 $\log_{10}$ and 3.11 $\log_{10}$ respectively. This is plausible since the vacuolar resident Salmonella are not exposed to a high dose of antimicrobial due to membrane barriers. In contrast, cytoplasm resident *Listeria* can directly interact with the drug molecules like gentamicin favoring efficient clearance. Intracellular escape of *Salmonella* from the cell is partially dependent on duration of infection. Thus, the observed reduction in *Salmonella* could be due to the escape of flaggelated bacilli from the SCV's and direct exposure to the free drug in the cell cytoplasm (23). In other words, the nanostructures may not be directly targeting the SCV but interacting with the flagellated *Salmonella* which are in cell cytoplasm. Development of DDS with an ability to release drug in a time dependent manner in the cell cytosol may be highly valuable for such treatment scenarios. Thus, it suggest that efficacy of this DDS is directly correlated/dependent on the location of the bacterium inside the cells.

In summary, our studies showed that the rate and route of uptake may be modified by increasing the amphiphilicity of the drug carrier. The efficacy of P85 DDS is dependent on the subcellular localization of bacteria. Higher clearance is achieved with the cytoplasm resident bacteria compared to the vacuolar resident bacteria. Future studies aiming to target the different intracellular niche of the bacterium may help develop an effective clearance strategy.

Acknowledgements

The authors are grateful to NSF DMR-0312046 and to Virginia Tech's Institute for Critical and Applied Technologies (ICTAS) for funding.

References:

1. **Bakowski, M. A., V. Braun, and J. H. Brumell.** 2008. Salmonella-containing vacuoles: directing traffic and nesting to grow. Traffic **9:**2022-31.
2. **Barclay, M. L., E. J. Begg, and K. G. Hickling.** 1994. What is the evidence for once-daily aminoglycoside therapy? Clin Pharmacokinet **27:**32-48.
3. **Batrakova, E. V., and A. V. Kabanov.** 2008. Pluronic block copolymers: evolution of drug delivery concept from inert nanocarriers to biological response modifiers. J Control Release **130:**98-106.
4. **Bromberg, L.** 2008. Polymeric micelles in oral chemotherapy. J Control Release **128:**99-112.
5. **Campos, M. G., H. R. Rawls, L. H. Innocentini-Mei, and N. Satsangi.** 2009. In vitro gentamicin sustained and controlled release from chitosan cross-linked films. J Mater Sci Mater Med **20:**537-42.
6. **Gamazo, C., M. C. Lecaroz, S. Prior, A. I. Vitas, M. A. Campanero, J. M. Irache, and M. J. Blanco-Prieto.** 2006. Chemical and biological factors in the control of Brucella and brucellosis. Curr Drug Deliv **3:**359-65.
7. **Gaymalov, Z. Z., Z. Yang, V. M. Pisarev, V. Y. Alakhov, and A. V. Kabanov.** 2009. The effect of the nonionic block copolymer pluronic P85 on gene expression in mouse muscle and antigen-presenting cells. Biomaterials **30:**1232-45.
8. **Hou, S. J., E. L. Chaikof, D. Taton, and Y. Gnanou.** 2003. Synthesis of water-soluble star-block and dendrimer-like copolymers based on poly(ethylene oxide) and poly(acrylic acid). Macromolecules **36:**3874-3881.
9. **Kataoka, K., A. Harada, and Y. Nagasaki.** 2001. Block copolymer micelles for drug delivery: design, characterization and biological significance. Adv Drug Deliv Rev **47:**113-31.
10. **Krupka, T. M., D. Dremann, and A. A. Exner.** 2009. Time and dose dependence of pluronic bioactivity in hyperthermia-induced tumor cell death. Exp Biol Med (Maywood) **234:**95-104.
11. **Lecaroz, C., C. Gamazo, and M. J. Blanco-Prieto.** 2006. Nanocarriers with gentamicin to treat intracellular pathogens. J Nanosci Nanotechnol **6:**3296-302.

12. **Lecaroz, C., C. Gamazo, M. J. Renedo, and M. J. Blanco-Prieto.** 2006. Biodegradable micro- and nanoparticles as long-term delivery vehicles for gentamicin. J Microencapsul **23:**782-92.

13. **Lutwyche, P., C. Cordeiro, D. J. Wiseman, M. St-Louis, M. Uh, M. J. Hope, M. S. Webb, and B. B. Finlay.** 1998. Intracellular delivery and antibacterial activity of gentamicin encapsulated in pH-sensitive liposomes. Antimicrob Agents Chemother **42:**2511-20.

14. **McClelland, M., K. E. Sanderson, J. Spieth, S. W. Clifton, P. Latreille, L. Courtney, S. Porwollik, J. Ali, M. Dante, F. Du, S. Hou, D. Layman, S. Leonard, C. Nguyen, K. Scott, A. Holmes, N. Grewal, E. Mulvaney, E. Ryan, H. Sun, L. Florea, W. Miller, T. Stoneking, M. Nhan, R. Waterston, and R. K. Wilson.** 2001. Complete genome sequence of Salmonella enterica serovar Typhimurium LT2. Nature **413:**852-6.

15. **Monack, D. M., D. M. Bouley, and S. Falkow.** 2004. Salmonella typhimurium persists within macrophages in the mesenteric lymph nodes of chronically infected Nramp1+/+ mice and can be reactivated by IFNgamma neutralization. J Exp Med **199:**231-41.

16. **Nagai, J., and M. Takano.** 2004. Molecular aspects of renal handling of aminoglycosides and strategies for preventing the nephrotoxicity. Drug Metab Pharmacokinet **19:**159-70.

17. **Neudeck, B. L., T. D. Alford, N. G. Faith, and C. J. Czuprynski.** 2008. The poloxamer P85 is protective against Listeria monocytogenes invasion. Foodborne Pathog Dis **5:**859-65.

18. **Perumal, O. P., R. Inapagolla, S. Kannan, and R. M. Kannan.** 2008. The effect of surface functionality on cellular trafficking of dendrimers. Biomaterials **29:**3469-76.

19. **Pothayee N., V. M. L., Ranjan A., Jain N. , Saeleem M, Sriranganathan N. and Riffle. J. S.** 2008. Aminoglycoside-ionopolymeric nanoplexes for treating intracellular pathogens. Polymer Preprints **49:**1037.

20. **Ranjan A, P. N., Seleem M, Jain J, Sriranganathan N , Riffle J. S. and Kasimanickam R.** 2009. Drug delivery using novel nanoplexes against a Salmonella mouse infection model J Nanopart Res **DOI 10.1007/s11051-009-9641-y**.

21. **Ranjan A, P. N., Seleem MN, Sriranganathan N, Kasimanickam R, Makris M, Riffle JS.** 2009. In-vitro trafficking and efficacy of core-shell nanostructures for treating intracellular Salmonella. **53**.

22. **Ranjan, A., N. Pothayee, M. N. Seleem, N. Sriranganathan, R. Kasimanickam, M. Makris, and J. S. Riffle.** 2009. In-vitro trafficking and efficacy of core-shell nanostructures for treating intracellular Salmonella. Antimicrob Agents Chemother.

23. **Sano, G., Y. Takada, S. Goto, K. Maruyama, Y. Shindo, K. Oka, H. Matsui, and K. Matsuo.** 2007. Flagella facilitate escape of Salmonella from oncotic macrophages. J Bacteriol **189:**8224-32.

24. **Vazquez-Boland, J. A., M. Kuhn, P. Berche, T. Chakraborty, G. Dominguez-Bernal, W. Goebel, B. Gonzalez-Zorn, J. Wehland, and J. Kreft.** 2001. Listeria pathogenesis and molecular virulence determinants. Clin Microbiol Rev **14:**584-640.

25. **Xia, S., X. P. Dun, P. S. Hu, S. Kjaer, K. Zheng, Y. Qian, C. Solen, T. Xu, B. Fredholm, T. Hokfelt, and Z. Q. Xu.** 2008. Postendocytotic traffic of the galanin R1 receptor: a lysosomal signal motif on the cytoplasmic terminus. Proc Natl Acad Sci U S A **105:**5609-13.

26. **Y. Tian, L. Bromberg, S. N. Lin, H. T. A., and K. C. Tam.** 2007. Complexation and release of doxorubicin from its complexes with pluronic P85-*b*-poly(acrylic acid) block copolymers. J.Control. Release **121:**137-145.

27. **Yang, Z., G. Sahay, S. Sriadibhatla, and A. V. Kabanov.** 2008. Amphiphilic block copolymers enhance cellular uptake and nuclear entry of polyplex-delivered DNA. Bioconjug Chem **19:**1987-94.

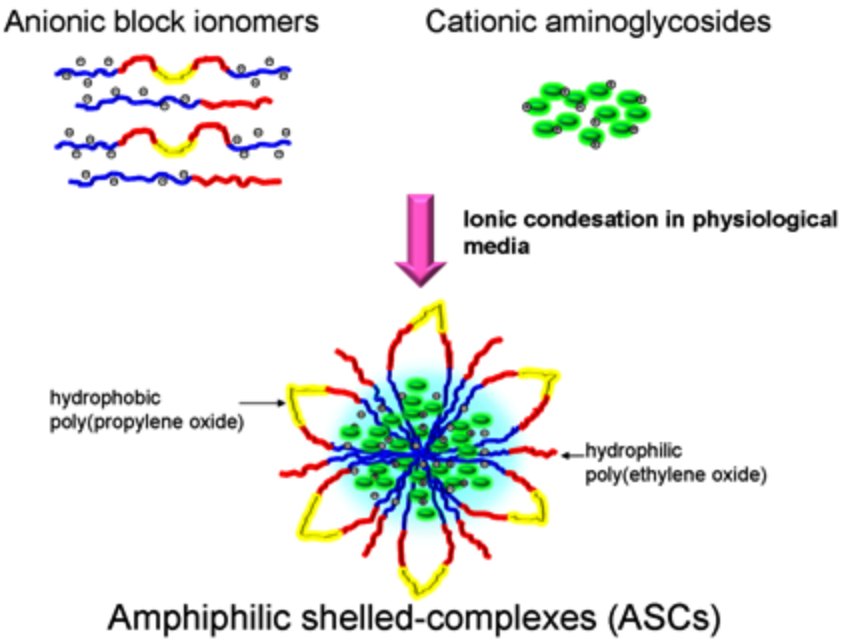

Fig. 3.1.1: Schematic representation for preparation of core-shell nanostructures encapsulating gentamicin

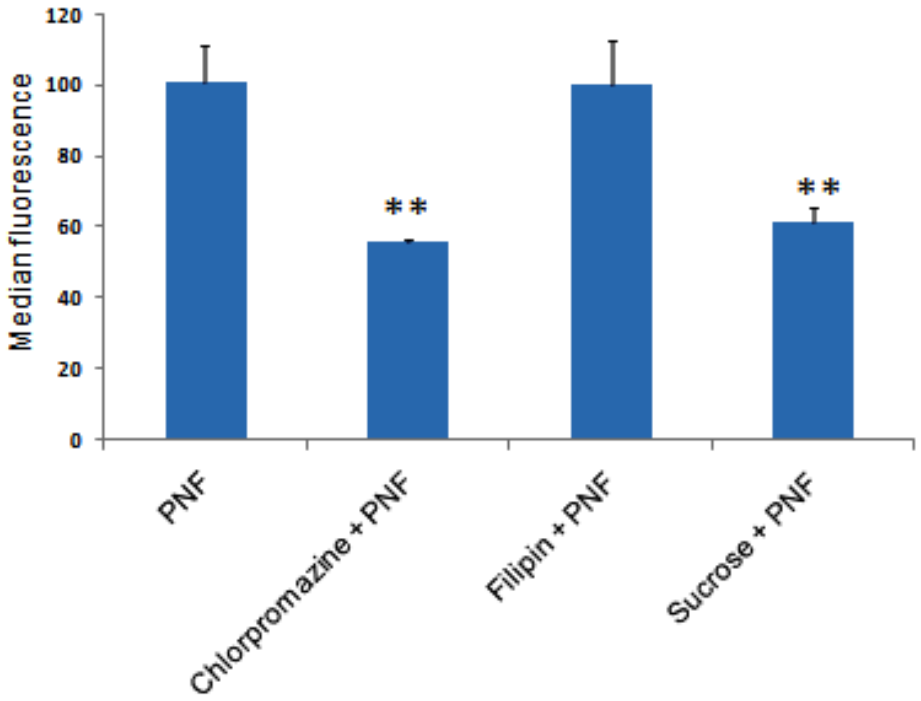

Fig.3.1.2. Median intracellular fluorescence intensity calculated from flow cytometry considering control (PNF) as 100 %. Each treatment represents mean of three measurements with error bars. Asterisk represents significant when compared to control ($p < 0.05$).

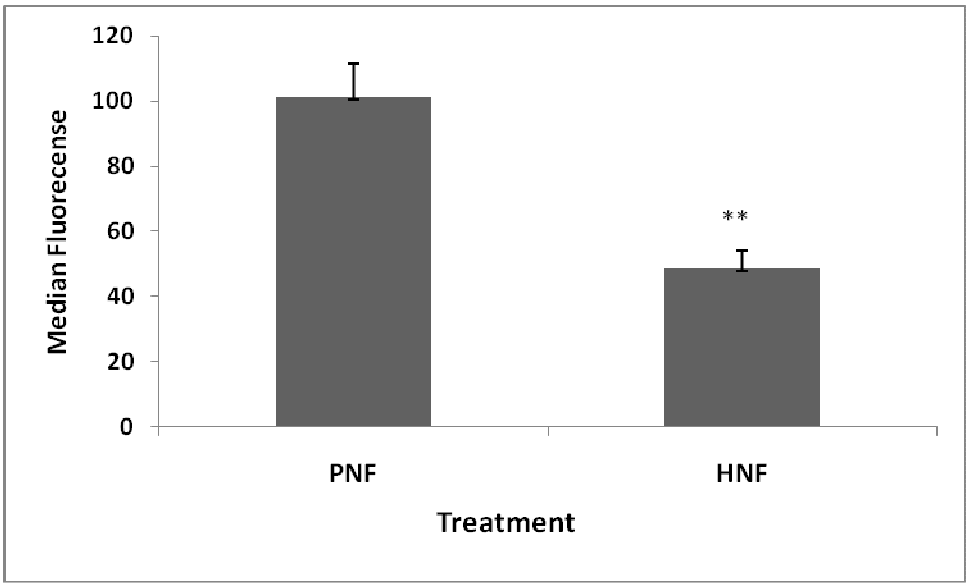

Fig.3.1.3. Median intracellular fluorescence intensity calculated from flow cytometry calculated for FITC labeled amphiphilic (PNF) and hydrophilic nanostructure (HNF) (represented by triplicate of three measurements). Asterisk represents significant when compared to control ($p < 0.05$).

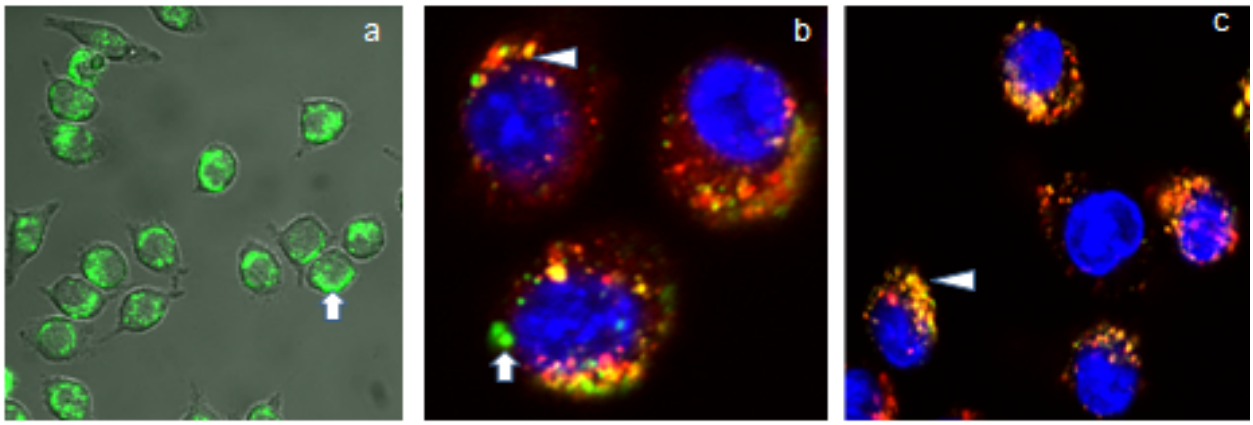

Fig 3.1.4: Confocal microscopy. (a) Uptake of PNF nanostructures into J774A.1 cells.(b) Colocalization of nanostructures with endosome/lysosome after incubation for 2 h. Subcellular colocalization of PNF (arrow) (b) and Alexafluor 488 (arrow head) (c) nanostructures are shown by yellow-to-orange (arrowhead) spots formed by green nanoparticles and red endosomes/lysosomes, showing that a majority of the Alexa-fluor appear to reside in endosomes whereas PNF nanostructructures is distributed all over the cell.

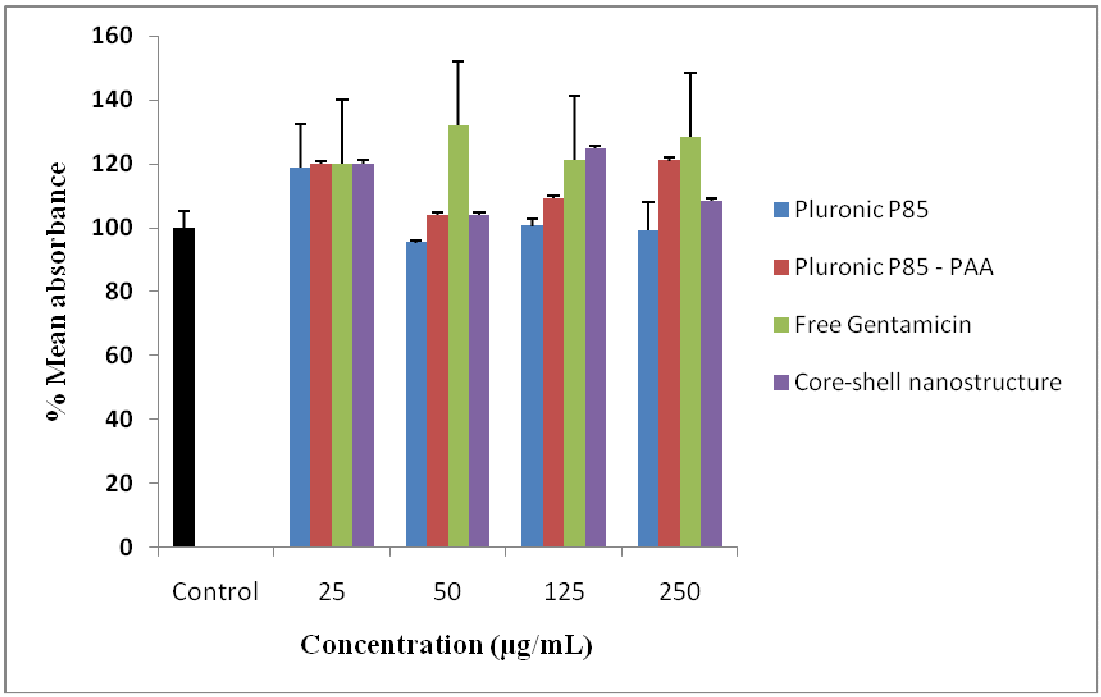

Fig.3.1.5: MTS assay showing the mean absorbance at wavelength of 490 nm after incubating J774A.1 cells with 50-250 µg mL^{-1} of core-shell nanostructures along with appropriate controls. Results are expressed as means ± SD of six measurements.

Group	Log CFU (±SD)	Log CFU reduction
Control	4.06 (± 0.16)	0.00
Free gentamicin	3.98 (± 0.05)	0.08
Polymer alone	3.91 (± 0.08)	0.15
Nanostructure	3.53 (± 0.20)	0.53**

Table 3.1.1: Killing of intracellular wild-type *S. typhimurium* LT2 in J774A.1 cells incubated with free gentamicin or nanostructure at a dose of 25 μg gentamicin/mL for 6 h. Each result represents the mean of triplicate assays ± SD performed together. Asterisks represent values found to be significantly different (confidence level, $t = 0.05$) from that for free gentamicin by statistical analysis (ANOVA followed by Tukey's procedure for multiple comparisons).

Group	Log CFU (±SD)	Log CFU reduction
Control	5.63 (± 0.35)	0.00
Free gentamicin	5.67 (± 0.14)	+ 0.04
Polymer alone	5.50 (± 0.10)	0.13
Nanostructure	2.46 (± 0.11)	3.17**

Table 3.1.2: Killing of intracellular wild-type *Listeria monocytogenes* in J774A.1 cells incubated with free gentamicin or nanostructure at a dose of 25 μg/mL for 6 h. Each result represents the mean of triplicate assays ± SD performed together. Asterisks represent values found to be significantly different (confidence level, $t = 0.05$) from that for free gentamicin by statistical analysis (ANOVA followed by Tukey's procedure for multiple comparisons).

Chapter 3

Improved drug delivery approach for intracellular *Salmonella*

Chapter 3.2

In-vivo toxicity and treatment efficacy of P85-core-shell nanostructure encapsulating gentamicin against *Salmonella* mouse infection model

(To be submitted)

Abstract

Pluronic P85 based core-shell nanostructures encapsulating gentamicin (NG) were designed in this study by blending sodium polyacrylate ($PAA^- Na^+$) and block copolymers of ($PAA^{-+}Na$-*b*-(pluronic- P85)-b-$PAA^{-+}Na$) and complexation with polycationic gentamicin. Synthesized NG had a hydrodynamic diameter of ~210 nm, zeta potentials of -0.7 (±0.2), and incorporated ~25% by weight of gentamicin. NG was administered *in-vivo* both by parenteral (IP) and oral route at multiple dosage of 5µg g^{-1} in AJ-646 mice infected with *Salmonella.* Parenteral administration of NG resulted in significant reduction of viable bacteria in the liver (0.40 $\log_{10}$) and spleen (0.72 $\log_{10}$) compared to free gentamicin (FG) at $p \leq 0.05$. Oral treatment of NG was not significant compared to FG suggesting ineffective targeting of intracellular *Salmonella* by this route. Histopathological evaluation of brain, heart, kidney, liver, spleen and lung at multiple dosages (three) of 5µg g^{-1} IP revealed no toxicity in NG treated mice. Thus, NG developed by this methodology can potentially improve targeting of intracellular pathogens including *Salmonella*.

Introduction

Gentamicin is one of the most commonly used aminoglycosides active against both Gram positive and Gram negative pathogens. Gentamicin is bactericidal and acts by binding to prokaryotic ribosomes impairing bacterial protein synthesis (16). Chemically, gentamicin is polar cationic molecules and requires aminated sugars joined in glycosidic linkages to a dibasic cyclitol for their potency. Despite their potent bactericidal activity *in-vitro*, gentamicin is poorly permeable across mammalian phagocytic membranes (15). Thus, limiting their efficacy against many intracellular bacterial pathogens like *Salmonella, Listeria, Brucella*. Along with poor

membrane permeability, cell uptake studies have shown that gentamicin internalize via endocytosis (23). Endocytic uptake may result in sub-cellular organelle dysfunction and an increase in minimum inhibitory concentration (MIC) of the gentamicin by many folds. Thereby, drastically reducing the intracellular antimicrobial efficacy (14). Thus, novel strategies are required to improve the intracellular gentamicin accumulation in order to achieve better efficacy against intracellular pathogens.

We had previously reported synthesis of core-shell nanostructures encapsulating gentamicin and anionic polymers in the cores with amphiphilic pluronic F68 shells to improve intracellular drug accumulation (20). Pluronics block copolymers are listed as pharmaceutical excipients in the United States and British Pharmacopoeia and are currently in the Phase I studies especially in the multidrug-resistant cancers due to their ability to overcome drug efflux systems (4, 12). Fundamentally, pluronic are synthetic amphiphilic copolymers consisting of ethylene oxide (EO) and propylene oxide (PO) blocks arranged in a triblock (A-B-A) structure (18). The triblock arrangement provides an advantage of altering the hydrophilic/hydrophobic balance (HLB) to suit a particular therapeutic application. For example, the HLB of pluronic F68 is 29 whereas that of pluronic P85 is 16 (12). Increased hydrophobicity of pluronic P85 may be beneficial especially for intracellular infection since it may favor improved uptake of nanostructure by the macrophages. Chemically, pluronic P85 copolymer is composed of ethylene oxide and propylene oxide units arranges as EO_{26}–PO_{40}–EO_{26} (7). Recently, pluronic P85 was shown to be protective against *Listeria* invasion in a murine model through transient depletion of host ATP levels in the mammalian cells (18). Therefore, in addition to pharmaceutical excipients, the direct application of pluronic P85 as a component of core-shell nanostructure encapsulating gentamicin for *in-vivo* treatment of intracellular infections may be highly interesting to explore.

Core-shell nanostructures have attracted considerable attention due to their unique ability in encapsulating either + vely or –vely charged therapeutic molecules (2). The unique ability is conferred to the core-shell structures mainly by fabricating the core to contain high amounts of ionic species and tailoring shell with specific hydrophobic/hydrophilic chemistry. This results in encapsulation of oppositely charged ionic species inside the cores and successful interaction of the shell's hydrophobic segment with the cell membranes. Furthermore, the incorporation of hydrophilic segment provide steric hindrance; thus aiding in dispersion in physiological medium.

The objective of this study was to develop core-shell nanostructure encapsulating charged gentamicin (NG) and test *in-vivo* efficacy and toxicity against an intracellular *Salmonella* mouse infection model. For *in-vivo* efficacy studies, NG and free gentamicin (FG) were administered via. oral and parenteral route. Administration of oral route is preferred by the patient for being convenient and may be used in outpatient setting (5). Triblock pluronic covalently conjugated with poly(acrylic acid) (PAA) encapsulating anti-neoplastic agent as excipients for sustained-release tablets orally have been explored extensively in cancer chemotherapy (3). It is noteworthy that pluronic-PAA are biocompatible, non-biodegradable and not absorbed into the systemic circulation. Thus oral administration can facilitate easier excretion from the patients. Therefore, to develop better treatment protocols, we investigated similarly the administration via. oral administration in antimicrobial therapy. Furthermore, considering that the nanostructure was non-biodegradable, we studied comprehensively the *in-vivo* toxicity of the NG upon parenteral examination.

Materials and Methods:

Preparation of the nanostructure (NG)

All chemicals were purchased from Sigma-Aldrich, USA unless otherwise noted. Pluronic P85™ (PEO-*b*-PPO-*b*-PEO) was kindly provided by BASF. *Poly(tert-butyl acrylate-b-PEO-b-PPO-b-PEO-b-tert-butylacrylate) or (PtBA-b-PEO-b-PPO-b-PEO-b-PtBA)* was synthesized via controlled Atom Transfer Radical Polymerization (ATRP) through a method adapted from the literature (10, 31). Initially, PtBA-*b*-PEO-*b*-PPO-*b*-PEO-*b*-PtBA copolymer (2.0 g, 1.09 x 10^{-2} eq of t-butyl ester groups) was dissolved in 30 mL of dichloromethane, then trifluoroacetic acid (5 mL, 6.50 x 10^{-2} mol) was added slowly over 30 min and the reaction mixture was stirred at room temperature overnight. The solvent was evaporated at 40 ^{o}C under vacuum and the residue was dissolved in TetroHydroFuran (THF) and subsequently dialyzed against 4 L of PBS through a cellulose acetate membrane (Mol. wt. cut off (MWCO) 3,500 g mol^{-1}) for 72 h. The poly(acrylic acid-*b*-PEO-*b*-PPO-*b*-PEO-*b*-acrylic acid) (PAA-*b*-PEO-*b*-PPO-*b*-PEO-*b*-PAA) was recovered by freeze-drying and followed by drying at 40 ^{o}C under vacuum. A representative procedure for preparing core-shell polymer-gentamicin nanostructures is provided. Core-shell nanostructures containing gentamicin wherein pentablock copolymers of $PAA^{-}{}^{+}Na$ (2500 MW)-*b*-PEO (1100 MW)-*b*-PPO (2300 MW)-*b*-PEO (1100 MW)-*b*-$PAA^{-}{}^{+}Na$ (2500 MW) were mixed with diblock

copolymers of $PAA^{-}{}^{+}Na$ (7100 MW)-*b*-PEO (2000 MW) and condensed with gentamicin. The PAA- 85-PAA copolymer described above (25 mg, 1.68 x 10^{-4} eq of anions) and 25 mg of PEO-PAA (1.63 x10^{-4} eq of anions) were charged to a 100-mL round-bottom flask and dissolved in 25 mL PBS. The solution was placed in a sonication bath and 5 mL of gentamicin sulfate solution (5.2 mg mL^{-1} gentamicin sulfate equal to 31 mg gentamicin, 3.31 x 10^{-4} eq of cations) was added via syringe to form a turbid dispersion. The resulting complexes were collected by ultra-centrifugation of the solution at 20,000 rpm for 15 min (Optima™ L-XP Ultracentrifuge, Beckman Coulter Inc.). The supernatant was removed and the sediment was washed twice with DI water. Finally, the complex was recovered by freeze-drying

Characterization of the nanostructure (NG)

The solute sizes and zeta potentials of the NG were characterized by Dynamic Light Scattering (DLS) with a Zetasizer 1000 HS with laser diffractometry (Malvern Instruments, Malvern, UK) at a scattering angle of 90^{o}. NG (1 mg) was dispersed in one mL of PBS and analyzed. Measurements were done in triplicate for each batch of particles. The results were taken as the average of three measurements. The amount of gentamicin in NG was determined as reported previously (19).

***In-vivo* efficacy of core-shell nanostructure (NG) against *Salmonella* Typhimurium**

S. Typhimurium LT2 was grown overnight in Luria-Bertani (LB) broth, centrifuged, washed in phosphate buffer saline (PBS) and serially diluted to achieve a final suspension containing 6x10^{4} colony forming units (CFU) per mL. Twenty five female AJ 646 mice (6-8 weeks old) were injected intraperitoneally (IP) with 100 µL of inocula containing 6000 CFU per mouse. 48 hours after infection, five AJ 646 mice/group [Groups: NG (PO), NG (IP), FG (oral), FG (IP) & No treatment] were treated with either FG (in PBS) or the NG in solution via. IP and PO route at a dosage of 5µg g^{-1} of body weight. The dosage was repeated in various groups twice at an interval of 24 h each post administration of the first dose. At day 3 (post 3^{rd} IP injection), the mice were euthanized, spleens and livers were removed aseptically, and organs were crushed and homogenized for 6-8 min in the presence of 2 mL of LB broth in a tissue homogenizer (Next Advance Inc., USA). Aliquots (20 µL) of the organ suspensions were serially diluted in 180 µL of LB broth to a maximum of 10^{5}-fold dilution. Subsequently, the dilutions were plated on

tryptic soy agar plates, incubated overnight at 37 °C, and the resulting grey mucoid, discreet colonies were counted for plates containing between 30 and 300 colonies.

***In-vivo* toxicity evaluation**

To assess toxicity of the NG, five Balb/c mice per group were administered IP 200 µL at a dosage of 5µg g^{-1} of body weight of NG, FG and PBS at an interval of 24 h each for three times. Forty eight h later (post 3rd IP injection), the brain, heart, lung, kidney, liver and spleen were harvested and assessed for histopathological changes. The organs were fixed in 10% neutral buffered formalin, routinely processed into paraffin blocks, and 5 micron sections were stained with haematoxylin and eosin on glass slides (Virginia-Maryland Regional College of Veterinary Medicine, Veterinary Teaching Hospital). Tissue samples were examined independently by light microscopy and scored by two veterinary pathologists. The pathologists were blinded to obtain unbiased assessment. The kidneys were scored on a scale of 0-4 based on the degree of inflammation as reported before (2, 8, 11). Briefly, a semi-quantitative scale consisting of whole numbers with scores from 0-4 was being given as (0) =unremarkable, (1) = minimum, (2) =mild, (3) =moderate, and (4) =marked with regard to changes. Changes include inflammation (infiltration of inflammatory cells), necrosis (morphologic changes of renal parenchyma cells consistent with degeneration and necrosis) and vascular disruptions (hemorrhage, edema and other signs of vascular leakage). The percentage of affected section of tissue being affected is what was used to score any change viz. 0% = unremarkable (0), 0-5% = minimal (1), 6-10%= mild (2), 11-20%= moderate (3),> 20% =marked (4). Previous research works have reported that clinical formulation of pluronic F68, Rheoth Rx in vascular medicine was withdrawn from Phase III studies due to renal toxicity (12). Though later studies showed that toxicity was due to presence of impurities and not because of F68, yet we decided to conduct renal function test to assess the suitability of NG. Therefore, blood from each mouse was collected in EDTA tube by retro-bulbar method and serum was separated by centrifugation at 1,500 rpm for 5 min. Following this, renal function test was performed from the serum of each mice group to assess blood urea nitrogen (BUN) and creatinine levels.

Statistical Analysis

The mean log CFU between groups were compared using ANOVA followed by Tukey's procedure for multiple comparisons. Statistical significance between various treatment groups was set up at $p \leq 0.05$.

Results

Properties of the nanoplexes

Dynamic light scattering (DLS) showed that the NG had mean intensity average diameters of ~ 210 nm. NG had small negative zeta potentials of -0.7 (±0.2) mv. Gentamicin concentration in NG based on the o-phthalaldehyde assay was 25% by wt.

***In-vivo* antibacterial efficacy of FG sulfate relative to the NG**

FG administered *in-vivo* at 5µg g^{-1} body weight in AJ 646 mice infected IP with 6000 CFU of *S.* Typhimurium did not reduce significantly the numbers of viable bacteria from the livers and spleens compared to those recovered from controls (Table 3.2.1). NG administered IP at dose similar to the FG reduced significantly the numbers of viable bacteria in the liver and spleen ($p \leq 0.05$). At 5µg g^{-1}, the numbers of viable bacteria remaining in the livers and spleens of infected AJ 646 mice treated with NG were 0.40 $\log_{10}$ and 0.72 $\log_{10}$ lower than those of the control (untreated). In contrast, oral therapy was not significant in reducing the viable number of bacteria in liver and spleen for the groups treated with FG or the NG suggesting that targeting was not effective/insufficient ($p \leq 0.05$).

***In-vivo* toxicity assessment**

Based on the individual data scored by the pathologists of brain, heart, lungs, kidney, liver and spleen, the median score did not differ significantly between NG, FG and PBS control (Table 3.2.2). Histopathologically, the predominant lesion seen in individual mice tissue was focal aggregates of mononuclear cells and increased protein deposition in the liver and kidney of NG and FG respectively (Fig. 3.2.1). Renal function was comparable in NG and FG treatment compared to control (Fig. 3.2.2). Mean BUN values (ref. range: 8-33 mg/dL) in control, FG and NG was 20.67 (±0.58), 21.5 (±1.92) and 16.5 (±1.74) respectively. Similarly, the creatinine levels (ref. range: 0.2-0.9 mg/dL) for control, FG and NG were 0.2 (±0.0), 0.2 (±0.0) and 0.175 (±0.05) respectively.

Discussion

In this research, we utilized an amphiphilic copolymer containing Pluronic P85 as the shell, and gentamicin was incorporated into the NG cores through cooperative electrostatic attractions. Similar methodology has applied previously to incorporate electro-statically cationic doxorubicin (DOX) into the cores of the nanostructures containing ionized PAA modified Pluronic P85 or PAA modified pluronic F87 (25, 26). These studies showed that the drug loading into the nanostructures is an enthalpically driven process. At a physiological pH of ~7.4, the loading of DOX into the macromolecular complexes were governed by both electrostatic and stacking interactions. Also, DOX was bound close to the stoichiometric proportion of 1:1 to the molar concentration of carboxyl groups in the P85-PAA copolymer. Interestingly, NG prepared via co-operative electrostatic interactions in our study had a drug loading of ~25% by weight of the polymer. Though gentamicin loading of 25% in NG is substantial, yet more investigation is required to understand the underlying reasons for not achieving a 1:1 cation to anion ratio in the NG as observed previously with DOX. The incorporation/loading of the charged species into the cores of the nanostructures may be dependent on both the nature of the drug and chemical structure of the copolymer (13) and this may have possibly influenced the loading in case of NG. The zeta potential of NG was low negative value in the range of -0.7 (±0.2) mV, suggesting effective shielding of the anionic core by the amphiphilic shell (24). In addition, size of NG was around ~210 nm which may be favorable for uptake by the macrophages (6).

For *in-vivo* treatment efficacy studies, BALB/c mice were infected with *S.*Typhimurium LT2 for 48 h (time required to infect liver/spleen macrophage) (21) and later were treated with the NG and FG by oral and parenteral IP routes. The results indicated that the treatment with FG was ineffective by both routes in the liver and the spleen (Table 3.2.1). In contrast, NG significantly reduced the viable bacterium in the spleen (0.72 $\log_{10}$) and liver (0.40 $\log_{10}$) after IP administration compared to FG and infected control ($p \leq 0.05$). However, oral route failed to achieve clinical success. This is in agreement with similar studies wherein the high polarity and cationic nature of the gentamicin results in scant absorption from gastrointestinal tract causing poor bioavailability (1). FG administered parenterally may achieve high bioavailability of FG, yet their short mean half life and rapid renal clearance may hinder *in-vivo* bacterial clearance

(17). Thus, poor cell membrane permeability coupled with quick clearance of FG from circulation could be a limiting factor in the therapy of intracellular *Salmonella*.

In contrast, NG appeared to translocate better to the *Salmonella* infected spleen and liver macrophage cells. This is evidenced by significant bacterial reduction in both liver and spleen upon IP treatment with NG (Table 3.2.1). We showed previously that the rate of internalization of the core-shell nanostructure by macrophage is dependent of shell chemistry (20). We observed improved internalization *in-vitro* upon changing the shell chemistry to amphiphilic from hydrophilic. Thus, NG with specific physico-chemical properties should be efficiently taken up by liver/spleen macrophage. Also, gentamicin encapsulation in a carrier improves both the half life and organ delivery as reported previously (28, 29). Hence, there is a strong probability of similar phenomenon happening in case of NG. However, for the present study, we could not experimentally determine the accumulation/amount of gentamicin in liver and spleen tissue. The o-phthaldehyde technique for gentamicin estimation in our study is based on derivatization of amino groups. Since, the liver or spleen contains lot of aminated protein; it was not possible to estimate the gentamicin amount accurately. This is because derivatization is non-specific and could have measure the amino groups of proteins in the tissue. A more robust technique will be using nanostructures doped with radioactive labeled [^{3}H] gentamicin and measuring by scintillation counting. Unfortunately, at present we don't have facility to perform the experimentation and will be a part of continuing research. However, the comparative better efficacy of NG suggests that filtration of drug was not rapid in contrast to FG.

Pluronic block copolymers based formulations are increasingly being studied in drug delivery studies. However, clinical application of pluronic as a potential drug carrier is dependent on it being non-toxic (12). In general, the toxicity of pluronic copolymers is proportional to their HLB (7). The more lipophilic the copolymer, the more severe are the lesions. For ex. the HLB of P85 and F68 is 16 and 29. Hence, these lesser lipophilic or more hydrophilic pluronics may be more favorable to be used as potential drug delivery carriers. Pluronic P85 has been shown to have a wide range of biological activity with negligible systemic toxicity (30). Studies reported to assess *in-vivo* toxicity of P85 upon intramuscular injection in mouse muscle for gene expression studies induces no toxicity after single injection (7). To improve the encapsulation efficiency of charged drugs, pluronics have further been modified with PAA end groups (3). Thus, in this study we

aimed to determine the *in-vivo* suitability of NG containing P85-PAA in shell for treatment of intracellular *Salmonella*.

At normal dosage of 5μg/gm body weight, BUN and creatinine levels of mice treated with FG and NG were comparable to PBS control levels (Fig. 3.2.2). This is plausible since the recommended dosage of gentamicin in mice is between 5-8 μg/gram body weights IP per day (22, 27). Free gentamicin can show nephrotoxic and ototoxic effects above 12 μg/gram especially in humans (9). Thus, any alteration in renal function was expected to be attributed to NG only. In the NG treated group, slightly lower values of BUN and creatinine was recorded compared to PBS control and FG (Fig. 3.2. 2). Extremely lower levels of BUN and creatinine may indicate hepatic insufficiency and low protein diets (8). However, the average levels of BUN and creatinine for NG in our experiment were slightly lower (-1.0) than the control and were within the normal reference values. Moreover, histopathological scoring of kidney tissue was normal for all the treatments. In addition to renal function test and scoring of kidneys, a comprehensive *in-vivo* study of various organs was performed independently by two anatomic pathologists to screen for microscopic lesions in other organs like brain, heart, liver, spleen and lung. Both evaluators did not notice any remarkable abnormal lesion with major tissue damage in PBS control, FG or NG organs (Table 3.1.2; Fig. 3.2.1). Thus, our observations suggest that the formulation may be relatively safe to be used for *in-vivo* treatment of intracellular infections at the dosage administered in this study.

In summary, the present study shows that comparatively better treatment efficacy can be achieved by incorporating gentamicin in pluronic-P85 based core-shell structures encapsulating gentamicin. At normal dosage, the NG is non-toxic *in-vivo* based on histopathological observations.

Future studies:

Future works aiming to study the biodistribution of NG and improving the specific intracellular targeting to the niche where the *Salmonella* reside in liver and spleen may enhance the suitability of the core-shell antimicrobial DDS systems.

References:

1. **Abu-Basha, E. A., N. M. Idkaidek, and A. F. Al-Shunnaq.** 2007. Comparative pharmacokinetics of gentamicin after intravenous, intramuscular, subcutaneous and oral administration in broiler chickens. Vet Res Commun **31:**765-73.

2. **Bajema, I. M., E. C. Hagen, B. E. Hansen, J. Hermans, L. H. Noel, R. Waldherr, F. Ferrario, F. J. van der Woude, and J. A. Bruijn.** 1996. The renal histopathology in systemic vasculitis: an international survey study of inter- and intra-observer agreement. Nephrol Dial Transplant **11:**1989-95.

3. **Barreiro-Iglesias, R., L. Bromberg, M. Temchenko, T. A. Hatton, C. Alvarez-Lorenzo, and A. Concheiro.** 2005. Pluronic-g-poly(acrylic acid) copolymers as novel excipients for site specific, sustained release tablets. Eur J Pharm Sci **26:**374-85.

4. **Batrakova, E. V., D. W. Miller, S. Li, V. Y. Alakhov, A. V. Kabanov, and W. F. Elmquist.** 2001. Pluronic P85 enhances the delivery of digoxin to the brain: in vitro and in vivo studies. J Pharmacol Exp Ther **296:**551-7.

5. **Bromberg, L.** 2008. Polymeric micelles in oral chemotherapy. J Control Release **128:**99-112.

6. **Chono, S., and K. Morimoto.** 2006. Uptake of dexamethasone incorporated into liposomes by macrophages and foam cells and its inhibitory effect on cellular cholesterol ester accumulation. J Pharm Pharmacol **58:**1219-25.

7. **Gaymalov, Z. Z., Z. Yang, V. M. Pisarev, V. Y. Alakhov, and A. V. Kabanov.** 2009. The effect of the nonionic block copolymer pluronic P85 on gene expression in mouse muscle and antigen-presenting cells. Biomaterials **30:**1232-45.

8. **Hanigan, M. H., E. D. Lykissa, D. M. Townsend, C. N. Ou, R. Barrios, and M. W. Lieberman.** 2001. Gamma-glutamyl transpeptidase-deficient mice are resistant to the nephrotoxic effects of cisplatin. Am J Pathol **159:**1889-94.

9. **Hatala, R., T. Dinh, and D. J. Cook.** 1996. Once-daily aminoglycoside dosing in immunocompetent adults: a meta-analysis. Ann Intern Med **124:**717-25.

10. **Hou, S. J., E. L. Chaikof, D. Taton, and Y. Gnanou.** 2003. Synthesis of water-soluble star-block and dendrimer-like copolymers based on poly(ethylene oxide) and poly(acrylic acid). Macromolecules **36:**3874-3881.

11. **Joss, N., S. Morris, B. Young, and C. Geddes.** 2007. Granulomatous interstitial nephritis. Clin J Am Soc Nephrol **2:**222-30.

12. **Kabanov, A. V., and V. Y. Alakhov.** 2002. Pluronic block copolymers in drug delivery: from micellar nanocontainers to biological response modifiers. Crit Rev Ther Drug Carrier Syst **19:**1-72.

13. **Kim, J. O., A. V. Kabanov, and T. K. Bronich.** 2009. Polymer micelles with cross-linked polyanion core for delivery of a cationic drug doxorubicin. J Control Release **138:**197-204.

14. **Lecaroz, C., C. Gamazo, and M. J. Blanco-Prieto.** 2006. Nanocarriers with gentamicin to treat intracellular pathogens. J Nanosci Nanotechnol **6:**3296-302.

15. **Lecaroz, C., C. Gamazo, M. J. Renedo, and M. J. Blanco-Prieto.** 2006. Biodegradable micro- and nanoparticles as long-term delivery vehicles for gentamicin. J Microencapsul **23:**782-92.

16. **Mingeot-Leclercq, M. P., Y. Glupczynski, and P. M. Tulkens.** 1999. Aminoglycosides: activity and resistance. Antimicrob Agents Chemother **43:**727-37.

17. **Nagai, J., and M. Takano.** 2004. Molecular aspects of renal handling of aminoglycosides and strategies for preventing the nephrotoxicity. Drug Metab Pharmacokinet **19:**159-70.

18. **Neudeck, B. L., T. D. Alford, N. G. Faith, and C. J. Czuprynski.** 2008. The poloxamer P85 is protective against Listeria monocytogenes invasion. Foodborne Pathog Dis **5:**859-65.

19. **Ranjan A, P. N., Seleem M, Jain J, Sriranganathan N , Riffle J. S. and Kasimanickam R.** 2009. Drug delivery using novel nanoplexes against a Salmonella mouse infection model J Nanopart Res **DOI 10.1007/s11051-009-9641-y**.

20. **Ranjan A, P. N., Seleem MN, Sriranganathan N, Kasimanickam R, Makris M, Riffle JS.** 2009. In-vitro trafficking and efficacy of core-shell nanostructures for treating intracellular Salmonella. **53**.

21. **Richter-Dahlfors, A., A. M. Buchan, and B. B. Finlay.** 1997. Murine salmonellosis studied by confocal microscopy: Salmonella typhimurium resides intracellularly inside macrophages and exerts a cytotoxic effect on phagocytes in vivo. J Exp Med **186:**569-80.

22. **Ristuccia, A. M., and B. A. Cunha.** 1982. Current concepts in antimicrobial therapy of prostatitis. Urology **20:**338-45.

23. **Sandoval, R., J. Leiser, and B. A. Molitoris.** 1998. Aminoglycoside antibiotics traffic to the Golgi complex in LLC-PK1 cells. J Am Soc Nephrol **9:**167-74.

24. **Tang, G. P., J. M. Zeng, S. J. Gao, Y. X. Ma, L. Shi, Y. Li, H. P. Too, and S. Wang.** 2003. Polyethylene glycol modified polyethylenimine for improved CNS gene transfer: effects of PEGylation extent. Biomaterials **24:**2351-62.

25. **Tian, Y., L. Bromberg, S. N. Lin, T. A. Hatton, and K. C. Tam.** 2007. Complexation and release of doxorubicin from its complexes with pluronic P85-b-poly(acrylic acid) block copolymers. J Control Release **121:**137-45.

26. **Tian, Y., P. Ravi, L. Bromberg, T. A. Hatton, and K. C. Tam.** 2007. Synthesis and aggregation behavior of pluronic F87/poly(acrylic acid) block copolymer in the presence of doxorubicin. Langmuir **23:**2638-46.

27. **VV, T.** 1998. Drug therapy in pet rodents. Veterinary Medicine **93:**988-991.

28. **Webb MS, B. N., Wiseman DJ, Saxon D, Sutton K, Wong KF, Logan P, Hope MJ.** 1998 Jan;. Antibacterial efficacy against an in vivo Salmonella typhimurium infection model and pharmacokinetics of a liposomal ciprofloxacin formulation. Antimicrob Agents Chemother **42(1):**:45-52.

29. **Webb, M. S., N. L. Boman, D. J. Wiseman, D. Saxon, K. Sutton, K. F. Wong, P. Logan, and M. J. Hope.** 1998. Antibacterial efficacy against an in vivo Salmonella

typhimurium infection model and pharmacokinetics of a liposomal ciprofloxacin formulation. Antimicrob Agents Chemother **42:**45-52.

30. **Weinberg, B. D., T. M. Krupka, J. R. Haaga, and A. A. Exner.** 2008. Combination of sensitizing pretreatment and radiofrequency tumor ablation: evaluation in rat model. Radiology 246:796-803.

31. **Y. Tian, L. Bromberg, S. N. Lin, H. T. A., and K. C. Tam.** 2007. Complexation and release of doxorubicin from its complexes with pluronic P85-b-poly(acrylic acid) block copolymers. J.Control. Release 121:137-145.

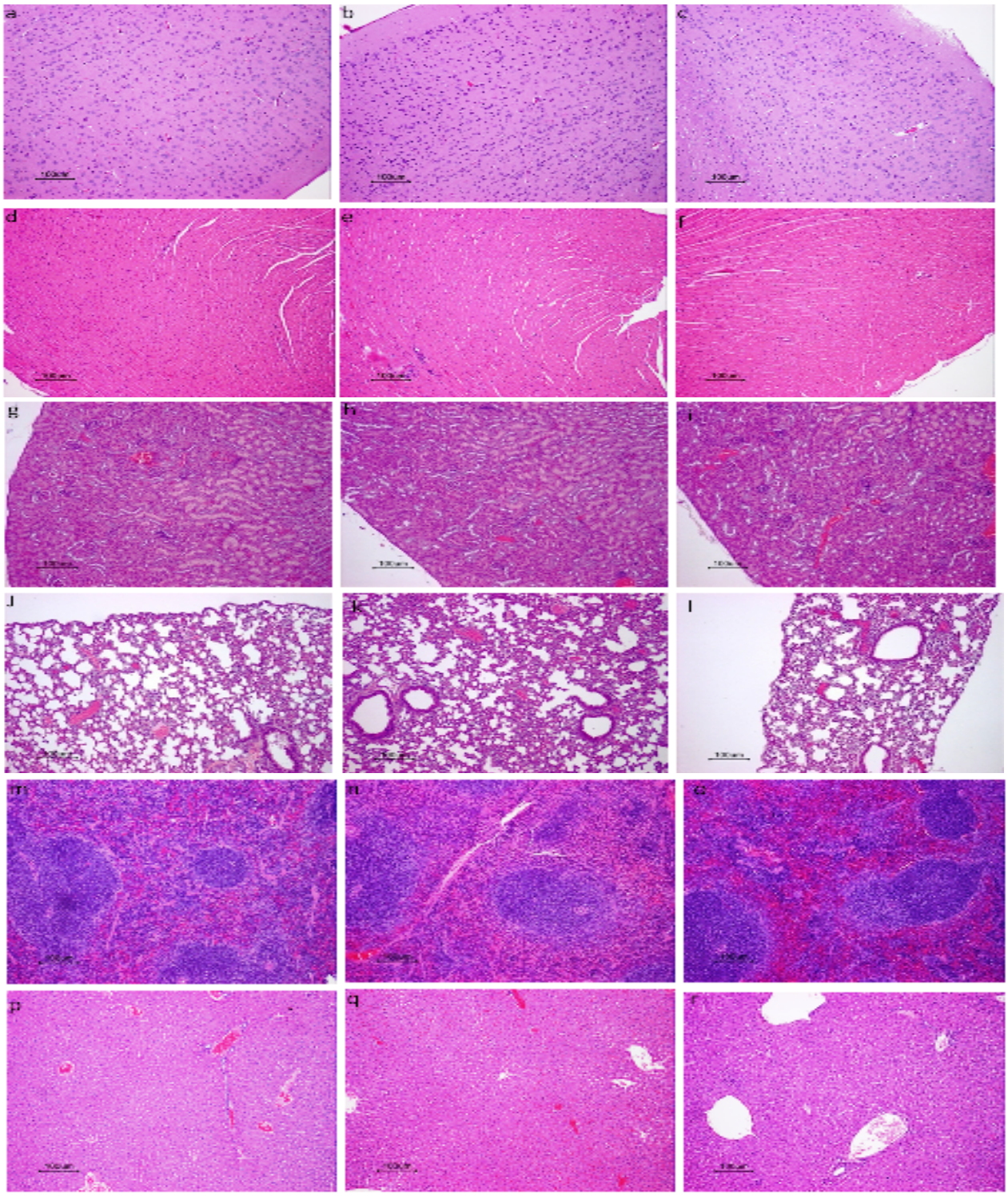

Fig. 3.2.1: Representative histopathological microscopic images of (a-c) Brain, (d-f) Heart, (g-i) Kidney, (j-l) Lung, (m-o) Spleen, and (p-r) Liver respectively of AJ-646 mice euthanized 5 days after intraperitoneal administration: (column 1: a,d,g,j,m and p) Untreated (PBS) control group; (b) (column 2: b,e,h,k,n and q) NG treated group; (column 3: c,f,i,l, and r) FG treated group. The tissues were hematoxylin and eosin stained. Scale bar represents 100 µm.

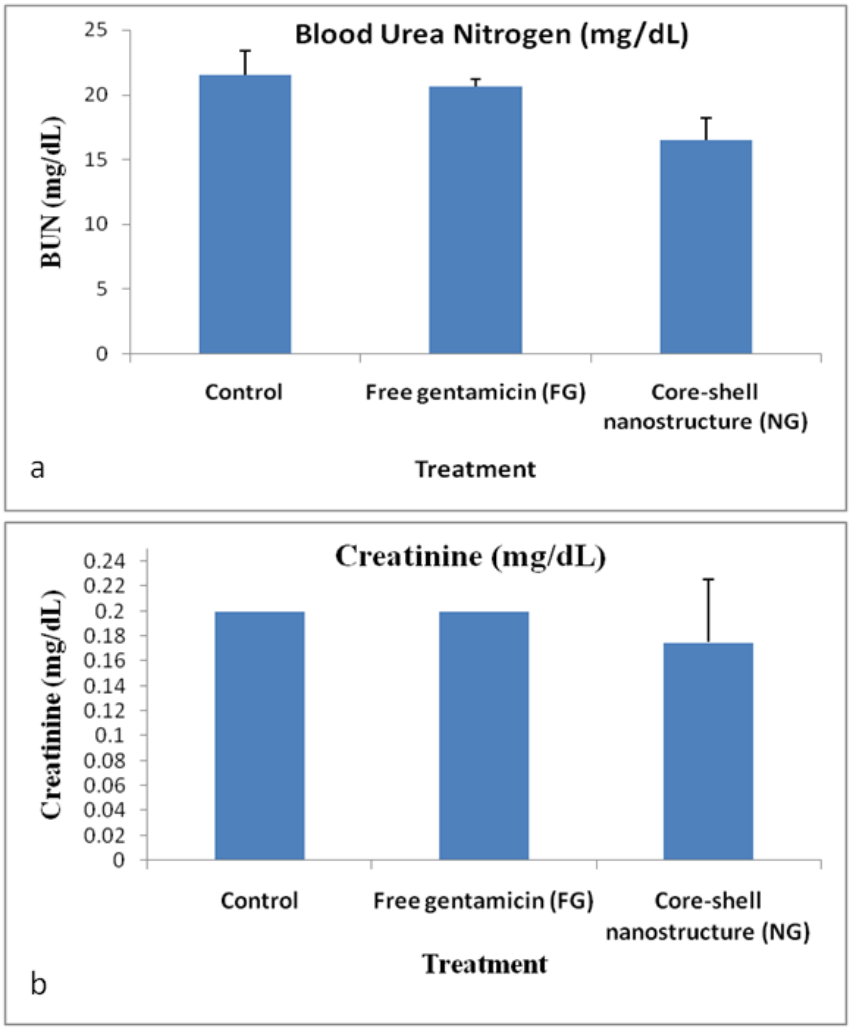

Fig. 3.2.2: Serum creatinine (a) and blood urea (b) values of BALB/c mice. (a) Mice were treated with core-shell nanostructure encapsulating gentamicin formulations (5 mg/kg) or free gentamicin (5 mg/kg) on days 1, 2 and 3 by intraperitoneal (IP) route. On day 5, blood from the control (PBS), free gentamicin and nanostructure mice was collected, serum creatinine and BUN values were determined.

(*Reference Range:* BUN: 8-33 mg/dL, Creatinine: 0.2-0.9 mg/dL; Source: Research Animal Resources, University of Minnesota)

Table 3.2.1: Killing of intracellular *Salmonella typhimurium* in AJ-646 mouse liver and spleen upon treatment with free gentamicin or core-shell nanostructure encapsulating gentamicin at triplicate dosage (Oral or IP) of 5µg/gm at an interval of 24 h each. Asterisks represent values found to be significantly different (confidence level, $t = 0.05$) from that of free gentamicin by statistical analysis (ANOVA followed by tukey's procedure for multiple comparisons).

Treatment Group	**Liver (log CFU)**	**Log CFU Reduction**	**Spleen**	**Log CFU Reduction**
Control	5.61±0.051	0.00	5.98±0.242	0.00
Free gentamicin IP	5.97±0.378	+0.36	5.63±0.072	0.35
Nanostructure IP	5.21±0.123	0.40**	5.26±0.384	0.72**
Free gentamicin Oral	5.86±0.427	+0.25	5.84 ± 0.27	0.14
Nanostructure Oral	5.84±0.781	+0.23	5.87±0.159	0.11

**Significant at P≤0.05 compared to free gentamicin and control.

Table 3.2.1: Mean value of histopathological scores of brain, heart, lungs, liver, kidney and spleen evaluated by two individual pathologist

Group	Brain	Heart	Lungs	Liver	Kidney	Spleen
Phosphate Buffer Saline Mice 1	0	0	0	0	0	0
Phosphate Buffer Saline Mice 2	0	0	0	0	0	0
Phosphate Buffer Saline Mice 3	0	0	0	0	0	0
Phosphate Buffer Saline Mice 4	0	0	0	0	0	0
Phosphate Buffer Saline Mice 5	0	0	0	0	0	0
Free gentamicin Mice 1	0	0	0	0.5	0	0
Free gentamicin Mice 2	0	0	0	0	0	0
Free gentamicin Mice 3	0	0	0	0	0	0
Free gentamicin Mice 4	0	0	0	0	0.5	0
Free gentamicin Mice 5	0	0	0	0	0	0
Core-shell nanostructure Mice 1	0	0	0	0	0	0
Core-shell nanostructure Mice 2	0	0	0	0	0	0
Core-shell nanostructure Mice 3	0	0	0	0	0	0
Core-shell nanostructure Mice 4	0	0	0	1	0	0
Core-shell nanostructure Mice 5	0	0	0	0	0	1

Kidney Scoring Protocol:

Scale	Percentage of tissue affected	Outcome
0	0%	unremarkable
1	0-5%	minimal
2	6-10%	mild
3	11-20%	moderate
4	> 20%	marked

Chapter 4

Overall Summary and Discussion

Intracellular bacterial pathogens like *Salmonella spp.*, evade killing by host phagocytic cells through various mechanisms and requires long-term antimicrobial therapy for effective clearance from the infected patient. Furthermore, patient non-compliance, indiscriminate antimicrobial use and cell membrane impermeability of drugs active against intracellular pathogens has the potential of creating drug resistant pathogens and chronic carrier state. Cell specific delivery of antimicrobials using polymeric carriers may help to reduce the dose and the frequency of administration that are required for the effective control of intracellular pathogens. Improved drug delivery to the specific infected cells/tissues can also drastically reduce the side effects commonly observed with classical antimicrobial therapy. The research described in this dissertation was aimed at establishment of methods to optimize the drug delivery system (DDS) and test the same in *in-vitro* and *in-vivo* against an intracellular *Salmonella* infection model.

Most of the DDS suffer from poor drug incorporation. Thus, our initial goal was to develop a core-shell nanostructure with high drug loading capacity. Since, gentamicin is polycationic, we hypothesized that its incorporation in anionic carriers like polyacrylates may be highly possible. Therefore, we attempted making core-shell nanostructures by mixing equal populations of an anionic carrier and polycationic drug. Stable dispersions of the hydrophilic core-shell nanostructures (N1) was obtained by incorporating block copolymers of poly(ethylene oxide-*b*-sodium acrylate) (PEO-*b*-$PAA^{-}\ ^{+}Na$) blended with the $PAA^{-}\ ^{+}Na$ homopolymer and complexed with polycationic gentamicin (PAPG). We reported that the core-shell nanostructures obtained by our novel technique can incorporate up to ~25% by weight of gentamicin which is 20-25 folds higher than the values reported previously, where gentamicin was loaded into hydrophobic microspheres or nanospheres. In addition to achieving higher drug loadings in the DDS, our i*n-vivo* studies of *Salmonella* infected AJ-646 mice treated with the N1 showed a reduced number of viable bacteria in the liver and spleen compared to a free gentamicin treated group.

Besides reporting the construction of a novel DDS with high drug encapsulation, we also devised new tools to enhance drug delivery for efficient intracellular *Salmonella* clearance. We demonstrated for the first time that the hydrophilic/hydrophobic nature of aminoglycoside drug

delivery vehicles can make a distinct difference in intracellular localization and bacterial clearance. We modified the hydrophilic core-shell nanostructures by incorporating into the shells amphiphilic copolymers containing pluronic-F68 $(PPO)_{68}$ which are somewhat more hydrophobic. We demonstrated that gentamicin encapsulation in core-shell nanostructures having $(PPO)_{68}$-PAA amphiphilic surfaces (N2) enhances the rate, modulates the route by augmenting non-endosomal delivery and significantly influence the therapeutic activity against intracellular *Salmonella in-vitro* and *in-vivo*. Furthermore, N2 protected mice against nephrotoxicity at higher dosage compared to free gentamicin. Thus, we believe that the novel approach described herein is highly promising and should be applicable for treatment of many intracellular pathogens like *Brucella, Salmonella* and *Mycobacterium.*

To achieve better efficacy and stability of core-shell nanostructure at the physiological pH of 7.4, temperature 37 °C and 0.1 NaCl, we investigated gentamicin encapsulated in core-shell nanostructure containing pluronic-P85 $(PPO)_{85}$ in the shell (N3). $(PPO)_{85}$ is relatively more hydrophobic than $(PPO)_{68}$ and has shown protection against Listeriosis in mice. In addition to evaluating the efficacy of N3, we also aimed to understand the correlation between sub-cellular localization of bacteria and clearance by N3. *In-vitro* intracellular delivery and efficacy studies against vacuolar resident Salmonella and cytoplasm resident *Listeria* showed that clearance by the N3 correlates directly with the bacterial localization inside the cell. Greater efficacy was observed against *Listeria* compared to *Salmonella*. Also, trafficking studies showed that N3 was taken up both through endosomal and fluid phase endocytosis pathways. Thus, we observed two important phenomenon which yielded valuable insight regarding the mechanism of bacterial killing by N3. First and foremost, we demonstrated effective targeting of cytoplasm resident bacteria, which is highly significant since many previously published DDS have reported pH dependent loss of gentamicin bioactivity in the endosomes. In addition, we found that effective targeting of bacteria which reside in specialized niches such as vacuoles inside the cell warrants further modification in the DDS. This is plausible since *Salmonella* was cleared less efficiently than *Listeria* upon treatment with N3, most likely due to the membrane barriers of *Salmonella* containing vacuoles preventing efficient gentamicin delivery.

We also investigated *in-vivo* treatment efficacy of N3 against an intracellular *Salmonella* mouse infection model. Studies done previously have shown that triblock pluronic covalently conjugated with poly(acrylic acid) (PAA) orally improves bio-availablity of many anti-cancer agents. Therefore, the efficacy of N3 to clear intracellular *Salmonella* was explored after oral and parenteral (IP) administration. We observed significant *Salmonella* reduction in infected liver and spleen upon IP administration. However, oral therapy with N3 was not effective in comparison to free gentamicin. We believe that gentamicin may be getting inactivated at low gastric pH and may not absorb from the gut. Hence, oral administration of N3 requires further research in order to apply them effectively in therapy of intracellular infection. At a dosage similar to a treatment dosage parenterally, *in-vivo* histopathological examination showed no abnormal toxicity in liver, spleen, brain, heart, kidney and lung. Renal function test showed normal BUN and creatinine level suggesting that the core-shell nanostructures were relatively non-toxic to kidney and *in-vivo*.

In summary, a novel method for delivery of cell impermeable gentamicin was developed by incorporating them into macromolecular complex. Core-shell nanostructure encapsulating gentamicin by this technique tremendously improved encapsulation efficiency. Upon modifying the shell of nanostructure to amphiphilic from hydrophilic by incorporating pluronic, the route, rate and efficacy of DDS was improved considerable *in-vitro* and *in-vivo*. Thus, the developed core-shell nanostructure can be potentially realized as a platform for efficient gentamicin delivery systems to treat intracellular pathogens.